Co-ordination & Organometallic Chemistry of Facially Capping Tridentate Triphosphorus Macrocycles and the Applications

A Thesis Submitted to Cardiff University

By

Lenali Vinodangi Wickramatunga

In Candidature for the Degree of

Doctor of Philosophy

July 2014

Department of Chemistry

Cardiff University

DECLARATION

This work has not been submitted in substance for any other degree or award at this or any other university or place of learning, nor is being submitted concurrently in candidature for any degree or other award.

Signed 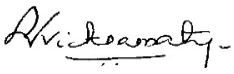 (Candidate) Date: 30/06/2014

STATEMENT 1

This thesis is being submitted in partial fulfilment of the requirements for the degree of PhD.

Signed 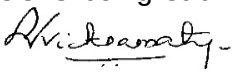 (Candidate) Date: 30/06/2014

STATEMENT 2

This thesis is the result of my own independent work/investigation, except where otherwise stated. Other sources are acknowledged by explicit references. The views expressed are my own.

Signed 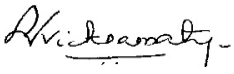 (Candidate) Date: 30/06/2014

STATEMENT 3

I hereby give consent for my thesis, if accepted, to be available for photocopying and for inter-library loan, and for the title and summary to be made available to outside organisations.

Signed 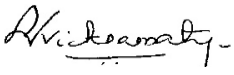 (Candidate) Date: 30/06/2014

STATEMENT 4

I hereby give consent for my thesis, if accepted, to be available for photocopying and for inter-library loans, **after expiry of a bar on access previously approved by the Academic Standards & Quality Committee.**

Signed.....(Candidate) Date.....

ACKNOWLEDGEMENTS

I would like to express my sincere gratitude to my supervisor Prof. Peter Edwards for giving me the opportunity to make my dream a reality. Not only am I indebted for your guidance and encouragement surrounding the phosphines, but also for the enthusiasm and understanding you have shown me about the life in a different environment in a different country.

Secondly, I would like to thank Dr. Paul Newman who has enormously helped me during the past years and Prof. Sudantha Liyanage, for his support and guidance over the years.

I would also like express my sincere appreciation to my parents; I can't express in words how much your continued support (both emotionally and financially) has meant to me. Also my sister, Vinidu, brother in law Malin and son Tharul for their support. Most importantly, I would like to thank and express my extreme gratitude to my husband, Nimal Tennakoon for the years of sacrifice, encouragement and continual support that have led to my accomplishments. Completion of this PhD would have been difficult without him. This thesis is dedicated to you all.

Many thanks are due to Dr. Ian Fallis, Dr. Ben Ward, Dr. Simon Pope, Dr. Dervisi and Dr. Amoroso for the invaluable advice, support and for being helpful.

I also wish to thank all the technical staff of the chemistry department, especially to Rob Jenkins, Robin Hicks and Simon for their help with the JEOL NMR spectrometer and Jamie, Gaz, Sham and Simon James and specially, Mal.

Finally, to my past and the present lab mates Brendon, Mark, Mauro, Neha, Sultan, Tim, Tom, Emily, Lara, Emily, Thusith and others, thank you for the unforgettable times.

Thank you so much.

ABSTRACT

The coordination chemistry of phosphine ligands was pioneered by Mann, Chatt, and others beginning in the 1930s.[1] Currently, phosphine compounds are sought as one of the most important classes of L-type ancillary ligands for transition metal complexes, particularly, because of their applications in a wide range of synthetically and catalytically valuable transition metal systems. There have been numerous efforts to understand the stereo-electronic properties of phosphine ligands and the nature of metal–phosphine bonding.[2] Despite extensive effort in this field, there is considerably less known about the coordination chemistry of the 12-membered tri-phospha macrocycles due to the difficulty of their synthesis. This thesis describes a detailed study of the chemistry of 1,5,9-trialkyl-1,5,9-triphospha cyclododecane ([12]-ane-P_3R_3)[3] ligands with copper, ruthenium, iron and cobalt metals.

Chapter 1, reviews the background chemistry of this research.

The radical-initiated coupling of three facially capping allylphosphine ligands on a neutral $(CO)_3Mo(0)$ template leads to the tri-secondary macrocycle, [12]-ane-P_3H_3 which then undergoes a two-step reaction involves deprotonation followed by alkylation. The macrocycle is then liberated from the template by oxidation of Mo, stereospecifically as the *syn-syn* isomer. The coordination chemistry of 12[ane]P_3Et_3, with copper(I) halides, is discussed in Chapter 2,

[1] (a) Leigh, G. J., Winterton, N., Eds., *Modern Coordination Chemistry: The Legacy of Joseph Chatt*, Royal Society of Chemistry, Cambridge, 2002. (b) Levason, W. In *The Chemistry of Organophosphorus Compounds*, Volume 1, Hartley, F. R., Ed., John Wiley & Sons, 1990, chapter 15

[2] (a) Song, S., Alyea, E. C., *Comments Inorg. Chem*., 1996, 18, 145-164. (b) Alyea, E. C., Song, S., *Comments Inorg.Chem.*, 1996, 18, 189-221. (c) Dias, P. B., Minas de Piedade, M. E., Martinho Simões, J. A., *Coord. Chem. Rev*., 1994, 135/136, 737-807. (d) Tolman, C. A., *Chem. Rev*., 1977, 77, 313-348.

[3] (a) Baker, R. J., Davies, P. C., Edwards, P. G., Farley, R. D., Liyanage, S. S., Murphy,D. M., Yong, B., *Eur. J. Inorg. Chem*., 2002, 1975-1984. (b) Baker, R. J., Edwards, P. G., *J. Chem. Soc., Dalton Trans.*, 2002, 2960-2965.

including a bimetallic Cu(I) species with a unique mono bridging halide atom. All the complexes have been fully characterized analytically and structurally.

Chapter 3 explores the coordination chemistry of triphosphacyclododecane ligands with Fe(0) and Co(0), which led to a range of novel macrocycle complexes, which have been characterised by multinuclear NMR, infrared spectroscopy, mass spectrometry and elemental analysis.

Chapter 4 discusses a series of novel bimetallic and monometallic Ruthenium(II) complexes, which were isolated and characterised in the course of reactions with the macrocycle ligands. The catalytic ability of one such complex (4.9) with respect to ring closing metathesis of diethyl diallylmalonate is described. GC-MS data provide insight to support conclusions drawn about the RCM reaction.

CONTENTS

Chapter 2: Ligand synthesis and coordination chemistry of [12]-ane-$P_3(CH_2CH_3)_3$ with group 11 metals

Copper(I) halides

ABBREVIATIONS

ABCN - 1,1'-Azobis-(cyclohexanecarbonitrile)

AIBN - 2,2'-Azabiisobutyronitrile

Ar - Aryl group

^{i}Bu - *iso*-butyl

^{n}Bu - *n*-butyl

^{t}Bu - *t*-butyl

Cp - cyclopentadienyl (C_5H_5)

Cp* - pentamethylcyclopentadienyl (C_5Me_5)

Cy - cyclohexyl

DCM - Dichloromethane

DMSO - Dimethylsulfoxide

EDTA - Ethylenediaminetetra-acetic acid

en - ethyl

Et - ethyl

GC-MS- Gas Chromatography-mass spectroscopy

IR - Infrared Spectroscopy

(s) - strong

(m) - medium

(w) - weak

(sh) - sharp

(br) - broad

L - Generic ligand

LAH - Lithium Aluminium Hydride

Me - methyl

M.S. - Mass Spectroscopy

NMR - Nuclear Magnetic Resonance

W

(s) - singlet

(d) - doublet

(t) - triplet

(q) - quartet

(m) - multiplet

(dt) - doublet of triplets

(dd) - doublet of doublets

(tt) - triplets of triplets

(br) - broad

$^{n}J_{xy}$ - n-bond coupling between atoms X and Y

Ph - phenyl

Ppm - parts per million

^{i}Pr - *iso*propyl

R - alkyl and aryl group

THF - Tetrahydrofuran

Triphos- $MeC(CH_2CH_2PPh_2)$

CHAPTER 1

INTRODUCTION

1.1 Introduction

Organometallic chemistry is an interdisciplinary science which continues to grow at a rapid pace. Organometallic chemistry is the study of chemical compounds containing at least one bond between a carbon atom of an organic compound and a metal.[1(a)(b)] Organometallic chemistry combines aspects of inorganic chemistry and organic chemistry. Research in organometallic chemistry involves the synthesis of transition metal complexes that exhibit new chemical properties, often via the design and introduction of new ancillary ligands. Homogeneous catalysis is the success story of organometallic chemistry. There has been a great increase in interest and activity in the area of homogeneous catalysis by transition metal complexes, to provide answers to problems in catalysis, biomedical imaging and also in the development of new materials. Phosphine ligands have been successfully used in these systems for past decades.

1.2: Overview – Significant Nature of Phosphine Ligands

Triaryl (e.g. triphenylphosphine) and trialkyl (e.g. trimethylphosphine) tertiary phosphines of the general formula PR_3, are one of the most common and important classes of ligands. According to the Covalent Bond Classification (CBC) method which was published by M. L. H. Green, PR_3 ligands can be classified as L-type ligands, which are neutral ligands that donate two electrons to the metal centre. These electrons can come from the lone pairs, pi or sigma donors.[1(a)] The bonds formed between these ligands and the metal are dative covalent bonds, which are also known as coordinate bonds. They are one of the few series of ligands, in which both the steric and electronic properties can be altered in a systematic and predictable way over a very wide range by varying R.[1(a)]

There are a huge number of reported transition metal complexes containing mono-, di- and polydentate chelating phosphine ligands. The range of the phosphorus substituents further enhance the variety of these ligands and of these complexes.[2] Figure 1.1 displays examples of phosphines exhibiting different steric and electronic properties where, PH_3 is the smallest known phosphine and $P(mesityl)_3$ one of the biggest according to Tolman's cone angles.[3]

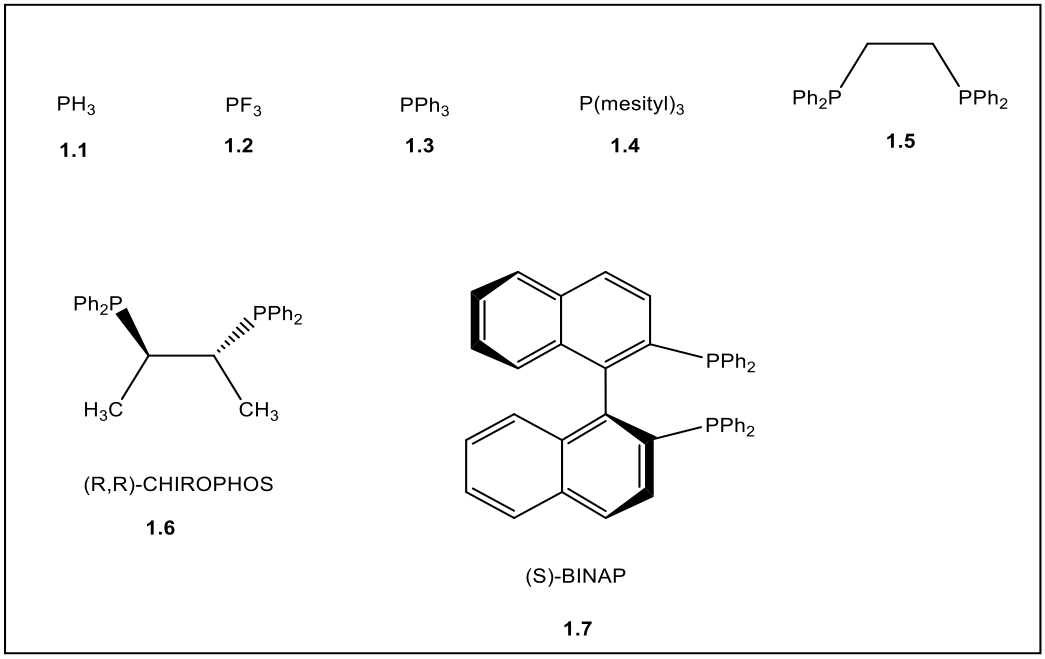

Figure 1.1: Few Phosphine ligands

The coordination chemistry of metal-phosphine complexes has developed dramatically since its appearance in 1857 by Hofmann[4a] and one of the first known example of phosphine complexes used in catalysis was discovered in late 1940s' by Reppe *et* al, that a complex of $Ni(CO)_2(PPh_3)_2$ increased the rate of olefin and acetylene polymerization[4b]. Another major discovery was by Wilkinson, $RhCl(PPh_3)_3$, a non-chiral phosphine, which increased the

hydrogenation of alkenes under mild conditions. Due to the trans effect of this phosphine, it has become an effective ligand for labilising the ligand, trans to the phosphine and it can be used to speed up the catalytic cycle involving dissociative mechanism as the bulky phosphines readily dissociate from the metal centre under mild conditions. The proposed mechanism for this has been outlined in Figure 1.2.[5]

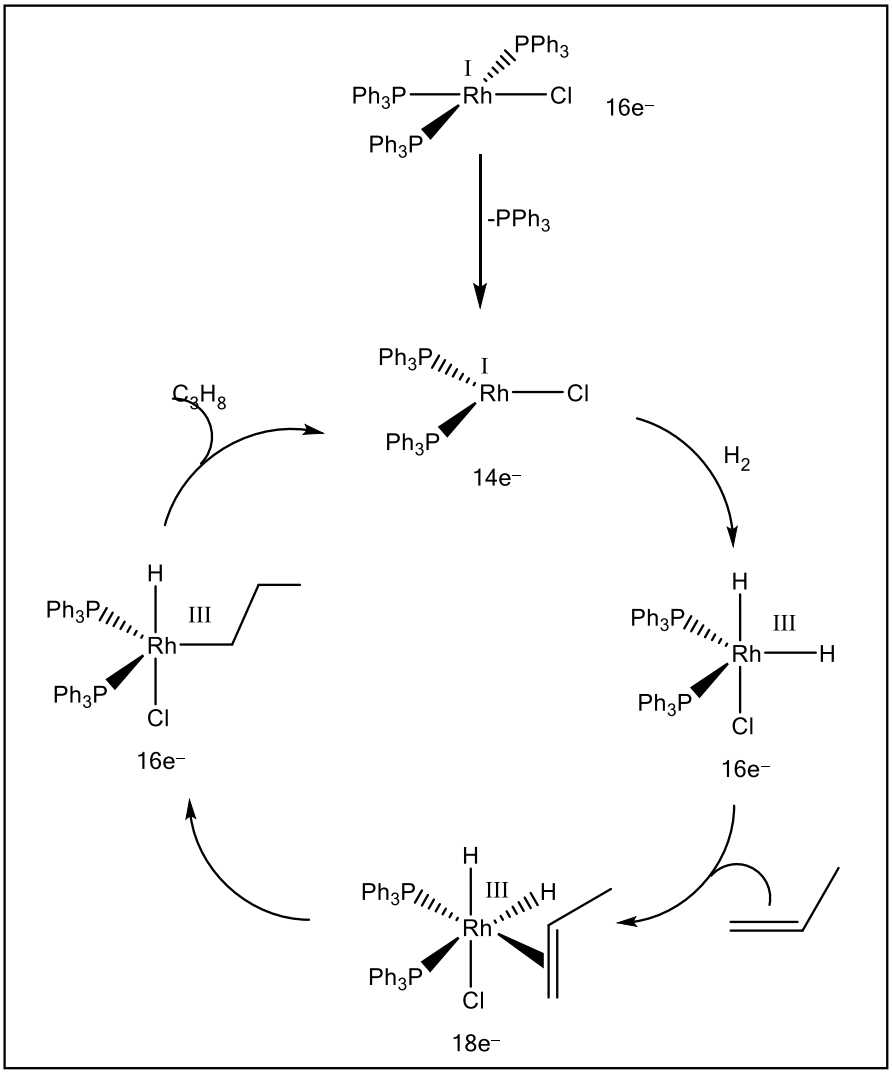

Figure 1.2: Catalytic hydrogenation of propylene by Wilkinson's catalyst.

Grubbs 1st generation catalyst $[Ru(Cl)_2(PCy_3)_2(CHPh)]$,[6] is another break through invention in olefin cross metathesis, ring closing and ring opening metatheses along with cyclic diene metathesis polymerisations.

Furthermore, Phosphine ligands are significant in asymmetric catalysis, due to their intrinsic capability to maintain their configuration, which results in stereospecificity being imparted on the ensuring products. This is immensely important in the fine chemical industries specially in the pharmaceutical sector. For an example, S-BINAP (1.7) is used in preparation of (1R,2S,5R)-menthol (Scheme 1.1) in a 94% ee, and was developed by Ryoji Noyori.[7]

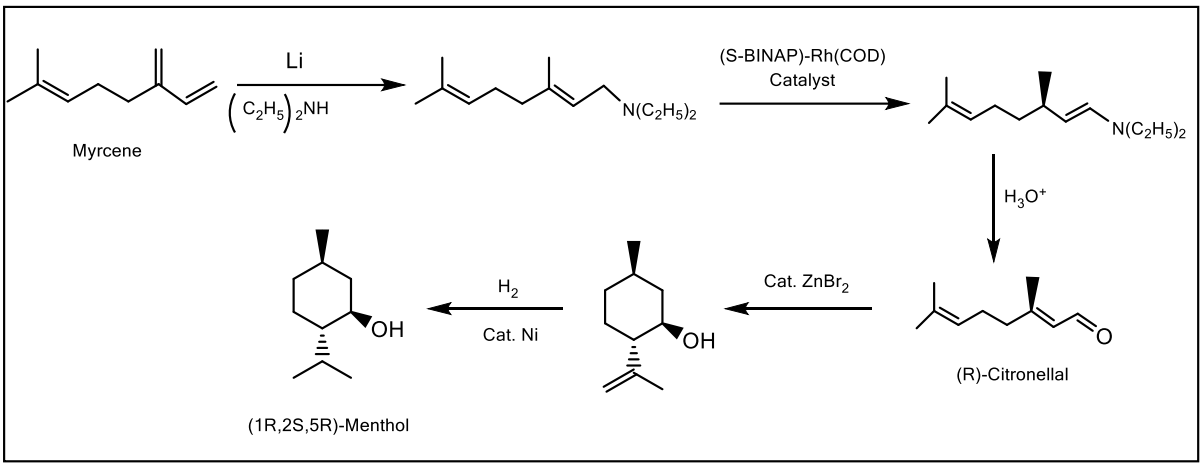

Scheme 1.1: Preparation of (1R,2S,5R)-Menthol

From the above mentioned few examples, it can be simply distinguish the value of the design and synthesis of phosphine ligands followed by their successive coordination chemistry to transition metals. A more comprehensive discussion of triphosphorus macrocyclic ligands in particular is presented below due to our extensive interest.

1.3: Phosphines as Ligands

1.3.1: Electronic Nature

1.3.1.1: σ-bonding:

Phosphines as well as other ligands containing group 15 donor atoms have a lone pair of electrons and exhibit a pyramidal geometry. They are able to act as electron pair donors (Lewis base), by virtue of the lone pair on the phosphorus atom, and coordinate to a metal centre through a σ-bond (Figure 1.3), and their electronic, steric, and stereochemical properties vary based on the substituents attached to the phosphorus atoms.[1] This can increase reaction rates and give greater control of the types of products formed.

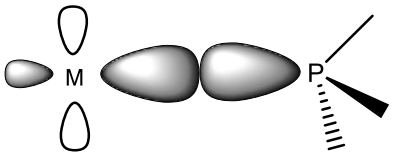

Figure 1.3: A representation of the σ- bond in the metal-phosphine complexes

The pK_a values of the conjugated acids HPR_3^+ established by Tolman, are a good indicator of the σ-bonding capacity of certain alkyl and aryl phosphines and if the pK_a value is high that indicates the strong σ-bonding to the metal.[8] They confirm that the trialkylphosphines are better donors than triarylphosphine, and that a tertiary phosphine ligand is a better donor than the corresponding secondary phosphine (Table 1.1). This does not take into account the π-acceptor nature of the phosphine, but it is a useful method to make comparison between phosphines.[9]

Phosphine	pK_a value	Phosphine	pK_a value
PCy_3	9.70	PMe_2Ph	6.50
PMe_3	9.65	PCy_2H	4.55
PEt_3	8.69	PBu_2H	4.51
PPr_3	8.64	PPh_3	2.73
PBu_3	8.43	$P(CH_2CH_2CH)_3$	1.37

Table 1.1: pKa values of the conjugated acids HPR_3^+ of the phosphines PR_3

1.3.1.2: π-bonding:

Unlike amines, phosphines can also act as π-acceptor ligands, due to the presence of empty orbitals of π-symmetry with respect to the metal ligand bond (Figure 1.4),[10] that forms a synergic metal-phosphine bond which can stabilize metal complexes in low oxidation states. Phosphines act as π-acid ligands, by back donation of electron density from the full or partially filled d-orbitals of the metal centre to the phsophine. It is currently established that the vacant 3d orbital combined with the σ*- antibonding molecular orbital of the P-R bond accepts the electrons from electron rich metals, and consequently the electronic nature of the substituents, R, have a large influence on the capacity of the complex to form these bonds.[11] As a result the increasing electronegativity of R, results in a larger extent of π-bonding in the metal complex. Thus, alkyl phosphines are less π-acidic, than aryl phosphines or phosphites with more electronegative substituents.[2,12,10]

Figure 1.4 represents how the combination of a phosphorus 3d and P-R σ* orbitals overlap leading to a well hybridised π-acceptor orbital.[11]

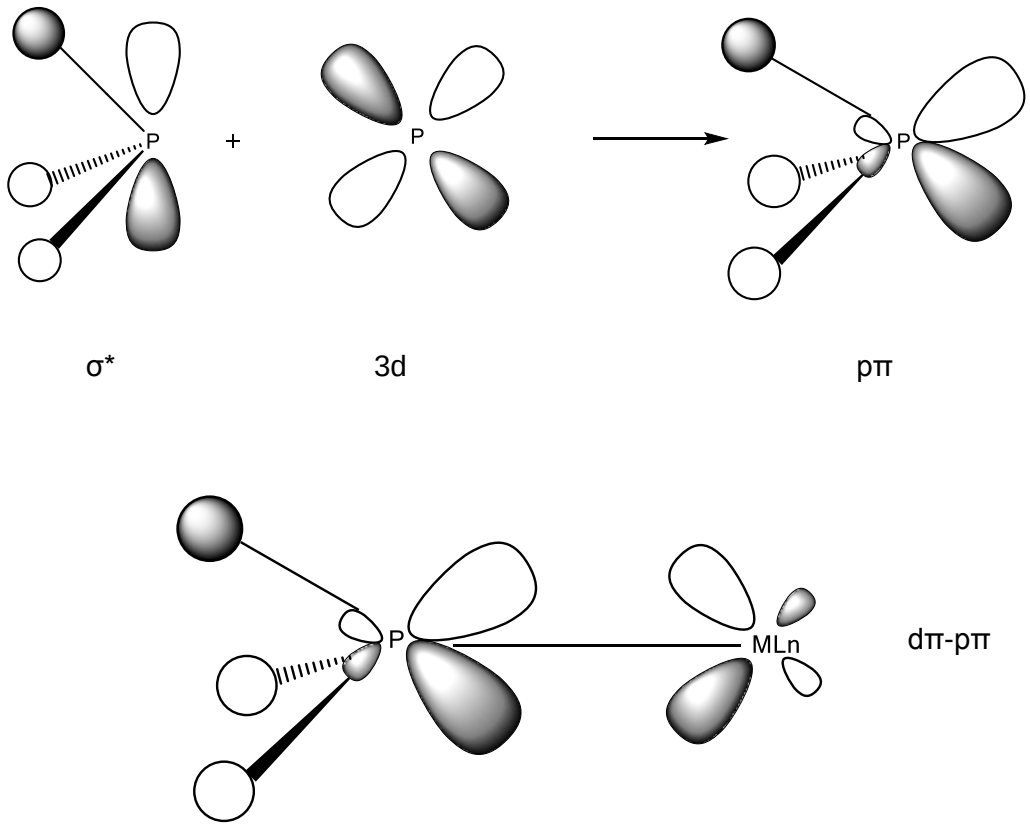

Figure 1.4: Metal-Phosphine bonding models

The dependence of the electronic effect of various PR_3, ligands on the nature of the R group has been quantified by Tolman, by comparing the $\nu_{(CO)}$ frequencies of ancillary carbonyl ligands in the IR spectrum for the complex $Ni(CO)_3L$.[3] Comparison of different phosphines can give the relative π-acidity. As electron density is removed by the phosphines, there is less back bonding to the carbonyl. π-Acidic phosphine ligands accept back donation from the nickel metal,

resulting in the decrease of the back donation from the metal to the CO ligand (M-CO) by competition for available π-electron density on the Ni atom. This essentially, reduces the amount of back bonding from the metal to the π^* orbital of the carbonyl ligands, which affords an increase in strength of the C-O bond resulting in a shift in the IR spectrum corresponding to $\nu_{(CO)}$. The reverse is observed for pure σ-donor phosphine and phosphite ligands (Table 1.2).

PR_3	CO stretch (v,cm^{-1})	PR_3	CO stretch (v,cm^{-1})
P(*t*-Bu)$_3$	2056	P(OMe)Ph$_2$	2072
PCy_3	2056	P(OPr^i)$_3$	2076
PBu_3	2060	PH_3	2083
PEt_3	2062	P(OPh)$_3$	2085
PMe_3	2064	PCl_3	2097
PPh_3	2069	PF_3	2111

Table 1.2: Increasing order of π-acidity of some phosphine complexes.

The order of increasing π-acid character for a series of ligands[12] is:

$PMe_3 \sim P(NR_2)_3 < PAr_3 < P(OMe)_3 < P(OAr)_3 < PCl_3 < CO \sim PF_3$

1.3.2: Steric Effect

The steric properties of phosphorus ligands have been exploited many times to control the reactivity of organometallic compounds in both stoichiometric and catalytic chemistry. Thus, much effort has been spent on quantifying the steric properties of phosphine ligands. This variation of the steric size is an important feature of phosphines as ligands, which can be adjusted by changing the substituents (R). For an example, the number of phosphine ligands

that can be arranged around a particular metal centre depends on the bulkiness of these ligands. Steric crowding at the reaction centre is usually assumed to inhibit associative reactions and facilitate dissociative reactions.[9]

Many attempts have been undertaken to define a reliable steric parameter complementary to the electronic parameter. Tolman has been credited with a systematic treatment of the steric properties of phosphorus ligands.[3] Tolman's parameter (θ), the angle of a cone which encompasses the Van der Waals surface of the phosphine ligand substituents with the apex at the metal and the R groups folding back as far as they are able in a space filling model. The relative sizes of ligands in terms of their cone angles θ, as shown below (Figure 1.4).

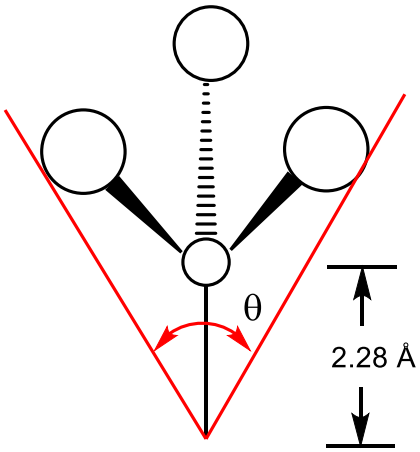

Figure1.4: Definition of Cone angle, θ

Different substituents on phosphorus cause a change in the size of the phosphine ligand as "seen" by the metal centre. More bulky substituents will increase this angle while less sterically

demanding substituents will decrease the angle (Table 1.3). Using suitable substituents allows us to tailor the stability and reactivity of any metal complexes formed.[3]

PR_3	θ(º)	PR_3	θ (º)
$P(t\text{-}Bu)_3$	182	$P(OPr^i)_3$	130
PCy_3	170	$P(OPh)_3$	128
PPh_3	145	PCl_3	124
$P(OMe)Ph_2$	132	PMe_3	118
PBu_3	132	PF_3	104
PEt_3	132	PH_3	87

Table 1.3: Cone Angles / º for selected Phosphine Ligands*.

*** Tolmen's original cone angle is measured from $R_3PNi(CO)_3$ complexes.**

Understanding the electronic and steric parameters of phosphine ligands can be useful in predicting reactivity and the behaviour of phosphine containing macrocycles.

1.4: Polydentate Ligands

A rising interest has been occurring in polydentate phosphine ligands, since the advantages of polyphosphines over comparable monodentate phosphines become clear.[13-15] Ligands that are able of forming more than one bond to a single metal atom can be termed polydentate, and when such metallacyclic complexes are formed, the resultant metal-ligand fragment is called a

chelate. Due to this chelate effect, such complexes are kinetically inert and thermodynamically more stable. It is more pronounced with five or six membered rings with very large and flexible rings the effect turns out to be insignificant. The formation constant β (or the logarithmic form), describes the affinity of a metal ion to a ligand, where the stabilisation properties arising from a chelate effect can be illustrated by this. Scheme 1.2 shows two pairs of equations for the formation of cadmium and nickel complexes.[16]

$Ni^{2+}(aq) + 6\ NH_3(aq) \longrightarrow [Ni(NH_3)_6]^{2+}(aq)$ $\log \beta = 8.61$

$Ni^{2+}(aq) + 3\ en(aq) \longrightarrow [Ni(en)_3]^{2+}(aq)$ $\log \beta = 18.28$

$Cd^{2+}(aq) + 4\ CH_3NH_2(aq) \longrightarrow [Cd(CH_3NH_2)_4]^{2+}(aq)$ $\log \beta = 6.52$

$Cd^{2+}(aq) + 2\ en(aq) \longrightarrow [Cd(en)_2]^{2+}(aq)$ $\log \beta = 10.6$

Scheme 1.2: Formation constants for Nickel and Cadmium, illustrating the chelate effect.

It can be seen from scheme 1.2, the complex formation for en in Nickel is 10^9 times more favourable than NH_3. The two reasons for this large increase in stability is the ligand is pre-organised, which is once one arm has bonded to the metal, the other is in a position to bond readily, being held in the outer coordination sphere and secondly, due to the entropic considerations which is the more significant reason.

$[Ni(NH_3)_6]^{2+}(aq) + 3\ en(aq) \longrightarrow [Ni(en)_3]^{2+}(aq) + 6\ NH_3(aq)$

4 species 7 species

This directs to a greater change in entropy. As the complexes on both sides of the equation contain 6 Ni-N bonds, ΔH is approximately unchanged which indicates the difference in Gibbs free energy mainly comes from the –TΔS component according to the $\Delta G^{\theta} = \Delta H^{\theta} - T\Delta S^{\theta}$, whereas for this complex ΔS = 86.5 $kJmol^{-1}$.[13-15]

Our main interest will focus on tridentate macrocyclic phosphine ligands (Figure 1.5).[15]

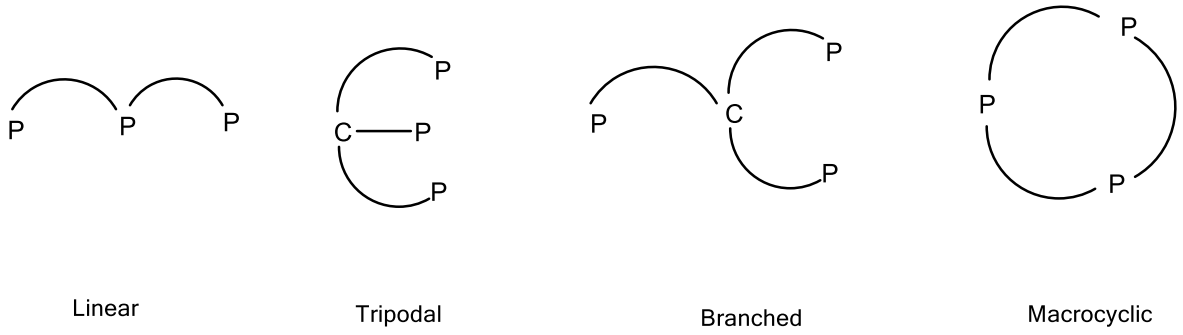

Figure 1.5: Tridentate Ligand types

1.6: Macrocyclic Ligands

Macrocyclic ligands are generally considered to be polydentate ligands which can be defined as a cyclic molecule, with three or more potential donor atoms within a ring of at least nine covalently bonded atoms, where each donor atom is separated by at least two heteronuclear atoms (usually carbon), from the adjacent donor atom.[17] There are various known examples of macrocycles with different donor atoms (Figure 1.6).[18]

The macrocylic ligand complexes are involved in a number of fundamental biological systems which has long been known.[11] For example, the porphyrin ring (1.10) of the iron-containing

haem proteins and the related chlorin complex of magnesium in chlorophyll, collectively with the corrin ring of vitamin B_{12} have all been studied for many years, which is evident that macrocyclic ligands are well-known in biology.[19-21]

Besides the biological uses, the clinical use of macrocycle ligands [(S)-2-(4-nitrobenzyl)-1,4,7,10-tetraazacyclodocecne-*N,N',N'',N'''*-tetraacetic acid] (1.11) to bind radioactive metals for chemotherapeutic applications or of paramagnetic complexes with lanthanides as imaging agents has become practice over the past few years.[21]

The extensive interest in this field is mostly based on the ability of macrocyclic ligands to form very stable complexes and their selectivity for different metals.[22]

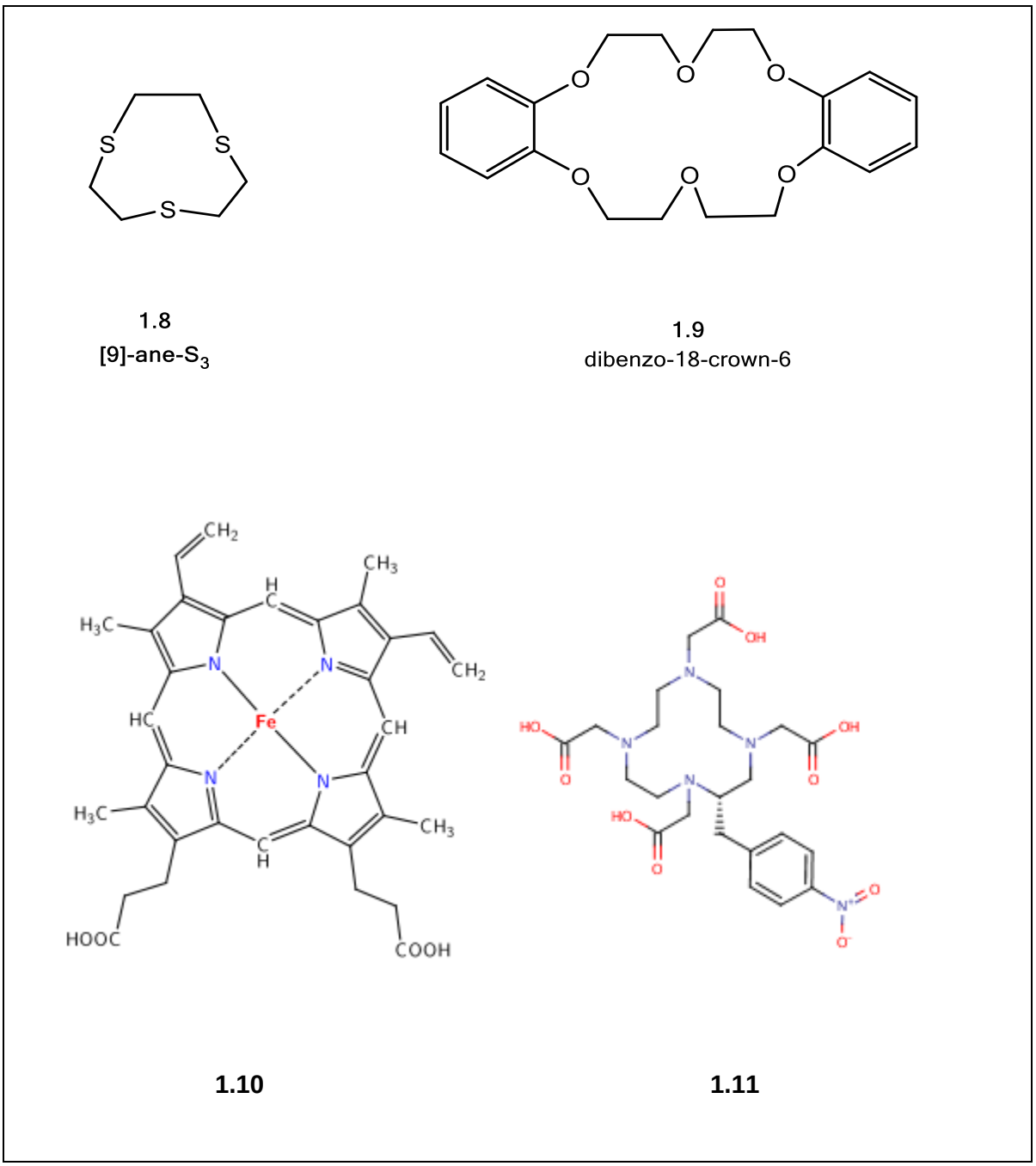

1.8
[9]-ane-S_3

1.9
dibenzo-18-crown-6

1.10

1.11

Figure 1.6: Examples of N, O, S containing macrocycles

1.6.1: Macrocyclic Coordination Effect

Unlike the chelate effect, the macrocyclic coordination effect is based on both entropy and enthalpy and macrocyclic ligands usually form kinetically and thermodynamically more stable complexes with metal ions.[23] For an example, Table 1.4 shows the ΔG values for the formation of the cyclic Ni^{2+} complex with 1.12 is more negative than that for the formation of the acyclic complex with 1.13.[23]

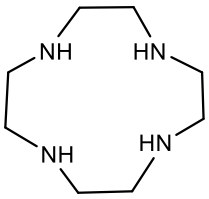

1.12

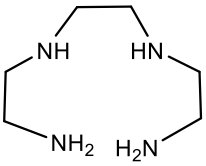

1.13

Ligand	Low-spin/ kJmol^{-1}			High-spin/ kJmol^{-1}		
	ΔH	TΔS	ΔG	ΔH	TΔS	ΔG
1.12	-78.2	49.3	-127.5	-100.8	24.3	-125.1
1.13	-66.1	21.7	-87.8	-80.3	10.9	-91.2

Table 1.4: Thermodynamic data of the formation of Ni(II) complexes at 298K

The ring size of the macrocycles also strongly influences the stability of the complexes.[23] The mismatch of the hole-size with the metal ion, leads to different consequences both in template synthesis or in the coordination chemistry of the macrocycles as for an example the formation of complexes where the macrocycle is partially bound to the metal centre.[22]

1.6.2: Synthesis of Macrocyclic Phosphine Ligands

Macrocyclic phosphines hold promise as incredibly stable ligands for applications requiring robust complexes.[24,25] But, unfortunately, there are only a few macrocyclic phosphine ligands known due to the difficulty in synthesizing them in good yield and handling the appropriate primary and secondary phosphine precursors as they are extremely toxic, air

sensitive, volatile and malodorous. A general synthesis of phosphine macrocycles can be one of two ways namely cycloaddition reactions and template synthesis.[26]

1.6.2.1: Cycloaddition Reactions

In this method, the desired product is prepared by a reaction between a nucleophilic and an electrophilic terminus in the absence of a metal template, which is purely a conventional organic reaction. Two ends of an acyclic molecule bearing suitable moieties react together forming a new bond creating the ring (Figure 1.7).

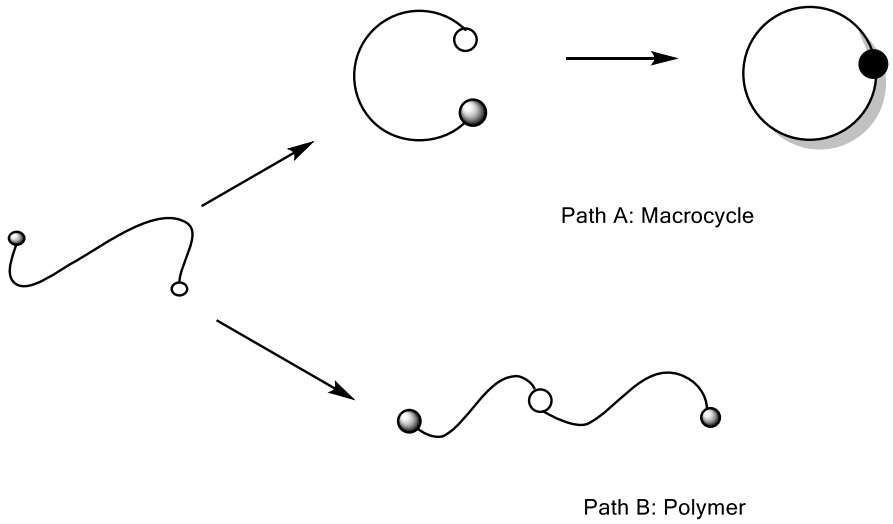

Figure 1.7: A schematic view of the cyclization step occurs during non-templated macrocycle synthesis.

To facilitate the cyclisation, the two reactive groups need to be close to each other, but, as this process displays unfavourable entropy, intermolecular reactions are more favourable than the intramolecular reactions, which are leading to the formation of polymers (Path B).

However, using high dilution conditions and slow addition of the reagents, can favour the intramolecular reactions, which led to the formation of the macrocycle (Path A).

In 1977, Kyba *et al.* synthesized 11-membered triphosphine (P3) macrocycles (1.14) and 14-membered tetraphosphine (P4) macrocycles (1.15) (Scheme 3) using a special high dilution apparatus.[27] Even using such an apparatus, the best yield of macrocycle was only 22%. In addition Ciampolini was successful in obtaining 18-membered mixed donor macrocycles[28-30] with four phosphorus atoms and two other donors including oxygen, nitrogen and sulphur (1.16).[31]

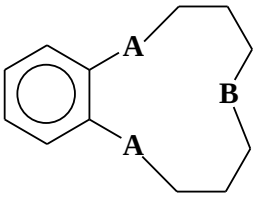

1.14

[11]-ane-A_2B
A= P, S, As
B= N, O, S, P, As

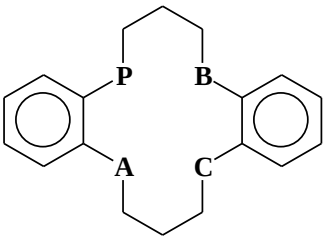

1.15

[14]-ane-PABC
A= P, S
B= N, O, S, P, As
C= N, O, S, P,

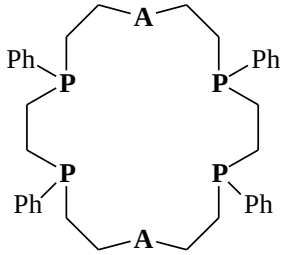

1.16

[18]-ane-P_4A_2
A=N, O, S

Figure 1.8: Various group 15 donor macrocycles prepared by high dilution reactions.

The above mentioned macrocycles were prepared by reaction of lithium or potassium salts of diphosphines with bis-electrophiles, with or without phosphino groups. Apart from the unwanted formation of oligomeric species, the lack of stereoselectivity in the reactions leads to the formation of various stereoisomers that reduces the yield of macrocycles.[32] This is illustrated in Kyba's [11]-ane-P_3 macrocycle which has three possible stereoisomers (Figure 1.9), containing a mixture of *syn* and *anti* configurations whereas the meso-trans isomer was collected in 5% by crystallization.[27,30] It is clear that, *syn,syn* isomer is essential for tridentate coordination to a single metal centre.

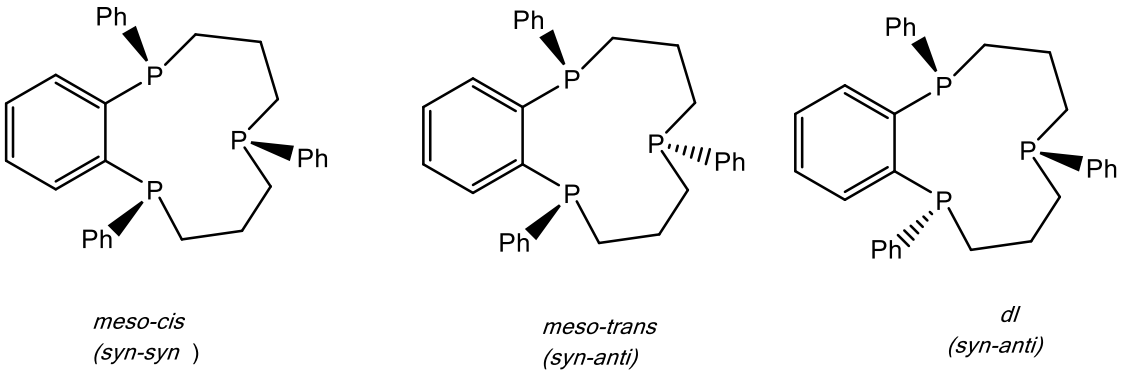

Figure 1.9: Various conformations of Kyba's [11]-ane-P_3 macrocycle

1.6.2.2. Template Method

The metal template acts as a collecting point, placing the precursor ligands in the ideal geometry and stoichiometry for the macrocyclization step (Figure 1.10). However, the role of the metal is not only conformational that is by placing the reactants in the correct special order for cyclisation but, may also function as a stabilising agent of otherwise unstable intermediates.[22] Unfortunately in most cases, the resulting macrocyclic ligands bind so strongly to the metal, that removal of the metal from the ligand is difficult, if not impossible.

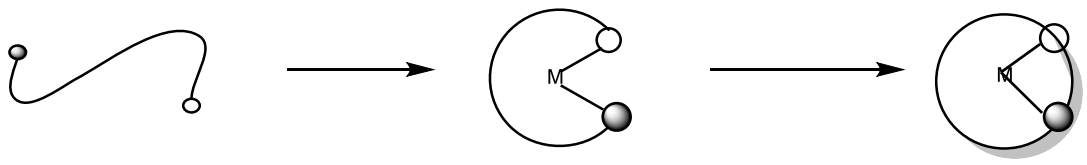

Figure 1.10: A schematic view of the cyclisation step involved in a template macrocycle synthesis.

The use of metal directed reactions can also induce more selectivity in the cyclisation due to the reduction of reactivity of the functional groups involved in the cyclisation process. Electrophilic functional groups have their electrophilic abilities reduced by the back-bonding effect of the metal, whereas nucleophilic functional groups have their electron density reduced by the electrophilicity of the cationic centre.[17] There are advantages in the template method; such as mild reaction conditions, high yields and the *in situ* preparation of metal complexes of themacrocyclic ligands and in many cases high stereo and conformational control of the reaction. Also, the disadvantages can be listed as; not all metal ions can act as a template for a desired reaction, a template reaction may not always give the expected macrocyclic product and it may not be easy to get the free macrocycle as an outcome of the strong coordination of the ligand to the metal resulting from the macrocyclic effect.[22]

The template methods also have been applied in the synthesis of phosphorus containing macrocycles. The first known example is a 15-membered mixed phosphorus thio macrocycle which was prepared using Ni(II) as the template metal in 1970 (Scheme 1.3).[17]

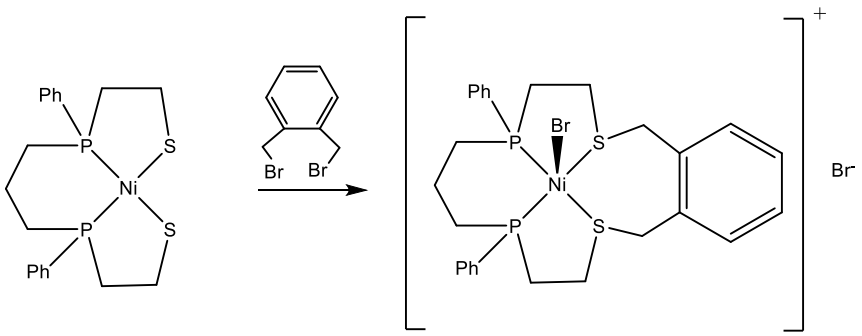

Scheme 1.3: The preparation of template synthesis Ni(II) macrocyclic complex.

Most of the previously known phosphorus macrocycles prepared by template method are tetradentate and built around Ni(II) or Pd(II) (Figure 1.11).[33-36]

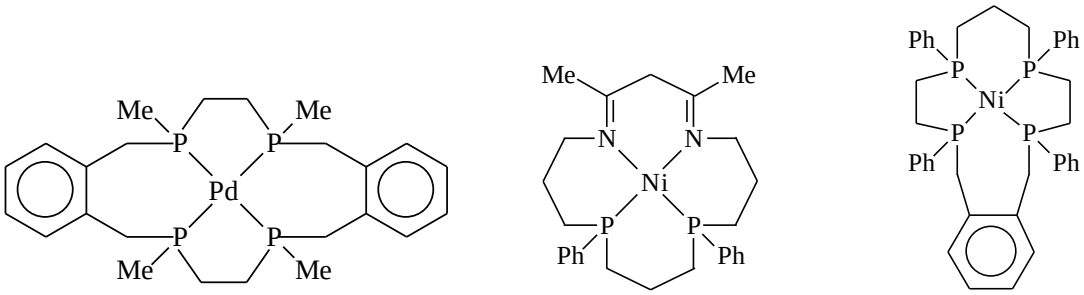

1.17 **1.18** **1.19**

Figure 1.11: Examples of complexes with phosphorus containing macrocycles.

Our main aim lies in the facially capping, triphosphine macrocycles, due to the fact that the three mutually *cis* coordination sites labilise the ligands on the opposite face by virtue of the trans effect (Figure 1.12).

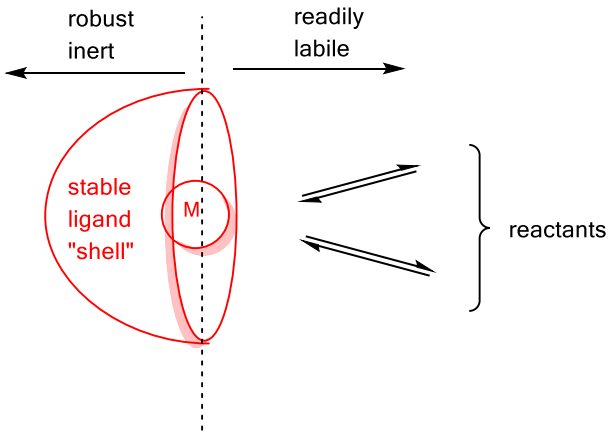

Figure 1.12: Kinetics of facially capping macrocycle

In 1982, Norman *et al.* synthesized the 12-membered P_3 macrocycle (1.21) from *fac*-Mo(allylphosphine)$_3$(CO)$_3$ (Scheme 1.4).[37] AIBN-initiated hydrophosphination of the terminal olefins around the Mo template gave the macrocycle in 85% yield. But, he failed to liberate the macrocycle from the metal template. Later, the Edwards group prepared the tertiary triphosphorus macrocycle (1.22) from 1.21 and also achieved the liberation of 12-membered tertiary triphosphorus macrocycle in 1996 by treating the 1.22 complex with bromine followed by strong base (NaOH) in ethanol (Scheme 1.5).[38-39]

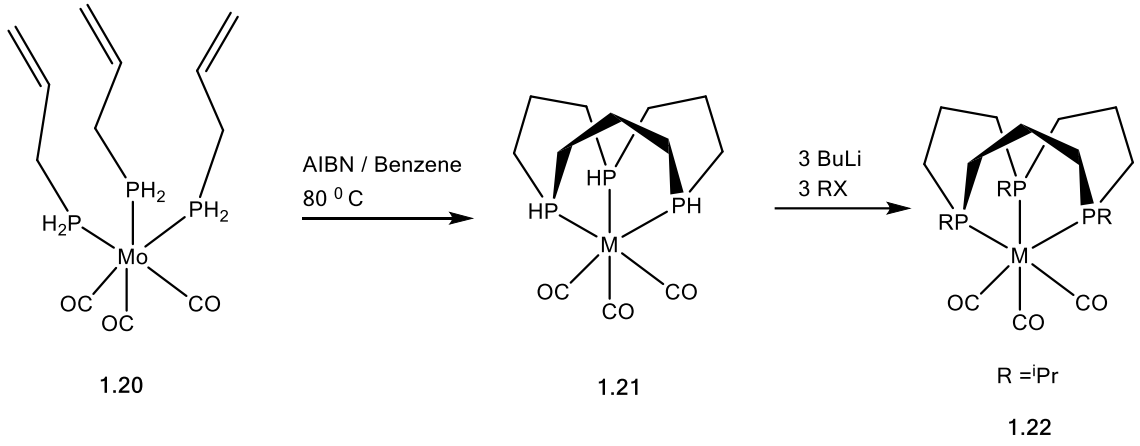

1.20 1.21 1.22

Scheme 1.4: Synthesis of 12-membered macrocycle

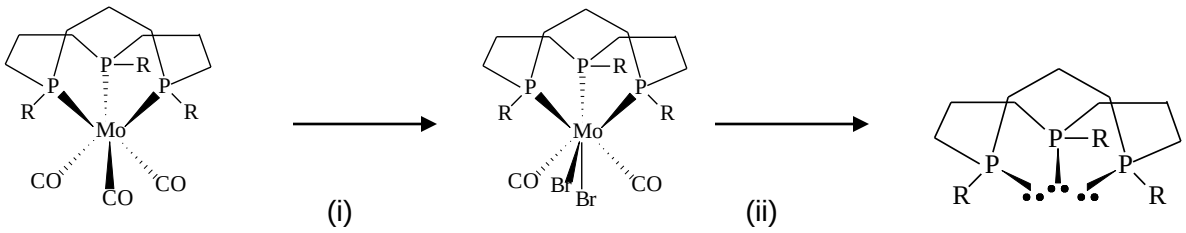

(i) Br, CH_2Cl_2 (ii) NaOH, EtOH

Scheme 1.5: Liberation of the free macrocycle

Furthermore, Edwards and co-workers, prepared various 9- (Scheme 1.6) and 10-membered triphosphorus macrocycles using different metals as templates.[40-44]

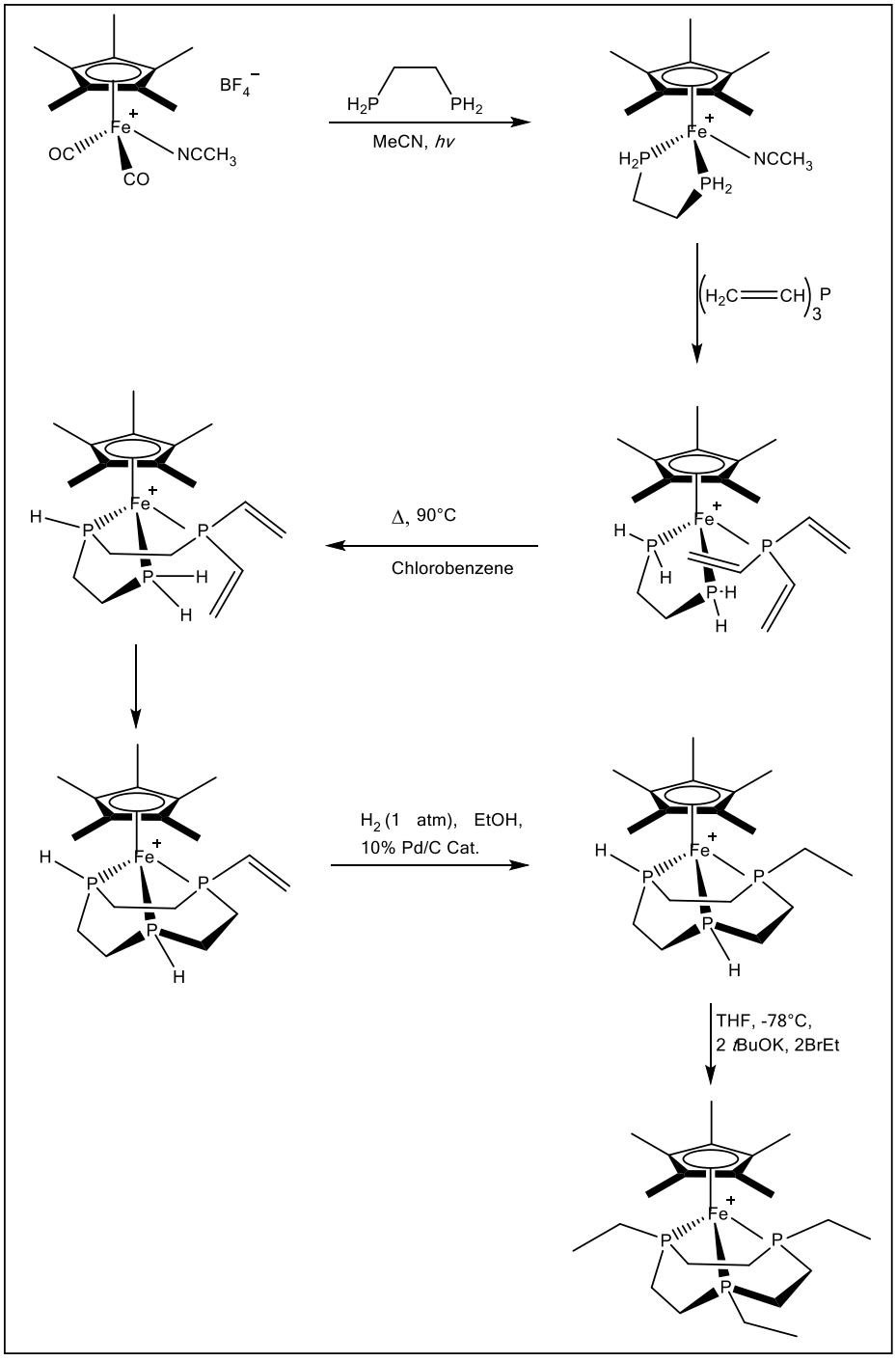

Scheme 1.6: The synthesis of 9-membered P3 macrocycle on an Fe(II) template

1.7. Liberation of P-containing Macrocycles

Once the macrocycle has been synthesised on a metal template, the demetallation/ liberation of the macrocycle from the metal ion can be divided into two main categories. It is either addition of a reagent to a solution of the macrocycle complex which chemically

modifies the donor atom and due to that the macrocycle becomes labile. For an example, several nitrogen containing macrocycles such as porphyrins are liberated after the addition of an excess of a strong acid.[45] Secondly, by addition of strongly competing ligands such as CN^-, $EDTA^{4-}$, OH^- or S^{2-} to the system, can induce the liberation. For phosphorus containing macrocycles the most commonly used agent is KCN[46,47] whereas H_2S[48] has been used less frequently.

In addition, the macrocyclic systems containing a kinetically inert metal ion, needed to tolerate oxidising or reducing agents in order to liberate the ligand. The labiliy of these ions then increased by disrupting the metal ion's electronic configuration by changing the oxidation state. For example strong oxidants such as halogens, H_2O_2 are greatly used in phosphorus macrocyclic systems.[39,49,50]

1.8. Aims of the Thesis

Phosphorus macrocyclic ligands are a fascinating class of ligands and of particular interest are the 12-membered triphosphamacrocycles in their free form. The potential advantages they present as such are their behaviour as six electron donors upon coordination to a metal as a

neutral analogue, and the stabilising ability under lower oxidation states of the metal centre. Furthermore, these tridentate triphosphorus macrocycles, will coordinate to a metal in a facile manner, forcing the remaining sites to be *cis* position, which is highly useful for homogeneous catalysis. As a consequence of the macrocyclic coordination effect, these complexes exhibit extra stability in a catalytic cycle, by inhibiting decomposition of the catalyst which finally, leads to more stable catalysis and higher yields of the product.

However, due to the experimental difficulties in synthesising and handling these complexes, the coordination chemistry of the [12]-ane-P_3R_3 macrocycles with transition metals has been restricted significantly.

Yet, a modified synthesis of 1,5,9-triethyl-1,5,9-triphosphacyclododecane and 1,5,9-triisopropyl-1,5,9-triphosphacyclododecane from a Molybdenum template will be discussed herein. This thesis will also focus on their subsequent coordination chemistry and organometallic behaviour with late transition metals including groups 8, 9 and 11 as well as the applications on phosphorus macrocycle chemistry.

1.9. Reference

1.(a) Crabtree, R. H., The *Organometallic Chemistry of the Transition Metals*, 5th ed., John Wiley & Son., New York, 2009, 99. (b) Toreki, R. (2003-11-20). "Organometallics Defined". Interactive Learning Paradigms Incorporated.

2. Collman, J. P., Hegedus, L. S., Norton, J. R., Finke, R. G., *Principles and Applications of Organotransition Metal Chemistry,* 2nd ed., University Science Books, Mill Valley, California, 1987.

3. Tolman, C. A., *Chem Rev.,* 1977, 77, 313.

4. (a) Reppe, V.W.; Schweckendeik, W.J. Justus Leibigs Ann. Chem.1948, 560, 104 116. (b) Hofman, A. W., *Justus Liebigs Ann. Chem.*, 1857, *103*,357.

5. Osborn, J. A., Jardine, F. H., Young, J. F., Wilkinson, G., *J. Chem. Soc. A.,*1966, 1711.

6. Grubbs, R. H., *Handbook of Metathesis,* Wiley VCH, 2003.

7. Akutagawa, S., *Topics in Catalysis,* 1994, 3, 271.

8. Tolman, C. A., *J. Am. Chem. Soc.,*1970, 92, 2953.

9. Astruc, D., *Organometallic Chemistry and Catalysis,* Springer verlag, Berlin, Heidelberg, 2007, 169.

10. Hill, A. F., *Organotransition Metal Chemistry,* The Royal Society of Chemistry, Cambridge, 2002.

11. Orpen, A. G., Connelly, N. G., *J. Chem. Soc. Chem. Commun.,* 1985, 1310.

12. Cotton, F. A., Wilkinson, G., *Advanced Inorganic Chemistry,* New York, 1980, 87.

13. Cotton, F. A., Hong, B., *Prog. Inorg. Chem.,* 1992, 40, 179.

14. Bianchini, C., Meli, A., Peruzzuni, M., Vizza, F., Zanobini, F., *Coord. Chem. Rev.,* 1992, 120, 193.

15. Meek, D. W., *Homogeneous Catalysis with Metal Phosphine Complexes,* ed. Pignolet, L. H., Plenum, New York, 1983, 257.

16. Cotton, F. A., Wilkinson, G., Murillo, C. A., Bochmann, M., *Advanced Inorganic Chemistry,* 6th ed., John Wiley & Sons., New York, 1999.

17. Constable, E. C., *Coordination chemistry of Macrocyclic Compounds,* Oxford University Press, Oxford, 1999.

18. Blake, A. J., Crofts. R. D., Reid, G., Schroder, M., *J. Organometal. Chem.,* 1989, 359, 371.

19. Corneilli, T. M., Lee, K. C., Whetstone, P. A., Wong, J. P., Meares, C. F., , *Bioconjugate Chem*. 2004,**15**,1392-1402.

20. Wei, L. H., Olafsen, T., Radu, C., Hildebrandt, I. J., McCoy, M. R., Phelps, R., Meares, C., Wu, A. M., Czernin, J., Weber, W. A., *J. Nucl. Med*., 2008, **49**, 11.

21. Miao, Z., McCoy, M. R., Singh, D. D., Barrios, O., Hsu, O. L., Cheal, S. M., MearesC. F., *Bioconjugate Chem*. 2008,**19**, 15.

22. Constable, E. C., *Metals and Ligand Reactivity,*Ellis Horwood Limited, Chichiester, 1990.

23. McAulife, C. A., *Comprehensive Coordination Chemistry,* Vol. 2, ed. Wilkinson, G., Gillard, R. D., McCleverty, J. A., Pergamon, Oxford, 1987.

24. Toulhoat, C.; Vidal, M.; Vincens, M. *Phosphorus, Sulfur Silicon Relat. Elem.* **1992**, *71*, 127-38.

25. Lambert, B.; Desreux, J. F. *Synthesis* **2000**, 1668-1670.

26. Caminade, A. M., Majoral, J. P., *Chem. Rev.,* 1994, 94, 1183.

27. Kyba, E. P.; Hudson, C. W.; McPhaul, M. J.; John, A. M. *J. Am. Chem. Soc.* **1977**, *99*, 8053-8054.

28. Vögtle, F.; Wittig, G. *J. Chem. Ed.,* **1973**, *50*, 650.

29. Davis, R. E.; Hudson, C. W.; Kyba, *J. Am. Chem. Soc.* **1978**, *100*, 3642-3643.

30. Kyba, E. P.; John, A. M.; Brown, S. B.; Hudson, C. W.; McPhaul, M. J.; Harding,A.; Larsen, K.; Niedzwiecki, S.; Davis, R. E. Triligating *J. Am. Chem. Soc.* **1980**,*102*, 139-147.

31. Ciampolini, M., Nardi, N., Zanobini, F., *Inorg. Chem. Acta.,* 1983, 76, L17.

32. Horner, L., Wallach, P., Kunz, H., *Phosphorus, sulfer, silicon, Rel. Elem.,* 1978, 5, 171.

33. Toulhoat, C., Vidal, M., Vincens, M., *Phosphorus, sulfer, silicon, Rel. Elem.,* 1992, 71, 127.

34. Bartsch, R., Hietkamp, S., Morton, S., Peters, H., Stelzer, O., *Inorg. Chem,* 1983, **22**, 3624.

35. Scanlon, L. G., Tsao, Y. Y., Cummings, S. C., Toman, K, Meek, D. W., *J. Am. Chem. Soc.,* 1980, **102**, 6849.

36. Lebbe, T., Machnitzki, P., Stelzer, O., Sheldrick, W., S., *Tetrahedron*, 2000, **56**, 157.

37. Diel, B. N.; Haltiwanger, R. C.; Norman, A. D. *J. Am. Chem. Soc.* **1982**, *104*, 4700-4701.

38. Coles, S. J.; Edwards, P. G.; Fleming, J. S.; Hursthouse, M. B., *J. Chem. Soc., Dalton Trans.* **1995**, 1139.

39. Edwards, P. G.; Fleming, J. S.; Liyanage, S. S.; Coles, S. J.; Hursthouse, M. B. *J. Chem. Soc., Dalton Trans.* **1996**, 1801.

40. Edwards, P. G.; Fleming, J. S.; Liyanage, *J. Chem. Soc., Dalton Trans.* **1997**, 193-198.

41. Jones, D. J.; Edwards, P. G.; Tooze, R. P.; Albers, T., *J. Chem. Soc., Dalton Trans.* **1999**, 1045-1046.

42. Edwards, P. G.; Newman, P. D.; Malik, K. M. A., *Angew. Chem., Int. Ed.* **2000**, *39*, 2922 - 2924.

43. Edwards, P. G.; Haigh, R.; Li, D.; Newman, P. D., *J. Am. Chem. Soc.* **2006**, *128*, 3818-3830.

44. Edwards, P. G.; Whatton, M. L., *Dalton Trans.* **2006**, 442-450.

45. Yashunsky, D. V., Ponomarev, G. V., Arnold, D. P., *Tetrahedron Lett.,* 1995, 36, 8485.

46. Deldonno, T. A., Rosen, W., *J. Am. Chem. Soc,* 1977, 99, 8051.

47. Riker-Nappier, J., Meek,D. W., *J. Chem. Soc. Chem. Commun.,* 1974, 442.

48. Lambert, B., Desreux, J. F., *Synthesis,* 2000, 12, 1668.

49. Price, A.J., Edwards, P. G., *Chem. Commun.,* 2000, 899.

50. Lebbe, T., Machnitzki, P., Stelzer, O., Sheldrick, W. S., *Tetrahedron,* 2000, 56,157.

CHAPTER 2

Ligand Synthesis & Coordination Chemistry of [12]-ane-$P_3(CH_2CH_3)_3$ with Group 11 metal Cu(I)X (X= Cl, Br, I)

2.1. Introduction

The coordination chemistry of macrocyclic ligands is a fascinating area of study in inorganic chemistry. There is a continued interest in synthesizing macrocyclic complexes, because of their potential applications in fundamental and applied sciences and importance in the area of coordination chemistry.

The study of metal-ligand interactions is the core of modern inorganic chemistry. Understanding of metal-ligand interactions allows to design and synthesize new complexes and materials that have the desired properties for targeted applications.[1]

2.1.1. The Chemistry of Tripodal Tridentate Phosphine Ligands

The triphosphamacrocycles normally act as rigid tridentate facially capping ligands which will favour particular coordination geometries and also as six electron donors and may be considered as neutral cyclopentadienyl analogous.[2a, 2b] In addition, the resulting metal species are stabilized by the macrocyclic effect of the ligand and may also influence the reactivity by stabilising specific oxidation states.

The range of known tripodal ligands containing phosphorus donor atoms is far less abundant than their nitrogen, oxygen and sulphur donor atom counterparts (Figure 2.1), which are due to the unavailability of the suitable phosphorus precursors as well as the sensitivity of many phosphorus complexes towards oxygen.

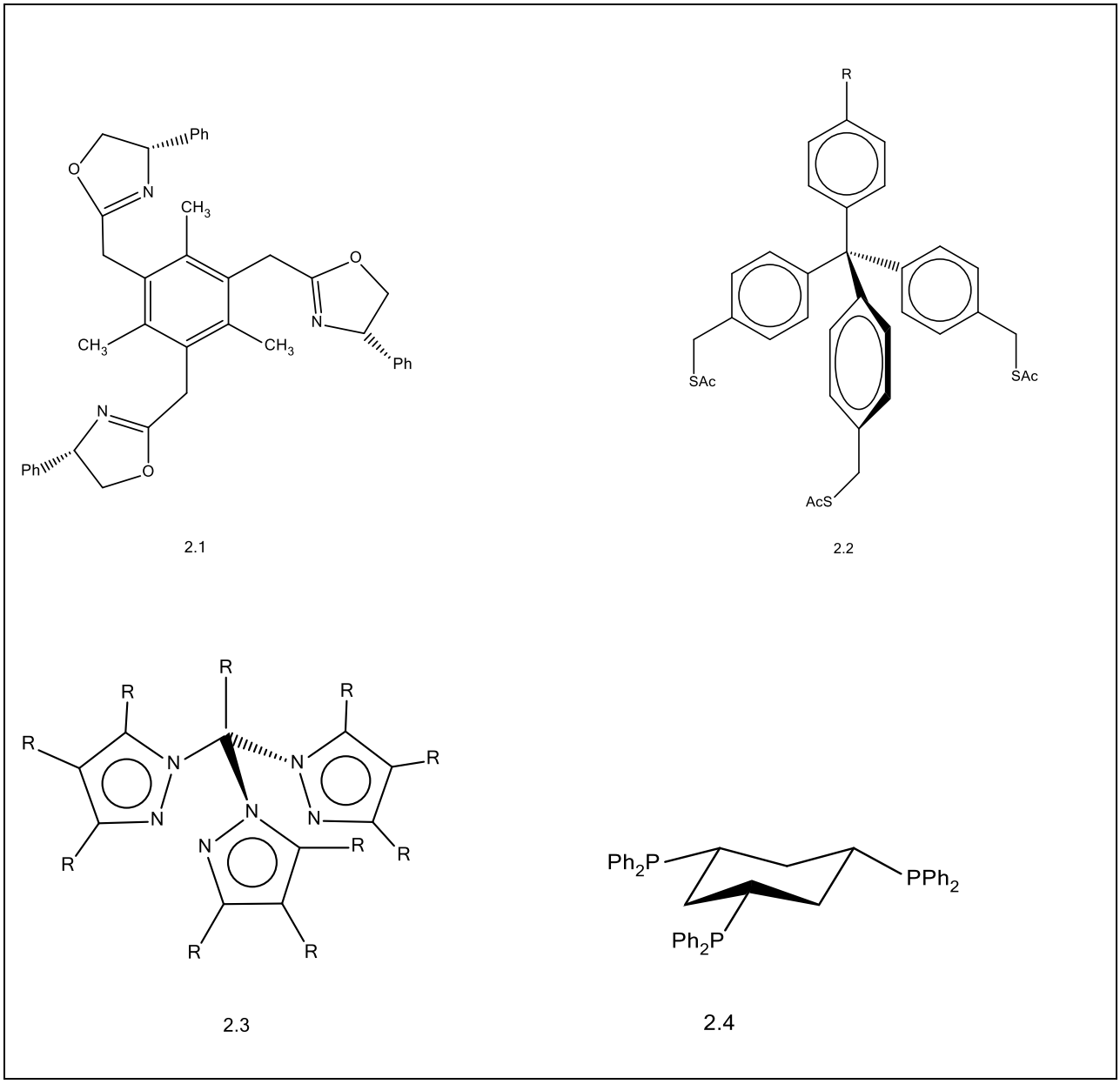

Figure 2.1: A few examples of Tripodal ligands with different donor atoms [3-7]

Tripodal phosphine ligands have advantages as same as other polydentate ligands in acting as multidentate donors and furthermore, the stereochemistry and stoichiometry of the complexes formed can be better controlled due to the structural restrictions of the backbone. Tripodal phosphine ligands are capable of coordinating either in a chelating style or in a bridging style. They have produced stable complexes with most of the *d*-block metals, exhibiting dissimilar coordination modes in a variety of stereochemistry.[8-11]

The main dominating factors of the geometry of these complexes are the nature of the metal and the ligand design. For example, triphos ligands generally coordinate to the metal centre occupying a facile position in tetrahedral, square/pyramidal, trigonal bipyramidal or octahedral geometries, whereas tripodal ligands may also favour a bridging mode aiding the formation of clusters.[10,11]

Among the known phosphorous containing macrocycles, triphospha macrocycles (P_3 macrocycle) with syn,syn,syn-P donors are of greater interest, due to their electronic analogy to η^5-Cp^- as tridentate, facially capping six electron donor ligands occupying three coordination sites. This imposes important structural influence on the metal centre (Figure 2.2), as such they force the remaining reaction sites into a mutually *cis* arrangement and may affect the shape distortions leading the coordination sphere with implications for modified reactivity. Due to their ligating ability as soft donor ligands, they may favour binding to higher electronegative metals with low oxidation states. Enhanced stability due to the macrocyclic coordination effect may also allow access to novel classes of complexes of electropositive metals.[12-14]

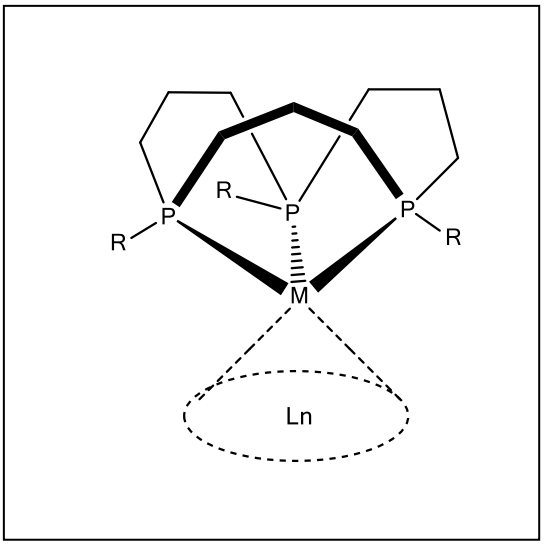

Figure 2.2: Coordination model of Triphosphamacrocycles

Given the widespread use of phosphorus ligands in transition-metal homogeneous catalysis, it can be expected that triphosphacyclododecane compounds hold substantial potential in this area. For example, these complexes have the ability to facially cap metal centres, resulting in their kinetic and thermal stability, while creating labile positions *cis* to the phosphorus coordination sites. The ability to electronically and sterically tune phosphorus donor atoms adds another degree of control that is ideal for catalytic systems.

2.2. Aims of Chapter 2

Chapter 2 discuses the synthesis of the macrocyclic phosphines, 1,5,9- triethyl-1,5,9-triphosphacyclidodecane, ([12]-ane-$P_3(Et)_3$) and 1,5,9-triisopropyl-1,5,9-triphospha cyclidodecane, ([12]-ane-$P_3(^iPr)_3$) and the coordination chemistry of ([12]-ane-$P_3(Et)_3$) with group 11 metal, copper(I) halides.

Early preparations of triphospha macrocycles were carried out by Kyba *et al*. through direct solution methods; however, only 11-membered rings containing benzyl backbones were obtained.[15] Norman *et al.* reported the first transition-metal synthesis of a [12]-ane-P_3H_3 macrocycle in 1982 via a template coupling of the tris(allylphosphine)tricarbonyl molybdenum(0) complex. [16,17] This was followed by the pioneering work of the Edwards *et al* in the template synthesis of numerous [12]-ane-P_3R_3 derivatives that were successfully removed from the metal templates by oxidation of the metal centre followed by base digestion.[18-20]

A novel consistent method for the conversion of the secondary phosphorous macrocycle into a tritertiary phosphorous macrocycle with less decomposition and high yield has been executed in this work.

2.3. Results and Discussion

2.3.1 Synthesis of 2-Propenylphosphine (Allylphosphine)

Aliphatic phosphines including allylphosphine are pyrophoric, malodorous, potentially highly toxic and as well as air sensitive and extremely volatile. All reactions had been carried out in a well-ventilated fume hood. The following methods are some of reported literature to prepare allylphosphine in high yields (Scheme 2.1 and Scheme 2.2).

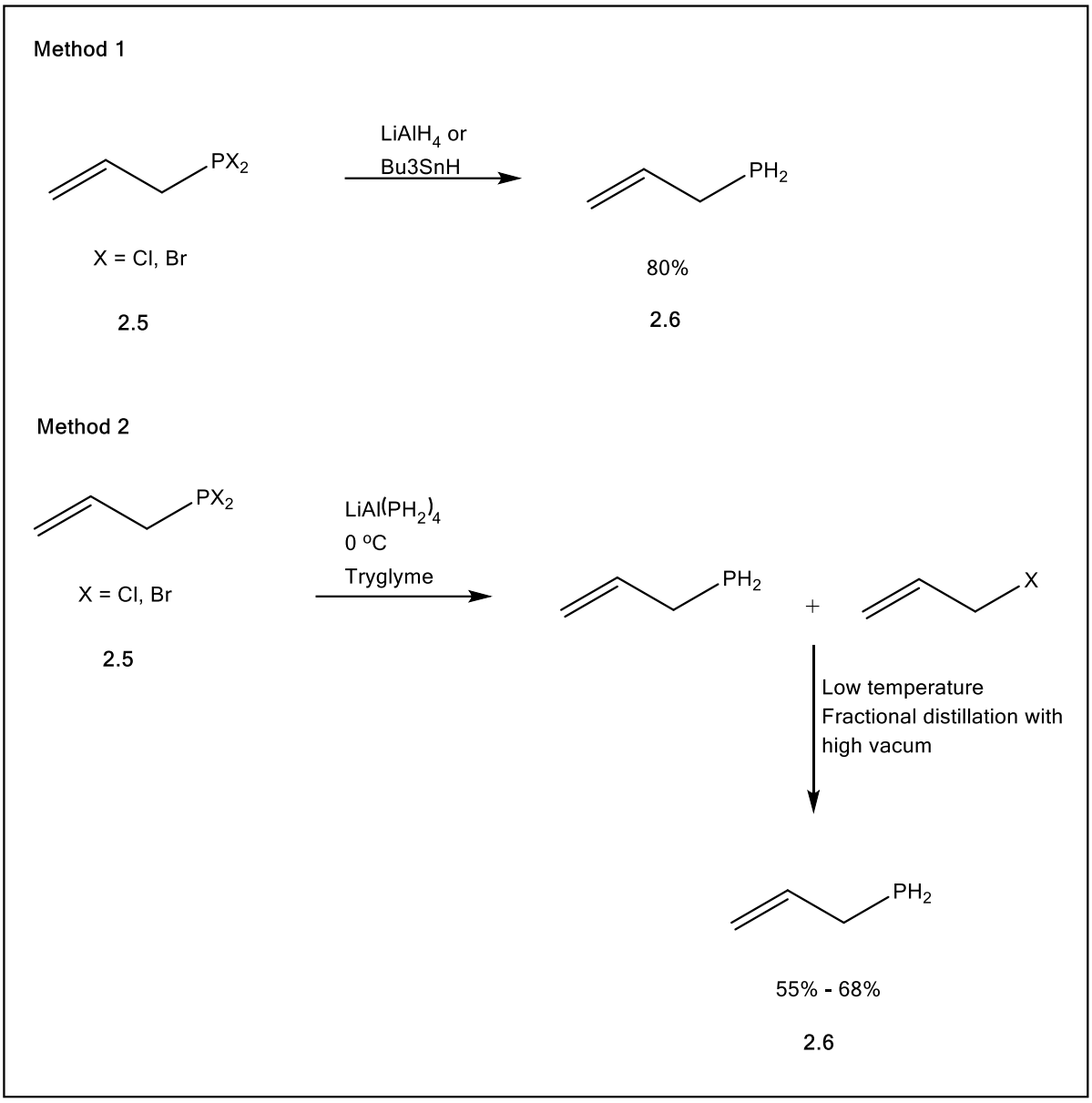

Scheme 2.1: Reported methods of synthesis of allylphosphine [18,19]

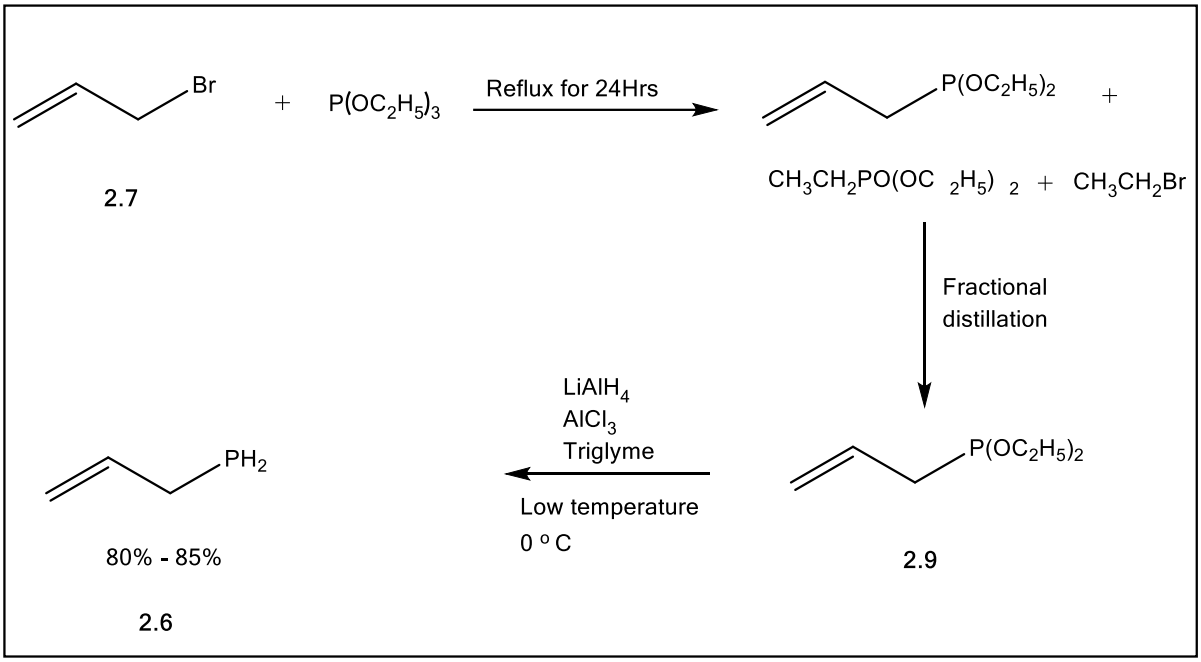

Scheme 2.2: The used synthetic route of Allylphosphine

The reaction of 2-propenylbromide with triethoxyphosphine was followed by the reduction of the formed triethylallyl phosphonate with $LiAlH_4$ and $AlCl_3$ in triglyme. The second step has been customized to prepare the 2-propenylphosphine in pure form. The flask containing the reducing mixture in triglyme was cooled to 0ºC, then the slow addition of the triethoxyphosphine during one hour was followed by another two hours of stirring. During and after the addition, the 2-propenylphosphine that formed was distilled off in vacuo from the reaction mixture and was collected by two cold traps during six hours for higher yield and high purity.

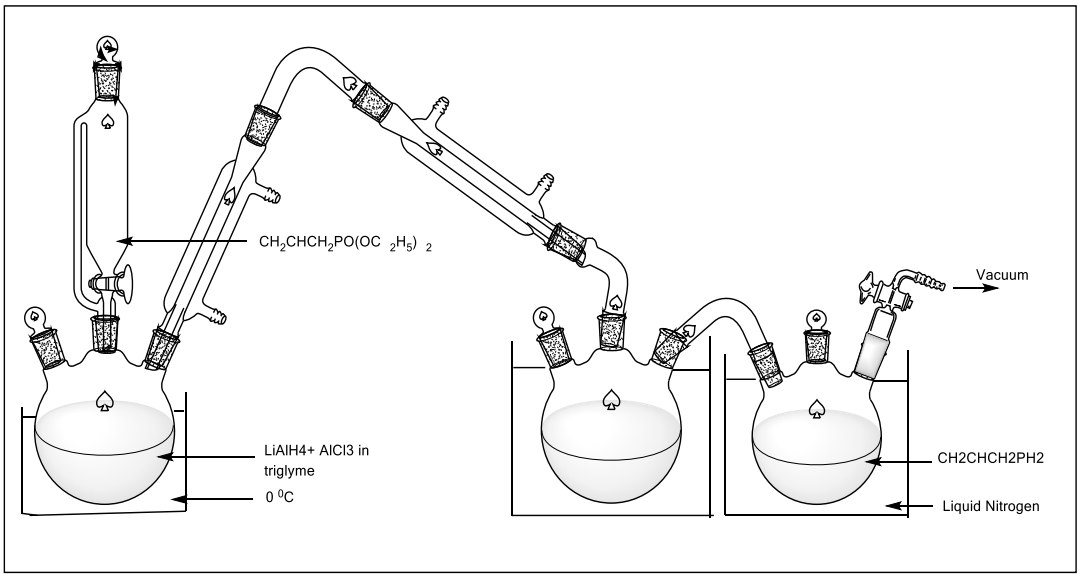

Figure 2.3: Apparatus for the synthesis of 2-Propenylphosphine

Allylphosphine was separated as a colourless liquid and the purity was checked by ^{1}H and $^{31}P\{^{1}H\}$ NMR spectroscopy.

2.3.2. Chromium(0) and Molybdenum(0) allylphosphine and Macrocycle complexes

In 1982, Norman et al. synthesized the 12-membered P_3 macrocycle from *fac*-Mo(allylphosphine)$_3$(CO)$_3$ with the reaction of allylphosphine and (η^6 – mesitylene)tris(carbonyl) molybdenum(0) metal precursor (Scheme 2.3).[16,17] AIBN-initiated hydrophosphination of the terminal olefins around the Mo template gave the macrocycle in 85% yield. The progress of the reaction, could be followed by $^{31}P\{^{1}H\}$ NMR spectroscopy with a single resonance (C_6D_6) at δ = - 57.9 ppm and the presence of the two carbonyl absorptions at U(CO) 1864 cm^{-1} and 1954 cm^{-1} confirms the *fac*-octahedral geometry.

The Edwards group later synthesized tungsten and chromium analogues.[18] Synthesis of the $W(CO)_3$(allylphosphine)$_3$ template from $W(CO)_3$(mesitylene) was similar to the synthesis of the Mo analogue (Scheme 2.3).

	$^{31}P\{^1H\}$ NMR	CO stretch / cm^{-1}
fac-$[W(CO)_3(CH_2CHCH_2PH_2)_3]$	- 80.1(t)	1935, 1825
fac-$[Cr(CO)_3(CH_2CHCH_2PH_2)_3]$	- 23.6 (t)	1932, 1834

The $Cr(CO)_3$(allylphosphine)$_3$ template could not be formed from the mesitylene complex but was synthesized instead from $Cr(CO)_3(MeCN)_3$. Radical-initiated intramolecular hydrophosphination of each of these templates then led to macrocyclization.

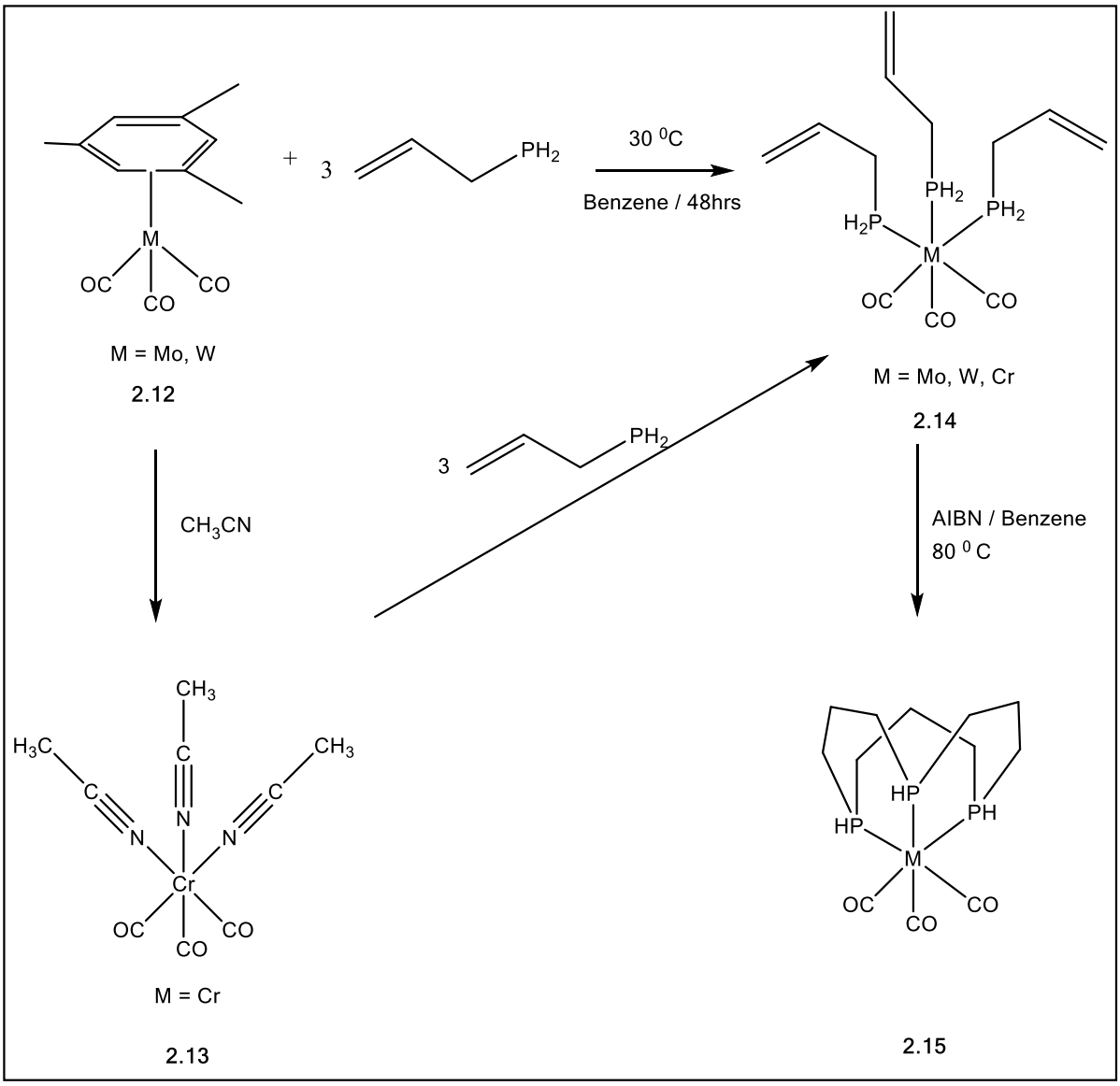

Scheme 2.3: Synthesis of the 12-membered macrocycle

In order to achieve the cyclization, Norman *et al* used AIBN as the catalyst and the cyclization was achieved in a free radical initiation path following stepwise process[17] (Scheme 2.4). The presence of these species (2.15, 2.16 and 2.17) was proved by the $^{31}P\{^{1}H\}$ NMR analysis as a

function of time.[17] This process has been modified by the use of 1,1'-Azobis-(cyclohexanecarbonitrile) (ABCN) as the free radical initiator due to the unavailability of AIBN and at 80ºC in toluene as same as the previous reaction conditions and was confirmed by the ^{31}P $\{^1H\}$ NMR a doublet is observed at δ = -32.1ppm consistent with a secondary phosphine with the downfield shift upon cyclization.

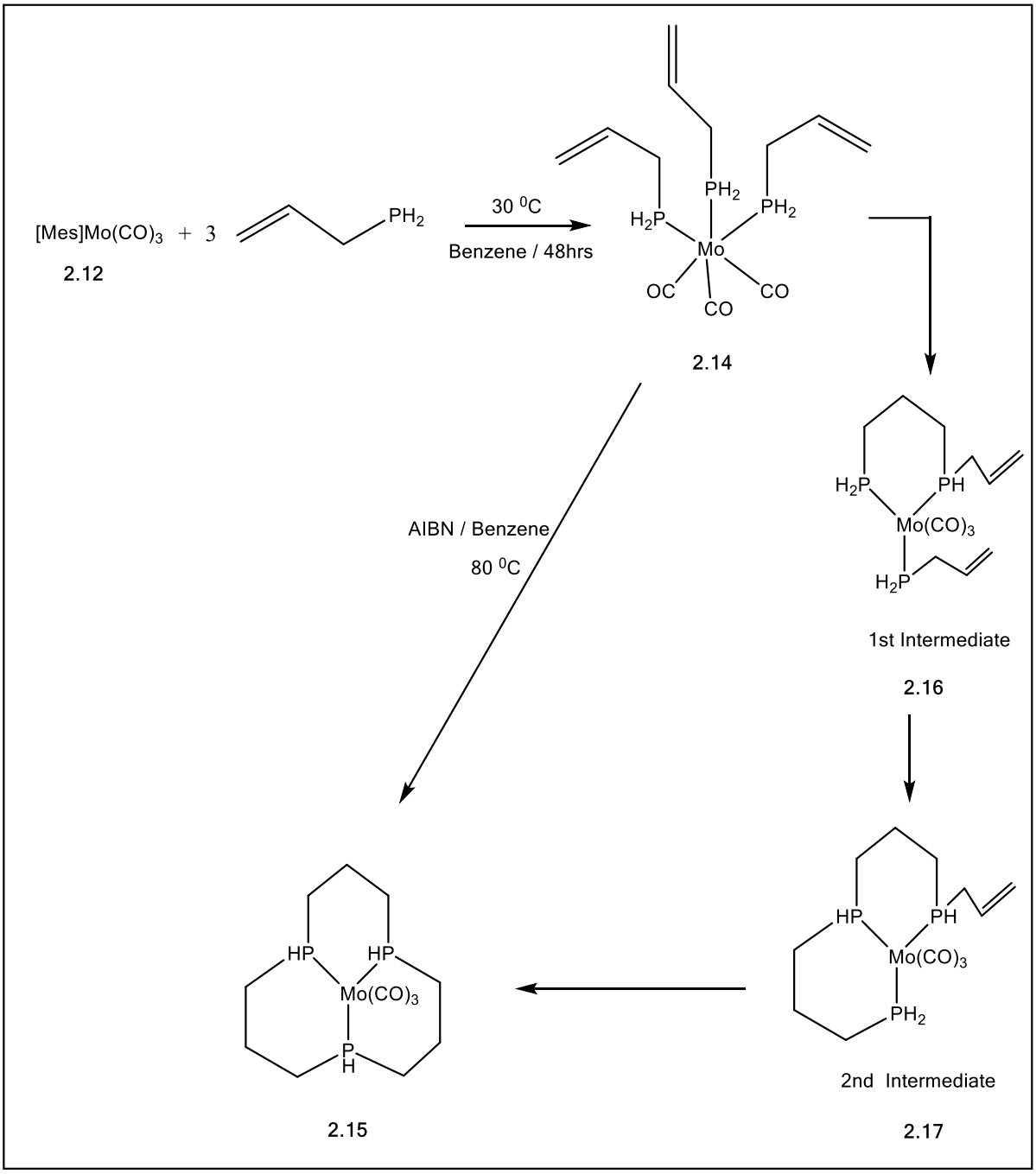

Scheme 2.4: Preparation of tricarbonyl[1,5,9-triphosphacyclododecane]molybdenum(0)

2.3.3. Synthesis of Tritertiary macrocycles

The tritertiary (1,5,9-triphosphacyclododecane)molybdenum(0) complexes have been prepared from the secondary phosphine macrocycle precursor complex tricarbonyl(1,5,9-triphosphacyclododecane)molybdenum(0). The synthetic routes involved either deprotonation of the trisecondary phosphine precursors followed by alkylation with alkyl halide or by radical-catalysed hydrophosphination of selected alkenes (Scheme 2.5).[18, 21-23]

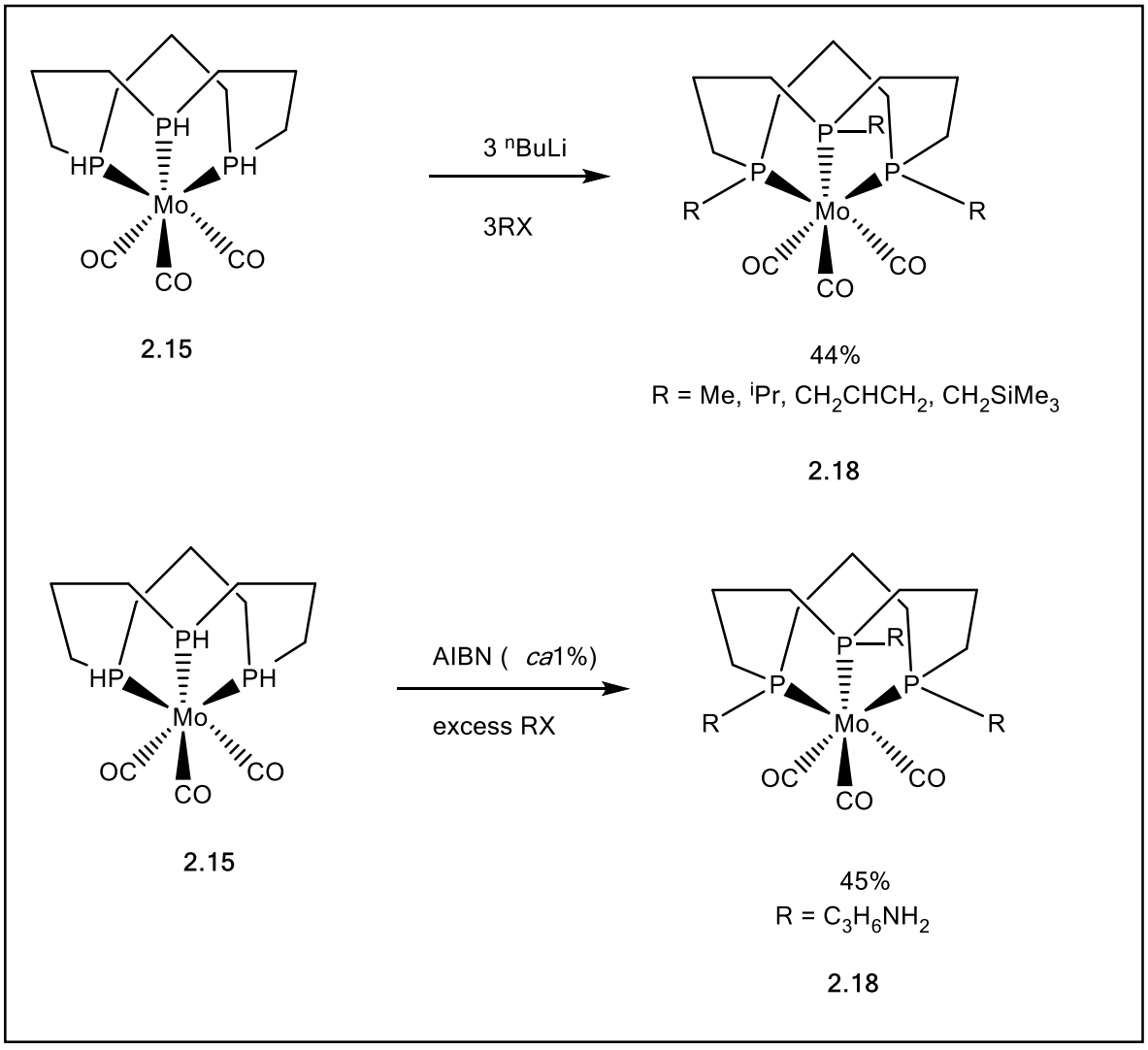

Scheme 2.5: Synthetic routes of tertiary phosphine macrocycles

We are using a different approach to synthese the tertiary phosphine macrocycles in high yield in a one pot process leading to an extremely effective system for the selective functionalisation of phosphines. Na-dimsyl (Na^+ $^-CH_2S(O)CH_3$), in DMSO has been used as an alternative solvent/base combination for the deprotonation of $[Mo(CO)_3\{cyclo\text{-}(HPC_3H_6)_3\}]$, where subsequent reaction of a slight excess of alkyl halide in DMSO results in the quantitative formation of the tritertiary phosphine macrocycle product (Scheme 2.6).

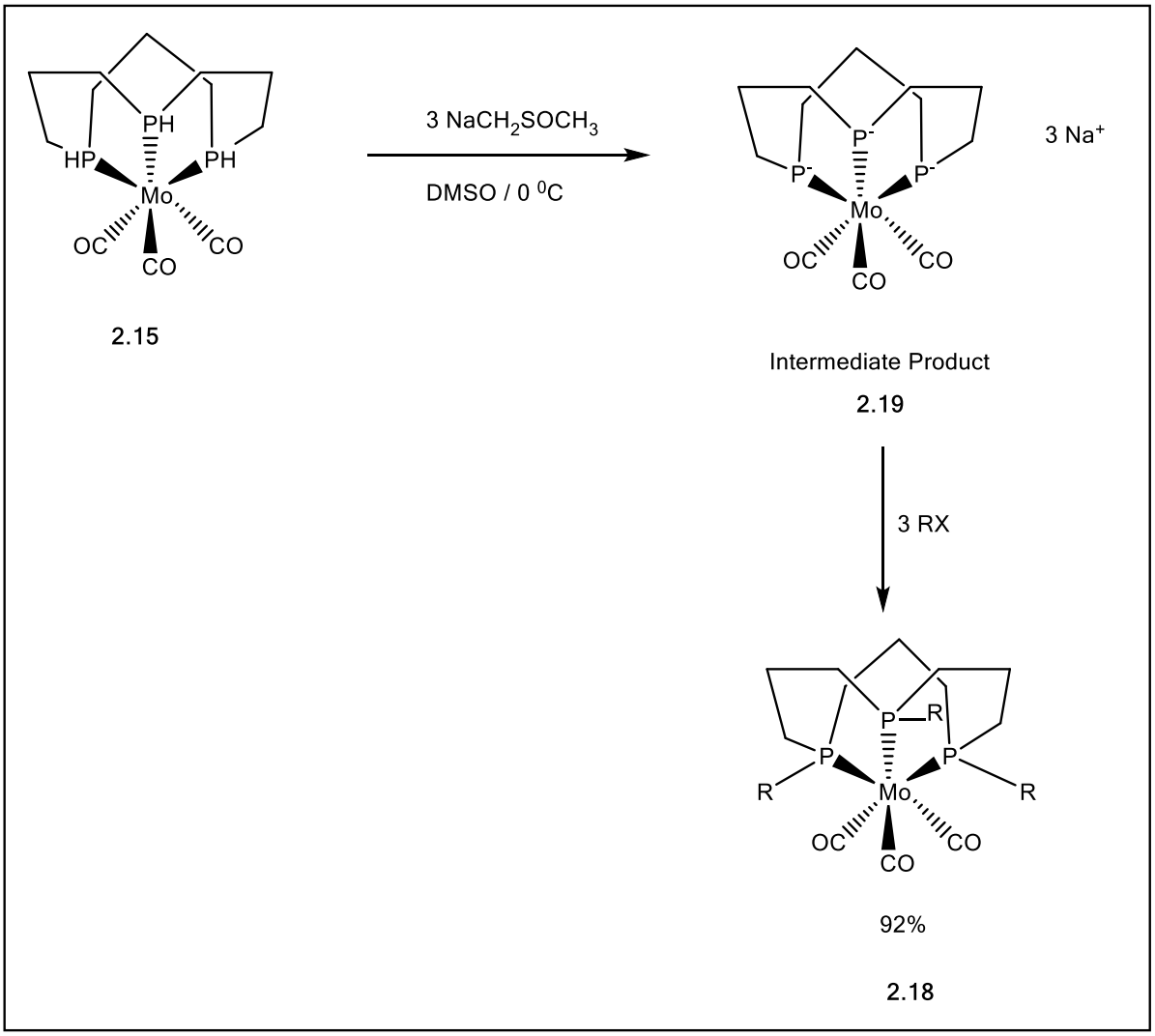

Scheme 2.6: Synthesis of tertiary phosphine macrocycles by reaction with RX followed by the deprotonation with Na-dimsyl

The attempts to isolate the intermediate product (2.19), was not successful due to its extreme air and moisture sensitivity. These reactions have been monitored by ^{31}P $\{^1H\}$ NMR spectroscopy, the isopropyl substituted tertiary macrocycle on molybdenum metal template appears at δ ^{31}P 12.1ppm and the ethyl substituted tertiary macrocycle appears at δ ^{31}P 4.4ppm as singlets respectively.

2.3.4. The Liberation of tri-tertiary macrocycle from the metal template

The molybdenum(0) tertiary macrocycle complexes have a d^6 electron configuration with an octahedral geometry. Due to the kinetic inertness of these Mo(0) complexes, it is difficult to demetallate: to overcome this difficulty and to facilitate the liberation a solution has been introduced, which is the oxidative addition of halogens to carbonyl complexes of Mo(0). It has been shown that a tricarbonyl cation is initially formed followed by the loss of CO and generation of neutral seven coordinate metal(II) complexes with prolonged stirring. This was then reacting with NaOH in ethanol followed by digestion of inorganic by-products in water causes a loss of colour in the mixture and the separation of a colourless oil. Extraction of this oil with petrol enables the isolation of colourless needles of the free macrocycle in high yields (80%) (Scheme 2.7).

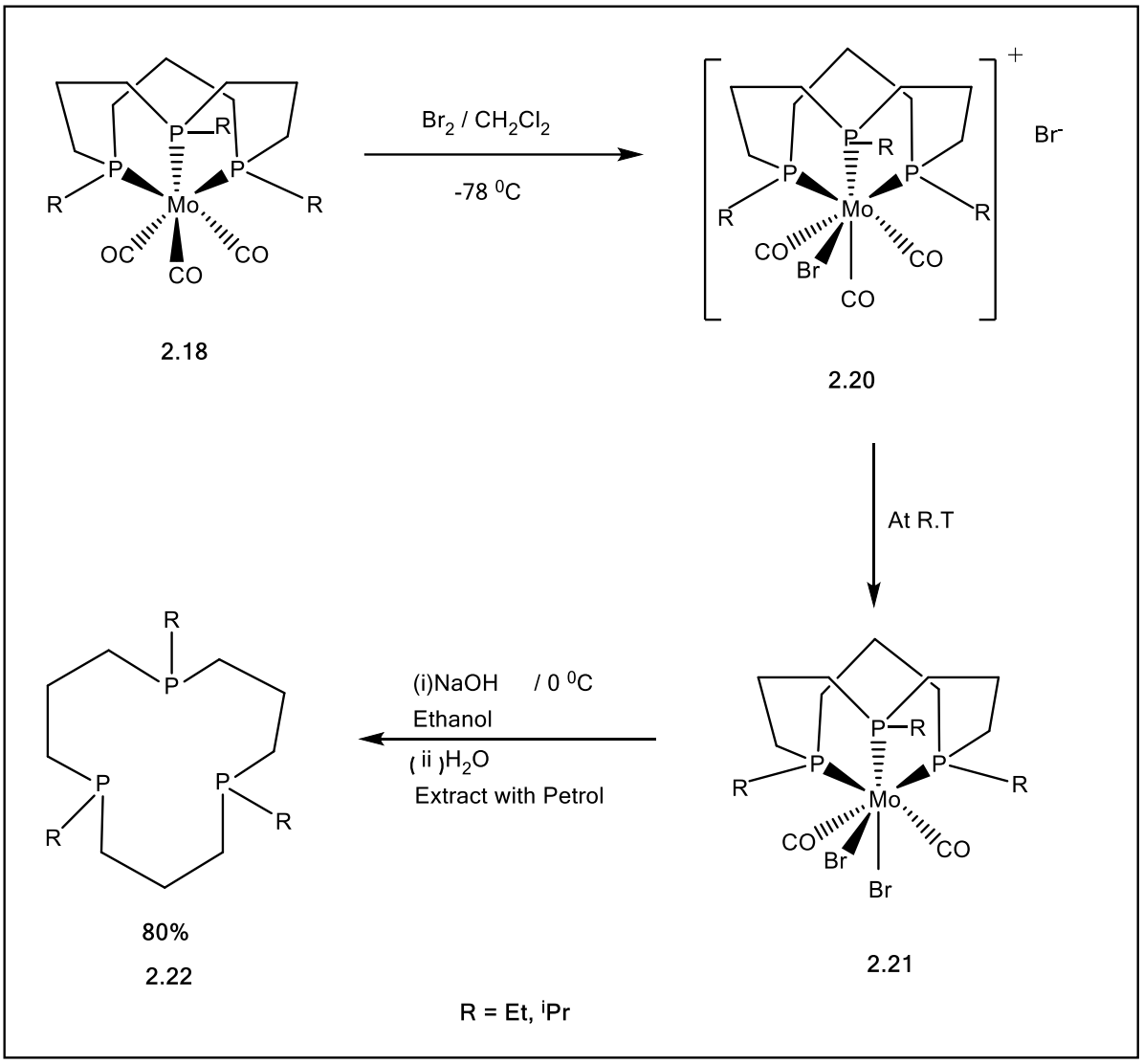

Scheme 2.7: Liberation of the macrocycle

Since there are two possible geometric isomers (Figure 2.4) of [12]-ane-P_3R_3, the spectra indicate that the liberation is stereospecific for all-*syn* stereochemistry as would be expected for a facially coordinating tridentate ligand since syn-anti isomer would require an A_2B pattern in the $^{31}P\{^1H\}$ NMR spectrum as well as more complex ^1H and ^{13}C NMR spectra.[24]

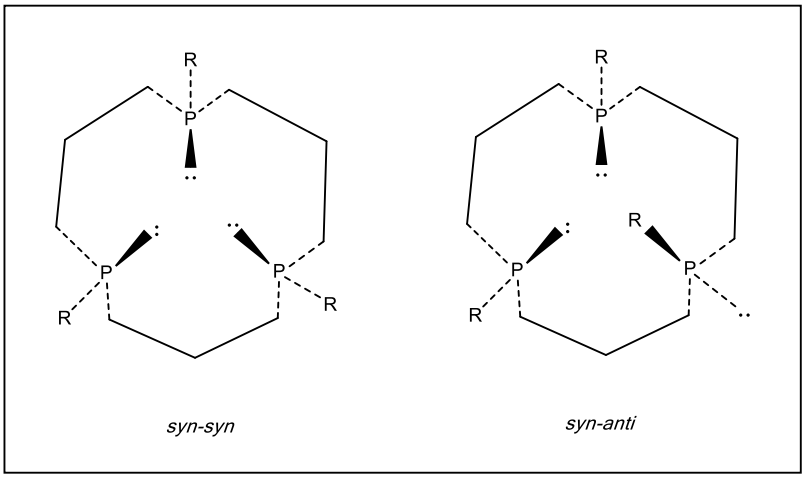

Figure 2.4: Possible conformation of [12]-ane-P_3R_3

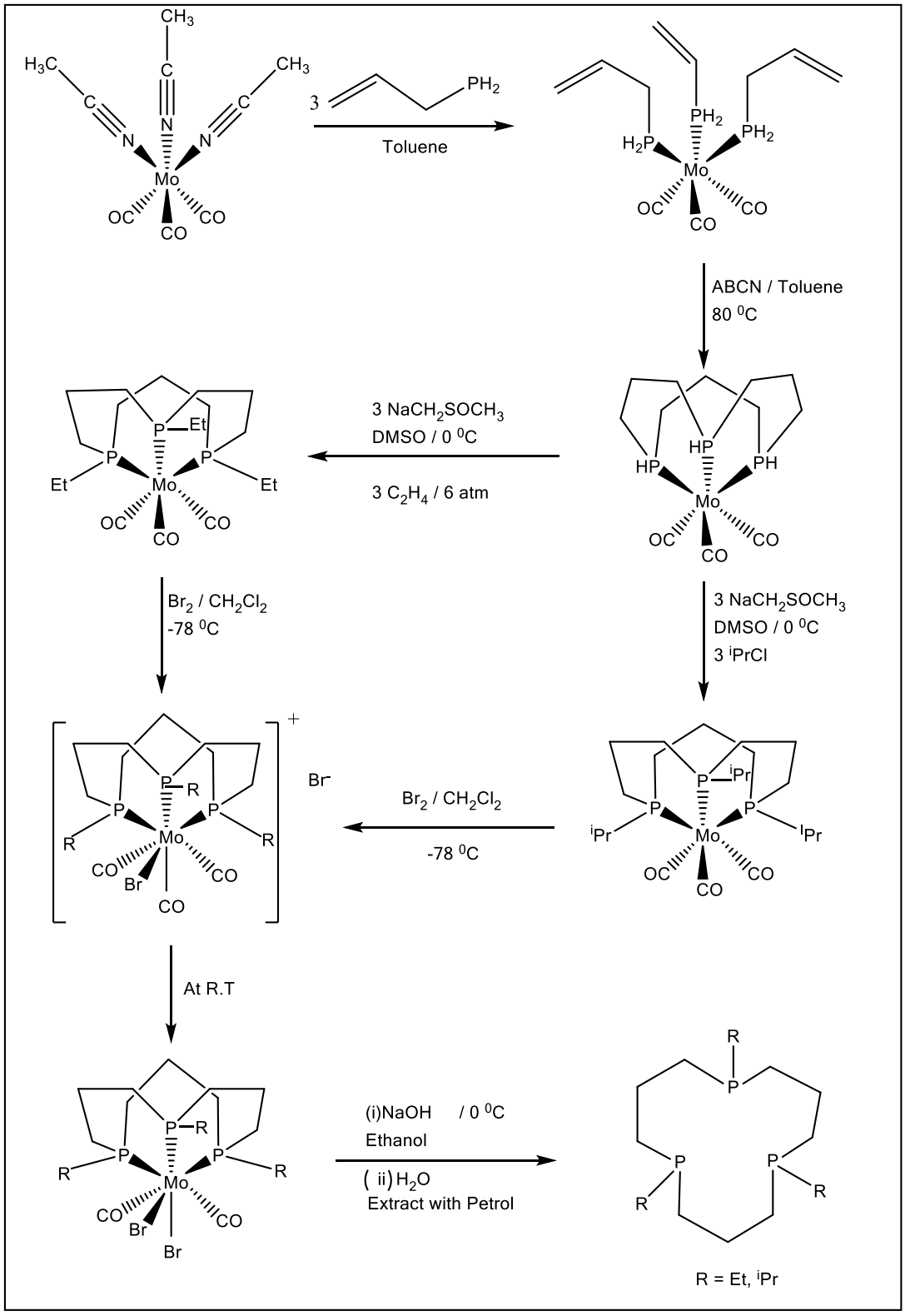

Scheme 2.8: The used synthetic route of [12]-ane-P_3R_3 (R = Et, ^{i}Pr)

2.3.5. New Copper(I) Chemistry

Copper(I) is a highly versatile metal from a coordination standpoint. Its extensive coordinative lability allows copper(I) to play a significant role in many catalytic and stoichiometric processes, including catalytic hydrocarbon functionalization reactions,[25-28] catalytic oxidation reactions,[29-33] and biomimetic dioxygen activation.[34-35] The electronic configuration of copper(I), [Ar] $3d^{10}$ involves a filled 3*d* shell and hence spherical symmetry for the Cu^+ ion. In the solid state the predominant geometry is tetrahedral about four coordinate Cu(I). Understanding and controlling the coordination sphere of a metal ion is often key to developing new reaction chemistry. Several well-defined copper(I) systems have been developed recently using ligands designed to control both steric and electronic factors that dictate reactivity profiles[36]. In contrast to the appearance of copper(I) containing macrocycles of S and N donor atoms, P containing copper macrocycles are rare.

Bimetallic complexes of copper(I) have been reported in the last decade which some complexes (Figure 2.6) having a shorter metal-metal distance than in the metal itself as in $[Cu_2(PhNNNPh)_2]$ (2.23), where the Cu-Cu distance of 2.45 Å is less than in metallic Cu (2.56 Å) and presumably indicates some interaction between the metal atoms[37], whereas in $M_2(form)_2$ (M=CuI; formH = p-$CH_3C_6H_4NCHNHC_6H_4$-p-CH_3) (2.24), which exhibits a metal-metal distance of 2.497(2) Å there is little or no direct metal-metal bonding. Valence shell *s* and *p* orbitals of the metals play a prominent role in metal-ligand bonding but do not provide a basis for metal-metal bonding.[38]

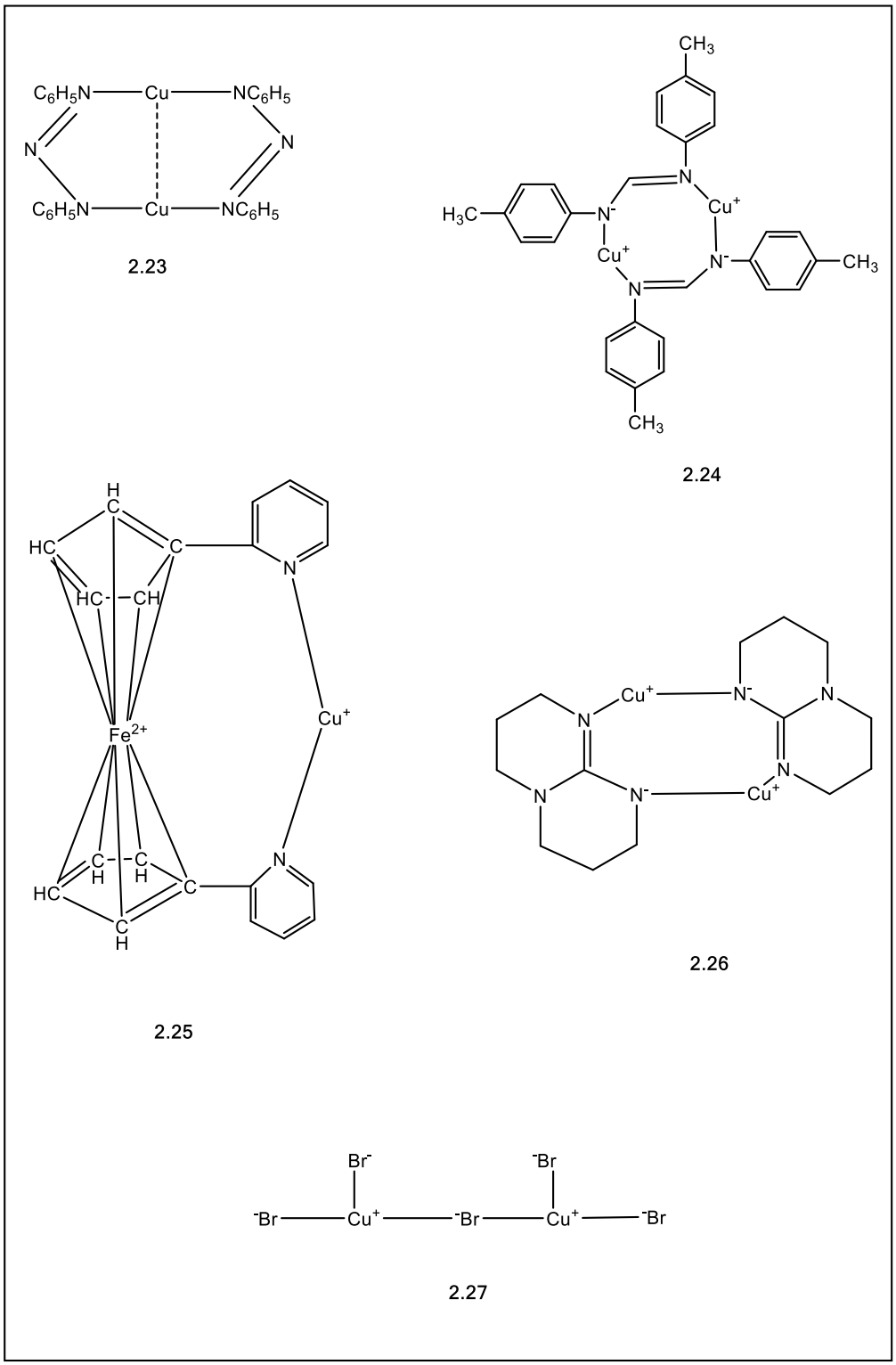

Figure 2.6: Known bimetallic complexes of Copper(I)

Bimetallic copper(I) complexes which exhibit a short Cu-Cu bond with single atom bridging units are much less common than two atom bridging structures. In these few existing complexes the bridging atom can be silicon as in $[Cu_2(Si(SiMe_3)_3)_2BrLi(THF)_3]$[39] , a sulphur atom in $[Cu_2L(CH_3CN)](PF_6)_2$[40] (L= 1,4-$[(EtSCH_2CH_2)_2NCH_2]_2C_6H_4$) or a bromide atom in $[N(CH_3)_4]_3[Cu_2Br_5]$ where the $[Cu_2Br_5]^{3-}$ anion is a discrete, trigonal-planar coordinated species and the bridging bromide ligand is situated on a two-fold axis (2.25).[41]

Equally, ligand unsupported intramolecular interactions with short Cu(I)-Cu(I) complexes are less common, but occur as in recent reported compounds such as $Cu_2(hpp)_2$, where hpp = ($C_7N_3H_{12}$), the anion derived from 1,3,4,6,7,8-hexahydro-2H-pyrimido[1,2-a]pyrimidine.[42] This contains a Cu(I)-Cu(I) unit with a short internuclear distance, 2.453(1) Å and these types of very short Cu(I) to Cu(I) distances can be attributed to a combination of strong Cu-N bonding and very short (~2.2 Å) bite distances for the ligands. Another example is $[Cu_3(2\text{-}(3(5)\text{-}pz)py)_3]_2 \cdot 2py$ featuring two planar pyrazolato-bridged trimetallic cores coupled exclusively via two metal-metal interactions (Cu-Cu = 2.905(3) Å) along one side of the metal triangles.[43] [CuL][$CuCl_2$] where L= 1,1'-bis(2-pyridyl)octamethylferrocene reveals a short Cu(I)-Cu(I) contact of 2.810(2) Å.[44,45]

So far no bimetallic phosphine complexes of copper(I) with a single halide bridge have been reported. In this chapter we discuss the bimetallic copper(I) phosphine complex containing a mono bridging halide and compare them with some copper(I) phosphine clusters.[46-47] In order to explore the potentially interesting chemistry of copper phosphine macrocycle complexes, the coordination chemistry of 1,5,9-triethyl-1,5,9-triphospha cyclododecane[1], [12]-ane-P_3Et_3, (L) with copper(I) halides has been studied.

2.3.5.1. Coordination Chemistry of [12]-ane-P_3Et_3 with Copper(I) halides

2.3.5.1.1. [12]-ane-P_3Et_3 with Copper(I) chloride

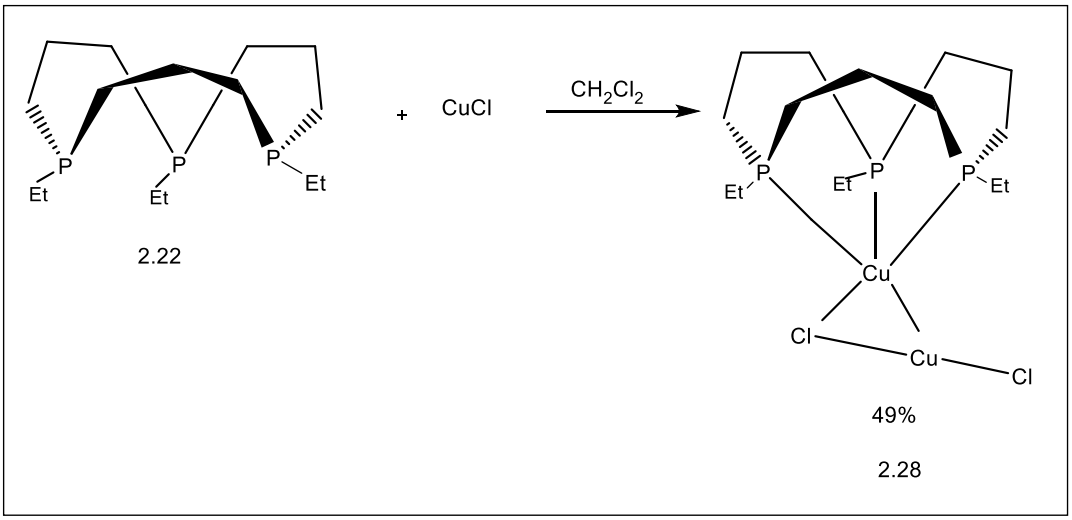

Scheme 2.9: Preparation of (μ-chloro)(η^3 -1,5,9-triethyl-1,5,9-triphosphacyclododecane)copper(I) copper chloride (2.28)

The 1:1 reaction of [12]-ane-$P_3(Et)_3$ (L), with CuCl (Scheme 2.9) in CH_2Cl_2 at room temperature gave rise to [LCu(μ-Cl)(CuCl)] (2.28) with 49% yield. The product is obtained as colourless crystals when recrystallised by slow diffusion of 40/60 petroleum ether into CH_2Cl_2. The crystalline solid was characterised by $^{31}P\{^1H\}$, ^1H and $^{13}C\{^1H\}$ NMR spectroscopy, mass spectrometry, IR spectroscopy and elemental analysis.

The diamagnetic binuclear complex exhibits a broad singlet at δ - 29.91 ppm in its $^{31}P\{^1H\}$ NMR spectrum in $CDCl_3$, shifted 3 ppm downfield compared to the free ligand. The $^{31}P\{^1H\}$ NMR data reported in Table 2.1 are for uncoordinated and copper coordinated triphos complexes for a comparison purpose.[48] The $^{31}P\{^1H\}$ signal of each compound exhibits a shift which is not

significantly different from that of the triphos ligand; accordingly this signal is assigned to the phosphorus atoms of the tripod triphosphane which shows very small Cu(I) coordination shifts as in the above complex 2.28. The broadness of the peak may be due to the ligand lability[49] and/or the electric quadrupole moment of $^{63/65}$Cu nucleus.[50a,b] When cooling to -70 ºC the $^{31}P\{^1H\}$ NMR shows a sharpening of the peak, without a significant shifting.

Compound	δ[a]/ppm
1,1,1-tris(diphenylphosphinomethyl)ethane	-26 (br)
[Cu(triphos)(phenothiazide)]	-30 (br)
[Cu(triphos)(para-thiocresolate)]	-29.2 (br)
[Cu(triphos)(benzotriazolate)]	-26.3 (br)
[Cu(triphos)(diphenylamide)]	-28.4 (br)
[Cu(triphos)(carbazolate)]	-24.6 (br)

Table 2.1: $^{31}P\{^1H\}$ NMR data for triphos compounds; measured in C_6D_6 solution at room temperature. (br = broad)

In the (2.28) ^{1}H NMR spectrum, resonances attributable to the α ($PC\mathit{H_2}$) ring protons fall in the region δ 1.85-1.95 ppm and those assigned to the β ($PCH_2C\mathit{H_2}$) ring protons fall in the region δ 1.50-1.65 ppm, where as the protons of ethyl $PCH_2C\mathit{H_3}$ resonate within the region of δ 1.10-

1.20 ppm and the PCH_2CH_3 hydrogens are observed at δ 1.65-1.70 ppm. In the $^{13}C\{^1H\}$ NMR spectrum, carbons assigned to PCH_2 are observed at δ 29.10 ppm and those due to PCH_2CH_2 are at δ 22.10 ppm while the carbons of ethyl PCH_2CH_3 at δ 20.9 ppm and the PCH_2CH_3 observed at δ 8.11ppm.

Complex 2.28 has also been characterised structurally by X-ray crystallographic methods as shown in Figure 2.7.

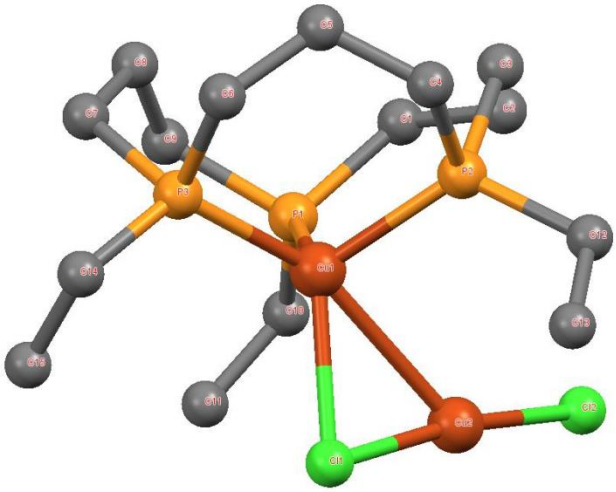

Figure 2.7: Molecular structure of (η^3 -1,5,9-triethyl-1,5,9-triphosphacyclododecane)copper(I) copper chloride, (2.28). For clarity hydrogen atoms have been omitted.

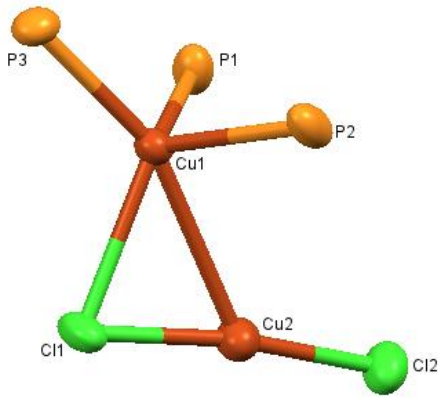

Figure 2.8: A view of the core geometry of 2.28 showing the atom numbering.

Thermal ellipsoids are shown at 50% probability level.

	Bond Lengths / Á		Bond angles / º
P(1)-Cu(1) P(2)-Cu(1) P(3)-Cu(1)	2.2444(10) 2.2441(10) 2.2492(10)	P(2)-Cu(1)-P(1) P(2)-Cu(1)-P(3) P(1)-Cu(1)-P(3)	104.56^0(4) 103.24^0(4) 104.41^0(4)
Cl(1)-Cu(2) Cl(1)-Cu(1) Cl(2)-Cu(2)	2.1368(10) 2.4024 (9) 2.1142(11)	Cu(2)-Cl(1)-Cu(1) Cl(1)-Cu(1)-Cu(2) Cl(1)-Cu(2)-Cu(1)	74.72^0(3) 48.26^0(3) 57.02^0(3)
Cu(1)-Cu(2)	2.7627(6)		

Table 2.2: Selected Bond Lengths and Bond Angles of [LCu(μ-Cl)(CuCl)] (2.28)

This binuclear structure consists of one five coordinate copper atom bonded to the tridentate macrocycle and one η^2 –$CuCl_2^-$ unit with a Cu(1)-Cu(2) distance of 2.7627(6) Å. This Cu-Cu interaction is unique in so far as it is solely supported by a single bridging chloride. The presence of electronegative substituents on a phosphine ligand in a metal complex is known to cause a decrease in the metal-phosphorus bond length compared with that in a corresponding -aryl or alkyl- phosphine complex.[63] This shortening has been ascribed to several different causes, such as lower steric requirements due to a smaller cone angle in fluorophosphines and phosphites, and contraction of the phosphorus lone-pair donor orbital.[64] In contrast to this 2.28, mono bridging copper(I) complex, $[Cu(tricyclohexylphosphine)Cl]_2$,[53] $[CuCl\{bis(diphenylphosphinothioyl)methane\}]_2$[36] and $[Cu(1\text{-}methylimidazoline\text{-}2\text{-}thione)_2Cl]_2$[36] complexes encompass longer Cu(1)-Cu(2) distances of 3.066(6) Å, 2.900(9) Å and 2.914(6) Å with symmetrical dinuclear chloride and sulphide bridges respectively.

The following table (Table 2.2) consists of selected bond lengths of known triphosphorus tripodal ligands for an evaluation purpose of M-P and P-P interactions of some Copper(I) complexes. The data table clearly shows the copper-phosphorus bond lengths in the P_3 macrocyclic complex 2.28 to be intermediate between those observed in complexes 2.32, 2.33, 2.35, 2.36, 2.37 and 2.34 which may be due to the steric contribution imposed by the bulky triphos, phenyl and cyclohexyl groups. However, Cu(1)-Cl(1) distance in 2.28, is significantly longer than the average values of 2.3203 Á in 2.33 and 2.3220 Á in 2.34 centrosymmetric complexes.

In 2.28 the first copper atom lies in a nearly tetrahedral environment, by only considering the three phosphorus atoms of the macrocycle and the Cl(1) atom. The second copper atom has a linear geometry which is quite common for Copper(I) complexes. The two copper atoms are bridged by a chloride with a compressed Cu(2)Cl(1)-Cu(1) angle of 74.72(3) Á, which can be compared with Cu-Cl-Cu angle of 83.4º in 2.34 that has a symmetrical arrangement of single atom bridges with a trigonal planer stereochemistry. The P-Cu-P bond angles of 2.28, lies within 103-104º where as the P(1)-Cu(1)-P(2), P(1)-Cu(1)-Cl(1) and P(2)-Cu(1)-Cl(1) bond angles of 2.33 which are 115.21º(4), 106.44º(4) and 110.82º(4), and its coordination of the Cu(I) ion is best described as distorted tetrahedral.

Complex	Bond lengths / Å	Reference
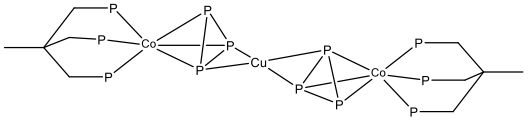 [{(triphos)CoP_3}$_2$Cu]PF_6.2THF 2.32	Cu-P(4) 2.360(2) Cu-P(5) 2.303(2) Cu-P(6) 3.528(2) Cu-P(7) 2.320(2) Cu-P(8) 2.329(2) Cu-P(9) 2.525(2)	51
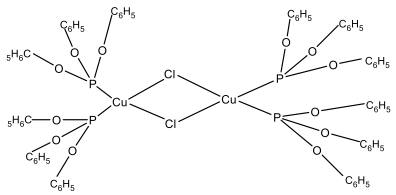 2.33	Cu(1)-Cl(1) 2.3584 (10) Cu(1)-Cl(1) 2.3822 (9) Cu(1)-P(1) 2.2321 (11) Cu(1)-P(2) 2.2420 (11)	52
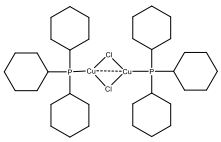 2.34	Cu(1)-Cl(1) 2.322 (4) Cu(1)-P(1) 2.183 (5)	53
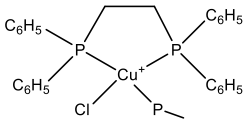 2.35	Cu(1)-Cl(1) 2.312 (4) Cu(1)-P(1) 2.291 (5) Cu(1)-P(2) 2.311 (4) Cu(1)-P(3) 2.284 (6)	54

Table 2.2: Selected interatomic distances of M-P and P-P interactions of some Cu(I) complexes

Complex	Bond lengths / Å	Reference
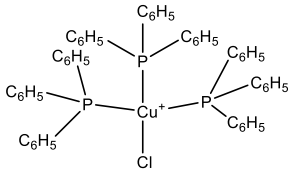 2.36	Cu(1)-Cl(1) 2.336 (4) Cu(1)-P(1) 2.384 (2) Cu(1)-P(2) 2.351 (2) Cu(1)-P(3) 2.355 (2)	55
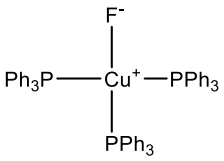 2.37	Cu(1)-F(1) 2.062 (6) Cu(1)-P(1) 2.325 (3) Cu(1)-P(2) 2.310 (3) Cu(1)-P(3) 2.316 (2)	49

Table 2.2: Selected interatomic distances of M-P and P-P interactions of some Cu(I) complexes

2.3.5.1.2. [12]-ane-P_3Et_3 with Copper(I) bromide

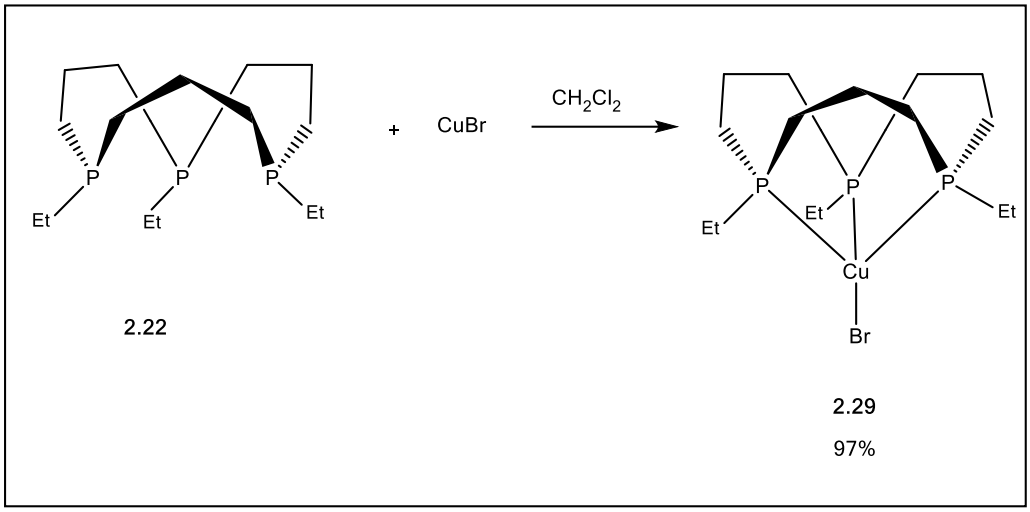

Scheme 2.10: Preparation of (η^3 -1,5,9-triethyl-1,5,9-triphosphacyclododecane)copper(I) bromide, (2.29)

Reacting [12]-ane-P_3Et_3, (L) with CuBr in a 1:1 ratio in CH_2Cl_2 resulted in the near quantitative isolation of 2.29 with 97% yield. Compound 2.29 has also been characterised structurally and analytically.

The complex is diamagnetic and its $^{31}P\{^1H\}$ NMR spectrum shows a broad singlet at δ -28.68ppm which indicates the coordination of the macrocycle to the metal centre. The ^1H NMR spectrum of 2.29 displays resonances at δ 1.93ppm and 1.61ppm which are attributable to the α ($PC\mathit{H_2}$) and β ($PCH_2C\mathit{H_2}$) ring protons respectively. Resonances due to the ethyl substituents are observed at δ 1.10ppm and δ 1.67ppm arising from the methyl and methylene groups correspondingly. The $^{13}C\{^1H\}$ NMR spectrum, shows peaks at δ 28.14ppm and δ 21.76ppm for the carbons of PCH_2 and PCH_2CH_2 , while the resonances assigned to the ethyl groups are found at δ 20.5ppm for PCH_2CH_3 and δ 8.50ppm for the PCH_2CH_3 environments.

The molecular structure determined by single-crystal x-ray techniques is shown in Figure 2.9.

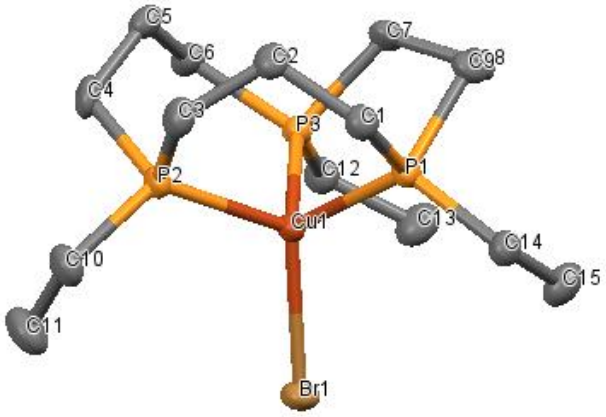

Figure 2.9: Molecular structure of (η^3 -1,5,9-triethyl-1,5,9-triphosphacyclododecane)copper(I) bromide, 2.29.
For clarity, hydrogen atoms have been omitted.

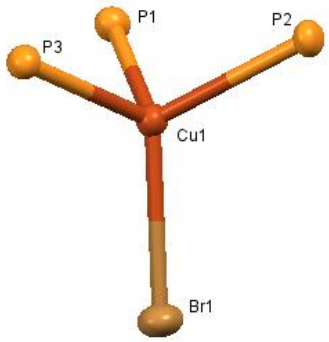

Figure 2.10: A view of the core geometry of 2.29 showing the atom numbering.

Thermal ellipsoids are shown at 50% probability level.

	Bond Lengths / Á		Bond Angles / º
Cu(1)-P(2)	2.2476(17)	P(2)-Cu(1)-P(3)	103.20^0(7)
Cu(1)-P(3)	2.2509(18)	P(2)-Cu(1)-P(1)	102.72^0(7)
Cu(1)-P(1)	2.2521(18)	P(3)-Cu(1)-P(1)	103.64^0(7)
Br(1)-Cu(1)	2.4300(10)	P(2)-Cu(1)-Br(1)	115.77^0(5)
		P(3)-Cu(1)-Br(1)	113.46^0(6)
		P(1)-Cu(1)-Br(1)	116.35^0(6)

Table 2.3: Selected Bond Lengths and Bond Angles of [L(CuBr)], (2.29)

The Cu(1)-Br(1) bond length of 2.4300(10) Á is shorter than that of [L(CuI)] (2.31) and lies between those reported for complexes of 2.39 (2.428(3) Á) and the average value of 2.593 Á in 2.40 (Table 2.4). On the other hand, the obstruction due to the P_3Et_3 ligand induces a significant lengthening of the average Cu-P distance in 2.29 (2.2502 Á) than 2.39 (2.206 Á) and 2.40 (2.228 Á)..

The bromo complex 2.29 has a more regular tetrahedral geometry than the binuclear chloro-complex and all mutually *cis*-donor atoms form significantly more obtuse bond angles than the ideal 109^0 bite angles P(2)-Cu(1)-Br(1) 115.77^0(5), P(3)-Cu(1)-Br(1) 113.46^0(6) and P(1)-Cu(1)-Br(1) 116.35^0(6). This remarkable connection of the macrocyclic bite angles may be a reason for the more regular tetrahedral geometry, as the macrocyclic unit restricts the random arrangement of the phosphorus units around the central metal atom. Similarly in 2.39[57] the

metal atom is tetrahedrally coordinated to 2,2´-bipyridine with a bond angle of 117.0(2)º. When these structures compared with 2.40,[58] the most important structural parameter observed is the steric repulsion of the phosphine aryl groups with those of the adjacent phosphines and with the nearby halogens. This concludes with the increase size of the phosphine groups it undergoes large distortions with less acute bond angles as in 2.40 resulting a distorted tetrahedral environment.

Complex	Bond distances/Á	Bond Angles/º
$CuBr(C_{10}H_8N_2)\{P(C_6H_5)_3\}]$	Cu(1)-Br(1) 2.428(3)	N(1)-Cu(1)-Br(1) 115.2(3)
(2.39)	Cu(1)-P(1) 2.206 (4)	N(2)-Cu(1)-Br(1) 108.8(4)
		N(1)-Cu(1)-P(1) 116.2(4)
		N(2)-Cu(1)-P(1) 114.8(4)
		Br(1)-Cu(1)-P(1) 117.0(2)
$CuBrP(t\text{-}Bu)_3$	Cu(1)-Br(1) 2.593	Br(1)-Cu(1)-Br(1) 95.3
(2.40)	Cu(1)-P(1) 2.228	Br(1)-Cu(1)-Br(1) 84.5

Table 2.4: Selected bond lengths (Á) and angles(º) for comparison purpose

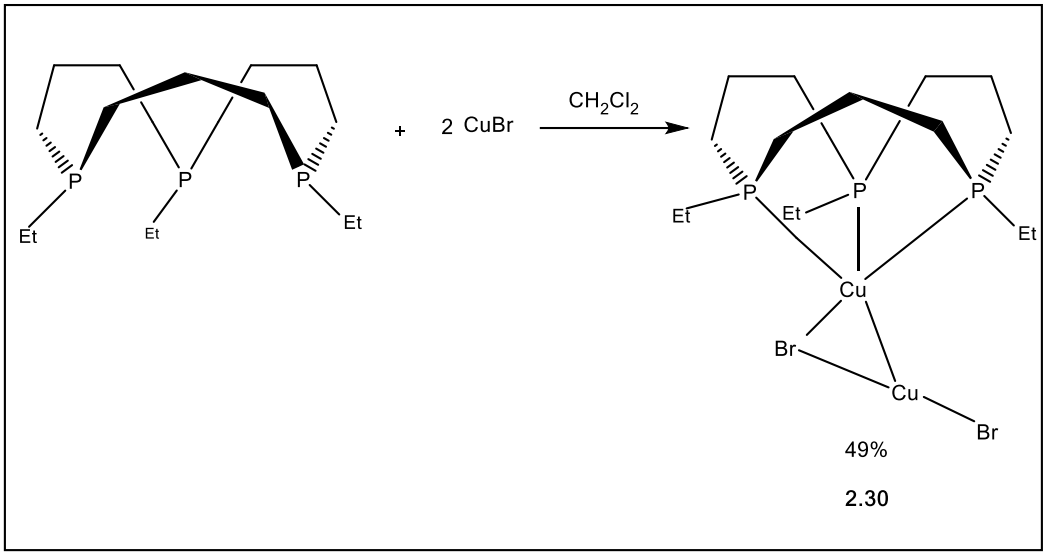

Scheme 2.11: Preparation of (μ-bromo) fac-(η^3 -1,5,9-triethyl-1,5,9-triphosphacyclododecane)copper(I) copper bromide (2.30)

Reaction of 1 equivalent of [12]-aneP_3Et_3, with 2 equivalents of CuBr in CH_2Cl_2 at room temperature gave [LCu(μ-Br)CuBr] (2.30) in 49% yield. Complex 2.30 was characterised by $^{31}P\{^1H\}$, ^1H and $^{13}C\{^1H\}$ NMR spectroscopy, mass spectrometry and IR spectroscopy as well as structurally and analytically.

This binuclear complex is diamagnetic and exhibits a broad singlet at δ – 28.14ppm in the $^{31}P\{^1H\}$ NMR spectrum in $CDCl_3$, shifted 4ppm downfield compared to the free ligand. Due to the broadness of the signal, a low temperature NMR study was performed and a sharpening of the signal was observed without a significant shifting at -70^0C. The characteristic resonances in ^1H NMR spectrum for α (PCH_2) ring protons fall at δ 1.85ppm and the β (PCH_2CH_2) ring protons fall at δ 1.58ppm. The protons of ethyl PCH_2CH_3 fall at δ 1.16ppm and the PCH_2CH_3 observed at δ 1.65ppm. The $^{13}C\{^1H\}$ NMR spectrum consists of four resonances assignable to the four

different carbon environments as; PCH_2 at δ 29.69 ppm, PCH_2CH_2 at δ 21.44 ppm, PCH_2CH_3 at δ 22.28 ppm and PCH_2CH_3 at δ 8.54 ppm.

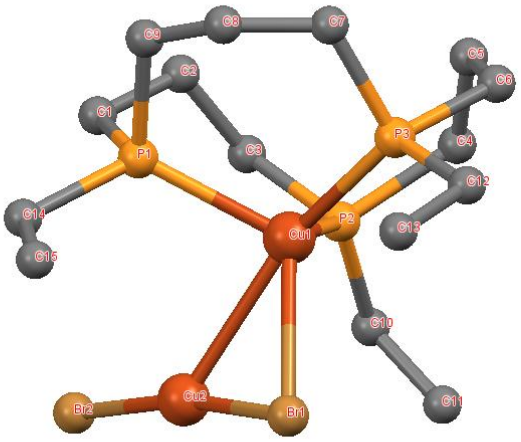

Figure 2.11: Molecular structure of (η^3 -1,5,9-triethyl-1,5,9-triphosphacyclododecane)copper(I) copper bromide, 2.30. For clarity, the hydrogen atoms have been omitted for clarity.

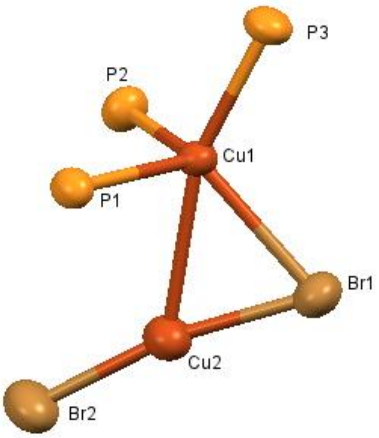

Figure 2.12: A view of the core geometry of 2.30 showing the atom numbering.

Thermal ellipsoids are shown at 50% probability level.

	Bond Lengths / Á		Bond Angles / º
Cu(1)-P(3) Cu(1)-P(1) Cu(1)-P(2)	2.2397(13) 2.2536(13) 2.2560(14)	P(3)-Cu(1)-P(1) P(3)-Cu(1)-P(2) P(1)-Cu(1)-P(2)	105.02^0(5) 104.29^0(6) 104.04^0(5)
Cu(1)-Br(1) Cu(2)-Br(2) Cu(2)-Br(1)	2.5265(8) 2.2337(10) 2.2598(10)	Cu(2)-Br(1)-Cu(1) Br(1)-Cu(1)-Cu(2) Br(1)-Cu(2)-Cu(1)	67.78^0(3) 51.37^0(3) 60.85^0(3)
Cu(1)-Cu(2)	2.6779(10)		

Table 2.5: Selected Bond lengths and bond angles of [LCu(μ-Br)CuBr], (2.30)

This bimetallic complex (2.30), shows a significant distorted tetrahedral geometry around the first copper atom with a unique mono bridging bromide atom. In the structures of 2.28 and 2.30 determined by X-ray crystallographic analysis, the two copper atoms are bridged by either a chloride or a bromide atom and the Cu(1)-Br(1)-Cu(2) angle 67.78^0(3) is more acute than the Cu(1)-Cl(1)-Cu(2) 74.72^0(3) angle. This coincides with a shorter Cu(1)-Cu(2) distance of 2.6779(10) Á for Br compared to 2.7627(6) Á for Cl, which points to a Cu-Cu interaction. The average Cu-Br (2.340 Á), Cu-P (2.2464 Á) and Cu-Cu (2.6779(10) bond lengths are significantly shorter than the average values of 2.404 Á, 2.569 Á and 2.992 Á found in

$[Cu_2(triphenylphosphine)_3Br_2]$[59]. Similarly in this two-atom bridging complex the Cu-Br-Cu angle is more acute (71.9º) than the complex 2.30 and continued a mixed trigonal/tetrahedral stereochemistry around each copper atom.

2.3.5.1.3. [12]-ane-P_3Et_3 with Copper(I) iodide

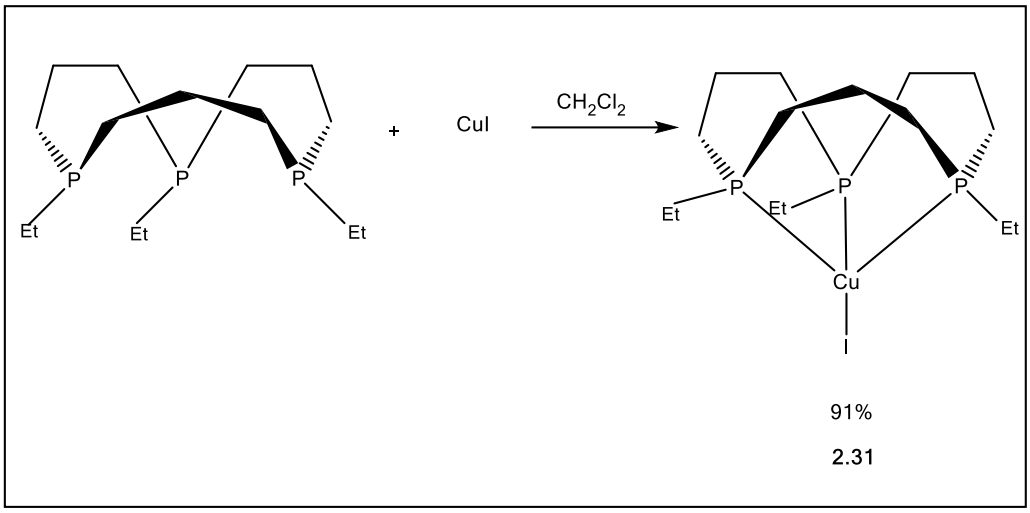

Scheme 2.12: Preparation of (η^3 -1,5,9-triethyl-1,5,9-triphosphacyclododecane)copper(I) iodide, (2.31)

The reaction of [12]-aneP_3Et_3 (L), with CuI in CH_2Cl_2 gave the [LCuI] (2.31) monomer with 91% yield. The resulting diamagnetic complex shows a broad singlet at δ -29.29ppm in $^{31}P\{^1H\}$ NMR spectrum indicating the coordination of the macrocycle to the metal centre. The ^1H NMR spectrum and the $^{13}C\{^1H\}$ NMR spectrum (In experimental section), consist of resonances assignable to four different hydrogen and carbon environments that are closely analogous to the spectra observed for complex 2.28.

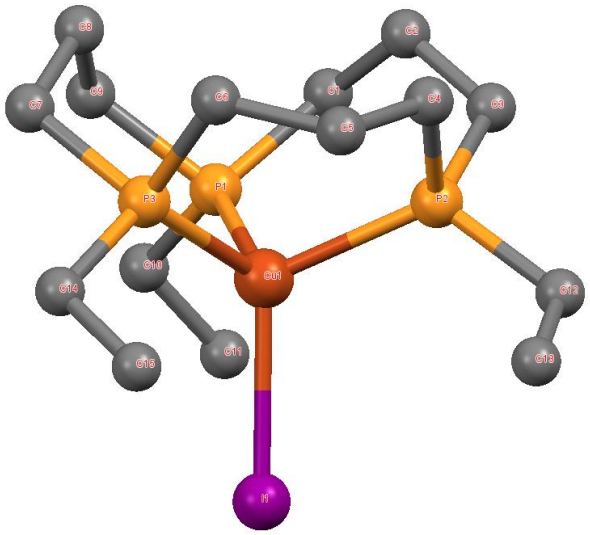

Figure 2.13: Molecular structure of (η^3 -1,5,9-triethyl-1,5,9-triphosphacyclododecane)copper(I) iodide, 2.31. For clarity, hydrogen atoms have been omitted.

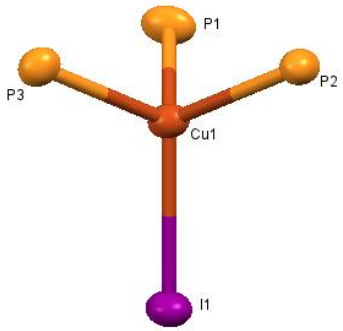

Figure 2.14: A view of the core geometry of 2.31 showing the atom numbering.

Thermal ellipsoids are shown at 50% probability level.

	Bond Lengths / Á		Bond Angles / º
P(1)-Cu(1) P(2)-Cu(1) P(3)-Cu(1)	2.243(2) 2.253(10) 2.233(11)	P(3)-Cu(1)-P(1) P(3)-Cu(1)-P(2) P(1)-Cu(1)-P(2)	103.3^0(4) 104.26^0(8) 103.4^0(4)
Cu(1)-I(1)	2.5944(10)	P(3)-Cu(1)-I(1) P(1)-Cu(1)-I(1) P(2)-Cu(1)-I(1)	114.8^0(3) 115.15^0(7) 114.4^0(3)

Table 2.6: Selected Bond Lengths and Bond Angles of [L(CuI)], (2.31)

The X-ray crystal structure of 2.31 shows a tetrahedral geometry around the copper atom with almost no distortions with the bond angles that range from 103-104º for P-Cu-P and 114-115º for P-Cu-I. The Cu(1)-I(1) bond distance 2.5944 (10) Á is longer than the [L(CuBr)] (2.29) as expected from the relative covalent radii of the halogens. Also the donor atoms form considerably less obtuse bond angles than the expected 109^0 in an idealised tetrahedral geometry.

The Cu-I bond length of complex 2.31(2.5944 Á) is intermediate between those in the binuclear bridging iodide complexes [Cu(N,N´-diisopropylethynediamne)I_2][60] (2.661 Á) and [Cu_2I_2(dimethylaminophenyldimethylarsine)$_2$][61] (2.53 Á).

2.3.5.1.4. [12]-ane-$P_3{}^iPr_3$ with Copper(I) halides

As same as the [12]-ane-P_3Et_3 coordination chemistry with Cu(I) chloride, [12]-ane-$P_3{}^iPr_3$ coordination chemistry with Cu(I) chloride results in the formation of a bimetallic, diamagnetic complex of {[12]-ane-$P_3(^iPr)_3$}Cu(μ-Cl)CuCl (2.41), with a significantly distorted tetrahedral geometry in a similar fashion[62]. Geometrically, there is no clear significant difference between the ethyl and isopropyl substituted macrocyclic complexes but, spacially there is a clear difference between them. The isopropyl substituted macrocyclic unit of the copper complex has a much shorter Cu(1)-Cu(2) bond length of 2.7001(8) Å than that of the ethyl analogue.

In contrast to the ethyl substituted bromo complexes 2.29 and 2.30, only a mononuclear structure {[12]-ane-$P_3(^iPr)_3$}CuBr (2.42) is observed in the isopropyl substituted analogue. This difference may be a clear indication of the influence of P-substituents, where the bulky isopropyl groups destabilise the bridging arrangement of the larger Br^-.

There is no notable geometrical and special difference in the ethyl and isopropyl substituted macrocyclic complexes of ([12]-ane-P_3R_3)CuI (2.43).

Complex	Cu-P bond length /Å	Cu-X bond length /Å
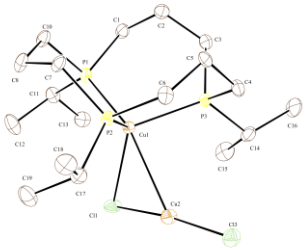 2.41	P(1) = 2.2383(13) P(2) = 2.2471(14) P(3) = 2.2416(14)	Cu(1)-Cl(1) = 2.4002(14) Cu(2)-Cl(1) = 2.1359(14) Cu(2)-Cl(3) = 2.1071(14)
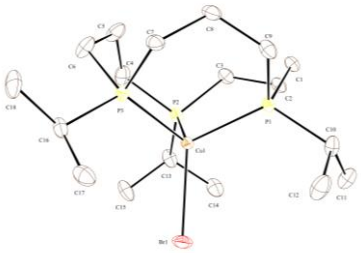 2.42	P(1) = 2.2483(7) P(2) = 2.2477(7) P(3) = 2.2592(7)	2.4410(4)
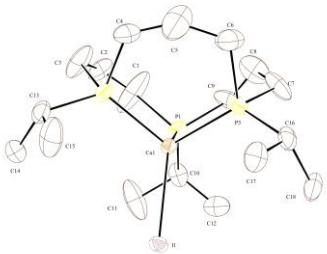 2.43	P(1) = 2.248(2) P(2) = 2.250(2) P(3) = 2.241(2)	2.5881(9)

Table 2.7: Selected interatomic distances (Å) of M-P and M- X of complexes of 2.41, 2.42 and 2.43

R = - CH_2CH_3

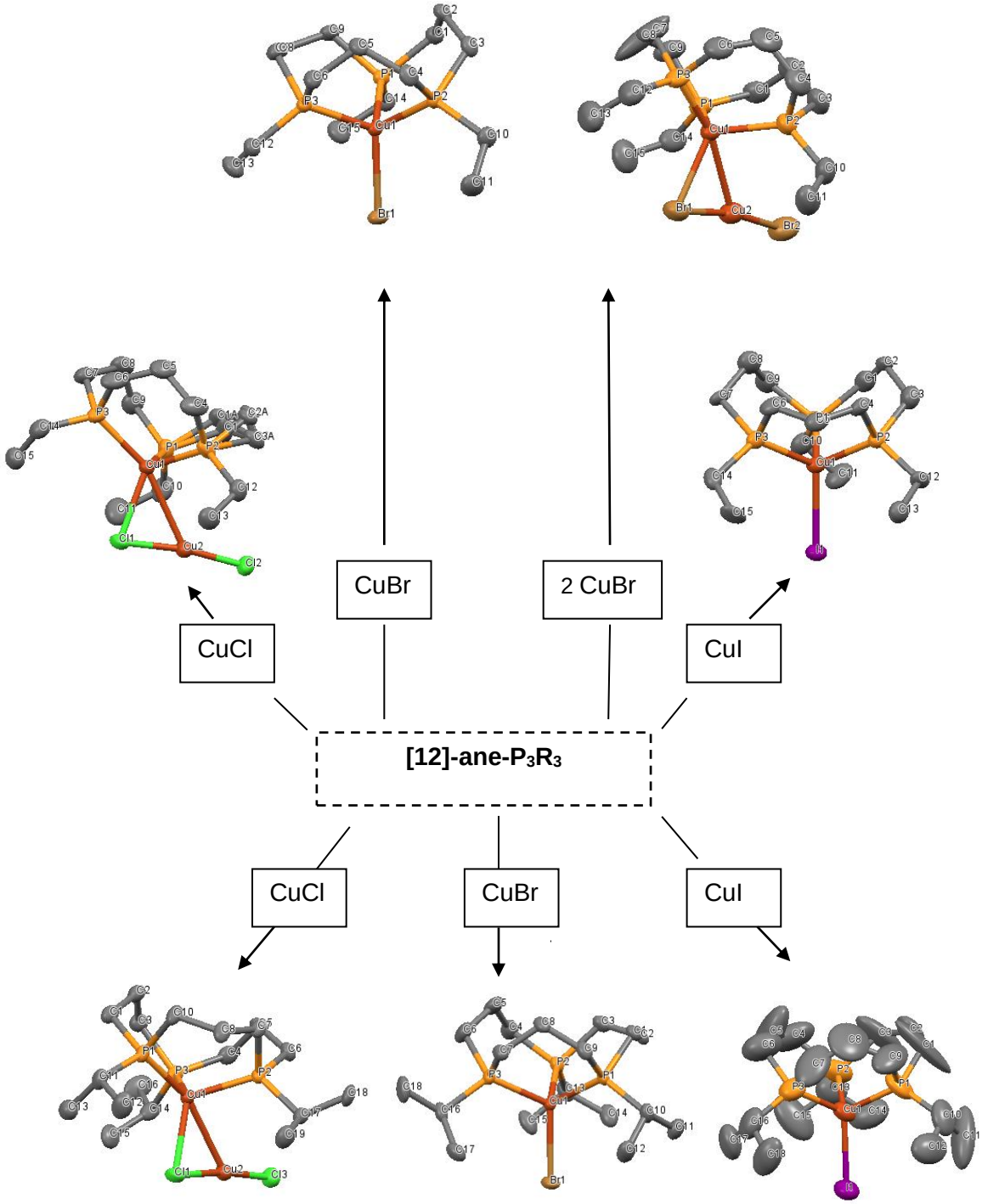

R = -CH-CH_3
|
CH_3

2.4. Conclusion

This study furnishes experimental evidence of [12]-ane-P_3Et_3 reactions with Copper(I) to support the existence of attractive Cu-Cu interactions in closed-shell d^{10} coordination compounds in which the macrocycle acts as a tridentate tris(phosphine) forming complexes with four coordinate tetrahedral geometries, or more heavily distorted five coordinate geometries with chloride and bromide mono bridging atoms. These diamagnetic compounds are restricted to a mutually *cis*-coordination environment.

The reaction of 12[ane]P_3Et_3 with copper(I) chloride gives rise to a bimetallic complex [$L(CuCl)_2$] (2.28), which has been fully characterised. It shows a significantly distorted tetrahedral geometry around the first copper atom with a mono bridging chlorine atom which is unique. The same reaction with copper(I) bromide affords the monomer [L(CuBr)] (2.29), with a 1:1 molar ratio showing a tetrahedral geometry, whereas a same type of bimetallic compound [$L(CuBr)_2$] (2.30), results with a 1:2 molar ratio showing a shortening of the Cu-Cu distance in the X-ray structure. The reaction with copper(I) iodide results in the monomer [L(CuI)] (2.31), illustrating a tetrahedral geometry for the copper atom with almost no distortion in the X-ray structure.

2.5. Experimental

2.5.1. General

Techniques and Instruments*:* All reactions were carried out in an atmosphere of dry argon. All solvents were dried by boiling under reflux over standard drying agents. The compounds allylphosphine[15] and *syn,syn*-1,5,9-triethyl-1,5,9-triphosphacyclododecane, [12]-ane-$P_3(Et)_3$ were prepared by literature methods.[19,20] All other reagents including Copper starting materials were obtained from the Aldrich Chemical Company and, where appropriate, were degassed before use. The NMR spectra were recorded on a Bruker DPX-500 instrument at 500 MHz (^{1}H), and 125.75MHz (^{13}C), Bruker DPX-400 instrument at 400 MHz and 100 MHz (^{13}C), Jeol Lamda Eclipse 300 at 121.65 MHz (^{31}P), 75.57 MHz (^{13}C). ^{1}H and ^{13}C chemical shifts are quoted in ppm relative to residual solvent peaks, and ^{31}P NMR chemical shifts quoted in ppm (δ) relative to 85% external H_3PO_4 (δ = 0ppm). The infra-red spectra were recorded on a Perkin Elmer 1600 or a Nicolet 510 FT-IR spectrometer and the samples were prepared under Argon atmosphere as a KBr disk. Mass spectra of all the samples have been measured by direct injection into a Waters Low Resolution ZQ Mass Spectrometer fitted with ESCI source. Elemental analysis was performed by London Metropolitan University Analytical Service.

X-Ray Crystallography*:* Data collections were carried out on a Bruker Kappa CCD diffractometer at 150(2) K with Mo $K\alpha$ irradiation (graphite monochromator). Empirical absorption corrections were performed using equivalent reflections. For the solution and refinement of the structures, the program package SHELXL 97 was employed. H atoms were placed into calculated positions and included in the last cycles of refinement.

2.5.2. Preparation of (μ-chloro)(η^3 -1,5,9-triethyl-1,5,9- triphosphacyclododecane) copper (I) copper chloride, 2.28

To a solution of [12]-ane-$P_3(Et)_3$ (0.49 mmol, 150 mg) dissolved in dichloromethane(15 ml) was added CuCl (0.49 mmol, 50 mg) in dichloromethane(15 ml) at room temperature. The solution was stirred for 3 hrs, during the time of the copper chloride dissolved. The colourless solution was then evaporated to give a white solid that was recrystallised by slow diffusion of 40/60 petroleum ether in to a CH_2Cl_2 solution of the complex to give **2.28** as white air-sensitive needles (0.247 mmol, 126 mg, 49.0%), Analysis found (calculated): C, 35.20 (35.72); H, 6.60 (6.59). MS(ES), *m/z*: 501.98 [46%, (M^+)]. NMR ($CDCl_3$): $^{31}P\{^1H\}$, δ -29.91 ppm. ^1H NMR (360 MHz, 27 ºC), δ (ppm): 1.88 (br m, PC*H*$_2$); 1.50 (br m, PC*H*$_2$C*H*$_2$); 1.68 (br m, PC*H*$_2$$CH_3$); 1.22 (br m, PCH_2C*H*$_3$). $^{13}C\{^1H\}$ NMR (90 MHz, 27 ºC), δ (ppm): 29.10 (dd, $^1J_{P\text{-}C}$ 17 Hz, $^3J_{P\text{-}C}$ 8 Hz, P*C*H_2); 22.10 (br s, PCH_2*C*H_2); 20.9 (d, $^1J_{P\text{-}C,}$ 10 Hz, P*C*H_2CH_3); 8.11 (br s, PCH_2*C*H_3). IR/cm^{-1}(KBr): 2968 s, 2902 s, 2843 m, 1451 m, 1420 m, 1380 m, 1255 s, 360 w, 703 m.

2.5.3. Preparation of (η^3 -1,5,9-triethyl-1,5,9- triphosphacyclododecane) copper(I) bromide, 2.29

To a solution of [12]-ane-$P_3(Et)_3$ (0.40 mmol, 122 mg) dissolved in dichloromethane(10 ml) was added CuBr (0.40 mmol, 48 mg) in dichloromethane(10 ml) at room temperature. The solution was stirred for 3 hrs, during the time of the copper bromide dissolved. The colourless solution was then evaporated to give a white solid that was recrystallised by slow diffusion of 40/60 petroleum ether in to a CH_2Cl_2 solution of the complex to give **2.29** as white air-sensitive

needles (0.32 mmol, 94 mg, 97.0%), Analysis found (calculated): C, 40.01 (40.08); H, 7.29 (7.40). MS(ES), *m/z*: 369.1094 (100%, $[M\text{-}Br]^+$), resolution mass spec actual (calc. mass): 369.1094 (369.1091). NMR ($CDCl_3$): $^{31}P\{^1H\}$, δ -28.68 ppm. ^1H NMR (360 MHz, 27 ºC), δ (ppm): 1.93 (br m, PCH_2); 1.61 (br m, PCH_2CH_2); 1.67 (br m, PCH_2CH_3); 1.10 (br m, PCH_2CH_3). $^{13}C\{^1H\}$ NMR (90 MHz, 27 ºC), δ (ppm): 28.14 (dd, $^1J_{P\text{-}C}$ 16 Hz, $^3J_{P\text{-}C}$ 10 Hz, PCH_2); 21.76 (br s, PCH_2CH_2); 20.5 (d, $^1J_{P\text{-}C,}$ 8 Hz, PCH_2CH_3); 8.50 (br s, PCH_2CH_3). IR/cm^{-1}(KBr): 2968 s, 2902 s, 2843 m, 1451 m, 1420 m, 1380 m, 1255 s, 360 w, 667 m.

2.5.4. Preparation of (μ-bromo) (η^3-1,5,9-triethyl-1,5,9-triphosphacyclododecane) copper(I) copper bromide, 2.30

To a solution of [12]-ane-$P_3(Et)_3$ (0.40 mmol, 122 mg) dissolved in dichloromethane(10 ml) was added CuCl (0.80 mmol, 96 mg) in dichloromethane(10 ml) at room temperature. The solution was stirred for 3 hrs, during the time of the copper bromide dissolved. The colourless solution was then evaporated to give a white solid that was recrystallised by slow diffusion of 40/60 petroleum ether in to a CH_2Cl_2 solution of the complex to give **2.30** as white air-sensitive needles (0.392 mmol, 96 mg, 49.0%), Analysis found (calculated): C, 30.22 (30.37); H, 5.43 (5.61). MS(ES), *m/z*: 369.1092 (100%, $[M\text{-}CuBr_2]^+$), resolution mass spec actual (calc. mass): 369.1092 (369.1091). NMR ($CDCl_3$): $^{31}P\{^1H\}$, δ -28.14 ppm. ^1H NMR (360 MHz, 27 ºC), δ (ppm): 1.85 (br m, PCH_2); 1.58 (br m, PCH_2CH_2); 1.65 (br m, PCH_2CH_3); 1.16 (br m, PCH_2CH_3). $^{13}C\{^1H\}$ NMR (90 MHz, 27 ºC), δ (ppm): 29.69 (dd, $^1J_{P\text{-}C}$ 16 Hz, $^3J_{P\text{-}C}$ 10 Hz, PCH_2); 21.44 (br s, PCH_2CH_2); 22.28 (d, $^1J_{P\text{-}C,}$ 8 Hz, PCH_2CH_3); 8.54 (br s, PCH_2CH_3). IR/cm^{-1}(KBr): 2968 s, 2902 s, 2843 m, 1451 m, 1420 m, 1380 m, 1255 s, 360 w, 667 m.

2.5.5. Preparation of (η^3 -1,5,9-triethyl-1,5,9-triphosphacyclododecane) copper(I) iodide, 2.31

To a solution of [12]-ane-$P_3(Et)_3$ (0.40 mmol, 122 mg) dissolved in dichloromethane(10 ml) was added CuCl (0.40 mmol, 76 mg) in dichloromethane(10 ml) at room temperature. The solution was stirred for 3 hrs, during the time of the copper iodide dissolved. The colourless solution was then evaporated to give a white solid that was recrystallised by slow diffusion of 40/60 petroleum ether in to a CH_2Cl_2 solution of the complex to give **2.31** as white air-sensitive needles (0.356 mmol, 178 mg, 98.0%), Analysis found (calculated): C, 36.40 (36.26); H, 6.71 (6.69). MS(ES), *m/z*: 369.1103 (100%, $[M-I]^+$), resolution mass spec actual (calc. mass): 369.1103 (369.1091). NMR ($CDCl_3$): $^{31}P\{^1H\}$, δ -29.29 ppm. ^1H NMR (360 MHz, 27 ºC), δ (ppm): 1.87 (br m, PCH_2); 1.65 (br m, PCH_2CH_2); 1.67 (br m, PCH_2CH_3); 1.20 (br m, PCH_2CH_3). $^{13}C\{^1H\}$ NMR (90 MHz, 27 ºC), δ (ppm): 28.43 (dd, $^1J_{P-C}$ 17 Hz, $^3J_{P-C}$ 8 Hz, PCH_2); 22.80 (br s, PCH_2CH_2); 20.60 (d, $^1J_{P-C,}$ 10 Hz , PCH_2CH_3); 8.37 (br s, PCH_2CH_3). IR/cm^{-1}(KBr): 2968 s, 2902 s, 2843 m, 1451 m, 1420 m, 1380 m, 1255 s, 360 w, 480 m.

2.6. References

1. Ed. Bruce, D. W., O'Hare, D., *Inorganic Materials*, 2nd Edition, John Wiley & Sons, New York, 1996.

2. (a) Baker, R. J., Davies, P. C., Edwards, P. G., Farley, R. D., Liyanage, S. S., Murphy,D. M., Yong, B., *Eur. J. Inorg. Chem*., 2002, 1975-1984. (b) Baker, R. J., Edwards, P. G., *J. Chem. Soc., Dalton Trans.*, 2002, 2960-2965.

3. Wei, L., Padmaja, K., Youngblood, W. J., Lysenko, A. B., Lindsey, J. S., Bocian, D. F., *J. Org. Chem.,* 2004, 69, 1461.

4. Wilkinson, G., *The Synthesis, Reaction, Properties and Applications of Coordinated Compounds,* Vol. 1, Pergamon, Oxford, 1987.

5. Kim, S. G., Kim, K. H., Jung, J., Shin, S. K., Ahn, K. H., *J. Am. Chem. Soc.* 2002, 124, 591.

6. Kaim, W., Titze, C., Schurr, T., Sieger, M., Lawson, M., Jordanov, J., Rojas, D., Gracia, A. M., Manzur, J., *Z. Anorg. Allg. Chem.,* 2005, 631, 2568.

7. Mayer, H. A., Otto, H., Kuhbauch, H., Fawzi, R., Steimann, M., *J. Organomet. Chem.,* 1994, 432, 347.

8. Bianchini, C., Meli, A., Peruzzini, M., Vizz, F., Zanobini, F., *Coord. Chem. Rev.,* 1992, 120, 193.

9. Cotton, F. A., Hong, B., *Prog. Inorg. Chem.,* 1992, 40, 179.

10. Mayer, H. A., Kaska, W. C., *Che. Rev.,* 1994, 40,179.

11. Meek, D. W., *Homogeneous Catalysis with Metal Phosphine Complexes,* ed. Pignolet, L. H., Plenum, New York, 1983, pp.257.

12. McAuliffe, C. A., *Comprehensive Coodination Chemistry*, Vol. 2, Perganon Prerss, Oxford, 1987, p. 989.

13. Levason, W., Reid, G., *Comprehensive Coordination. Chemistry II*, 2004, 1, pp. 475-484.

14. Stelzer, O., Langhans, K. P., *The Chemistry of Organophosphorus Compounds*, ed. Hartley, F. R., Wiley, New York, 1990, vol 1. Ch8, pp.192-254.

15. (6) Kyba, E. P., John, A. M., Brown, S. B., Hudson, C. W., McPhaul, M. J., Harding, A., Larsen, K., Niedzwiecki, S., Davis, R. E., *J. Am. Chem. Soc*., 1980, 102, 139

16. Diel, B. N., Haltiwanger, R. C., Norman, A. D., *J. Am. Chem. Soc.* 1982, *104*, 4700-4701.

17. Diel, B. N., Brandt, P. F., Haltiwanger, R. C., Hackney, M. L. J., Norman, A. D., *Inorg. Chem.,* 1989, *28*, 2811-2816.

18. Coles, S. J., Edwards, P. G., Fleming, J. S., Hursthouse, M. B., *J. Chem. Soc., Dalton Trans.* 1995, 1139.

19. Edwards, P. G., Fleming, J. S., Liyanage, S. S., Coles, S. J., Hursthouse, M. B., *J. Chem. Soc., Dalton Trans.* 1996, 1801.

20. Edwards, P. G., Fleming, J. S., Liyanage, S. S., *J. Chem. Soc., Dalton Trans.* 1997, 193-198.

21. Edwards, P. G., Whatton, M. L., Haigh, R., *Organometallics,* 2000, 19, 2652.

22. Edwards, P. G., Newman, P. D., Malik, K. M. A., *Angew. Chem. Int. Ed.,*2000, 39, 2922.

23. Treichel, P. M., Wong, W. K., *Inorg. Chim. Acta.,*1979, 33, 171.

24. Coles, S. J., Edwards, P. G., Fleming, J. S., Hursthouse, M. B., Liyanage, S.S., *Chem. Commun.,*1996, 293-294.

25. Ley, S. V., Thomas, A. W., *Angew. Chem., Int. Ed*. 2003, 42, 5400-5449.

26. Caballero, A., Diaz-Rodriguez, M. M., Belderrain, T. R., Nicasio, M. C., Trofimenko, S., Perez, P. J., *J. Am. Chem. Soc*. 2003, 125, 1446-1447.

27. Kirmse, W., *Angew. Chem., Int. Ed.* 2003, 42, 1088-1093.

28. Müller, P., Fruit, C., *Chem. Rev*. 2003, 103, 2905-2919.

29. Rovis, T.; Evans, D. A. Prog. Inorg. Chem. 2001, 50, 1-150.

30. Marko, I. E., Gautier, A., Dumeunier, R., Doda, K., Philippart, F., Brown, S. M., Urch, C., *J. Angew. Chem., Int. Ed*. 2004, 43, 1588-1591.

31. Lipshutz, B. H., Noson, K., Chrisman, W., Lower, A., *J. Am. Chem. Soc*. 2003, 125, 8779-8789.

32. Gao, J., Reibenspies, J. H., Martell, A. E., *Angew. Chem., Int. Ed*. 2003, 42, 6008-6012.

33. Gamez, P., Aubel, P. G., Driessen, W., Reedijk, L., *J. Chem. Soc. Rev*. 2001, 30, 376-385. 270.

34. Lewis, E. A., Tolman, W. B., *Chem. Rev*. 2004, 104, 1047-1076.

35. (a) Kim, E., Chufan, E. E., Kamaraj, K., Karlin, K. D., *Chem. Rev*. 2004, 104, 1077-1133.

(b) Mirica, L. M., Vance, M., Rudd, D. J., Hedman, B., Hodgson, K. O., Solomon, E. I., Stack, T. D. P., *J. Am. Chem. Soc.* 2002, 124, 9332-9333.

36. Wilkinson, G., ed., *Comprehensive Coordination Chemistry,* vol.5, Pergamon Press, Oxford, 1987, pp. 538-542

37. Wells, A. F., *Structural Inorganic Chemistry,* 4th ed., Clarendon Press, Oxford, 1975, pp. 879 – 881.

38. Cotton, F. A., Feng, X., Matusz, M., Poli, R., *J. Am. Chem. Soc.,* 1988, 110, 21, 7077-7083.

39. Heine, A., Herbst-Irmer, R., Stalke, D.,*J. Chem. Soc., Chem. Commun.,*1993, 23, 1729-1731.

40. Karlin, K. D., Hyde, J. R., Zubieta, J., *Inorg. Chim. Acta,* 1982, 66, 1, L23-L24.

41. Asplund, M., Jagner, S., *Acta. Chem. Scand.,* 1985, A39(1), 47-51.

42. Cotton, F. A., Feng, X., Timmons, D. J., *Inorganic Chemistry* (1998), 37(16), 4066-4069.

43. Singh, K., L., Jeffrey R., Stavropoulos, P., J. Am. Chem. Soc., 1997, 119(12), 2942-2943.

44. Siemeling, U., Vorfeld, U., Neumann, B., Stammler, H. G., Chem. *Commun. (Cambridge)*, 1997, 18, 1723-1724.

45. Poblet, Josep-M., Benard, M., *Chem. Commun. (Cambridge),* 1998, 11, 1179-1180.

46. Driess, M., Martin, S., Merz, K., Pintchouk, V., Pritzkow, H., Grutzmacher, H., Kaupp, M., *Angew. Chem. Int. Ed. Engl.,* 1997, 36(17), 1894-1896.

47. Driess, M., Faulhaber, M., Pritzkow, H., *Angew. Chem. Int. Ed. Engl.,* 1997, 36(17), 1892-1894.

48. Roderiques, S., Glueck, D. S., Cain, M. F., REU in Nanomaterials, 2009

49. Gulliver, D. J., Levason, W., Webster, M., *Inorg. Chimi. Acta.,* 1981, 52(2), 153-159.

50. (a) Ramaprabhu, S., Amstutz, N., Lucken, E. A. C., Bernardinelli, G., *J. Chem. Soc.,* 1993, 6, 871- 875. (b) Ramaprabhu, S., Lucken, E. A. C., Bernardinelli, G., *J. Chem. Soc.,*1993, 8, 1185 -1190.

51. Vaira, M. D., Ehses, M. P., Peruzzini, M., Stoppioni, P., *Polyhedron,* 1999, 18, 2331-2336.

52. Jian, F., Wang, K., Xiao, H., Qiao, Y., *Acta. Cryst.,* 2005, E61, m1324 - m1325.

53. Churchill, M. R., Rotella, F. J., *Inorg. Chem.,*1979, 18, 166.

54. Albano,v. G., Bellon, P. L., Ciani, G., *J. Chem. Soc., Dalton Trans.,* 1972, 18, 1938.

55. Barron, P. F., Dyason, J. C., Healy , P. C., *J. Chem. Soc., Dalton Trans.,* 1987, 5, 1099.

56. Khan, M. M. T., Paul, P., Venkatasubramanian, K., Purohit, S., *J. Chem. Soc., Dalton Trans.,* 1991, 12, 3405.

57. Zukerman-Schpector, J., Castellano, E. E., Oliva, G., Mauro, A. E., Roveri, M. R., *Acta Cryst.*, 1985, C41, 204-206.

58. Goel, R. G., Beauchamp, A. L., *Inorg. Chem.*, 1983, 22 (3), pp 395–400.

59. Negita, H., Hiura, M., Kushi, Y., Kuramoto, M., Okuda, T., *Bull. Chem. Soc. Jpn.,*1981, 54, 1247.

60. Haitko, D. A., *J. Coord. Chem.,* 1984, 13, 119.

61. Graziani, R., Bombieri, G., Forsellini, E., *J. Chem. Soc.,* 1971, 2332.

62. Pothupitiya, T. K., PhD Thesis, Cardiff University, 2010.

63. Cotton, F. A., *Inorg. Chem.,* 1964, **3**, 702-711.

64. Rudolph, R. W., Parry, R. W., *J. Am. Chem. Soc.,* 1967, **89**, 1621-1630.

CHAPTER 3

Coordination Chemistry of [12]-ane-P_3R_3 with Group 8 & 9 metals Fe(0) and Co(0)

3.1. Introduction

3.1.1. Iron Chemistry

Iron is by mass the most common element on Earth, forming much of Earth's outer and inner core, in contrast to the metal ruthenium, which is in the same group in the periodic table.[1] Like other group 8 elements, iron exists in a wide range of oxidation states, (−II) to (+VI), although (+II) and (+III) are the most common. Iron also occurs in higher oxidation states, an example being the potassium ferrate (K_2FeO_4) which contains iron in its +VI oxidation state. The discovery of ferrocene has led to a new branch of organometallic chemistry. Ferrocene itself can be used as the backbone of a ligand (e.g. dppf).[2]

Iron plays an important role in biology, forming complexes with molecular oxygen in hemoglobin and myoglobin; these two compounds are common oxygen transport proteins in vertebrates.[3] Iron is also the metal used at the active site of many important redox enzymes dealing with cellular respiration and oxidation and reduction in plants and animals. There is good precedent for complexes of these metals to be of value in catalytic applications (e.g. iron pentacarbonyl is an effective homogeneous catalyst for the hydrogenation of polyunsaturated fats).[4]

3.1.2. Cobalt Chemistry

Cobalt was first discovered in 1735 by George Brandt in Stockholm Sweden and it is a sturdy, gray metal which resembles iron and nickel.[5] Next to nickel and iron, cobalt is one of the three naturally occurring magnetic metals, which has a wide range of oxidation states of III, II, 0 and -I like other group 9 metals.

There are many uses for Cobalt; it is alloyed with chromium and tungsten to make a metal (e.g. stellite alloy) hard enough, to be used for high speed cutting tools and valves for internal combustion engines, the alloy alnico (Al + Ni + Co) is used to make extremely strong permanent magnets and cobalt compounds are also used in paints. Importantly, they are used as catalysts, e.g. cobalt carbonyl $Co_2(CO)_8$ is used to catalyse the hydroformulation reaction to produce an aldehyde or alcohol from an alkene.[5]

As Iron, cobalt plays an important role in biology. It is an essential trace element. Vitamin B_{12} (cobalamine) contains a cobalt atom and is necessary for the prevention of pernicious anaemia and the formation of red blood corpuscles. In plants cobalt is involved in nitrogen fixation by microorganisms.[5]

Iron and Cobalt carbonyls stabilised by phosphine donors have long been known.[6] Complexes with η^1-coordinated phosphines tend to labile and chelating ligands have been studied in order to enhance the stability of resulting complexes. Not surprisingly, larger chelate ring sizes have been shown to decrease stability[7] and rigid chelating ligands[8] enhance stability. This chapter aims in the study of kinetically robust 12-membered triphosphorus macrocycles based upon the 1,5,9-triphosphacyclododecane core ([12]-ane-P_3R_3) with Fe(0) and Co(0) carbonyls.

3.2. Results and Discussion - New Iron Chemistry

3.2.1. Synthesis of (dicarbonyl) fac-(η^3 -1,5,9-triethyl-1,5,9-triphosphacyclododecane) iron(0)

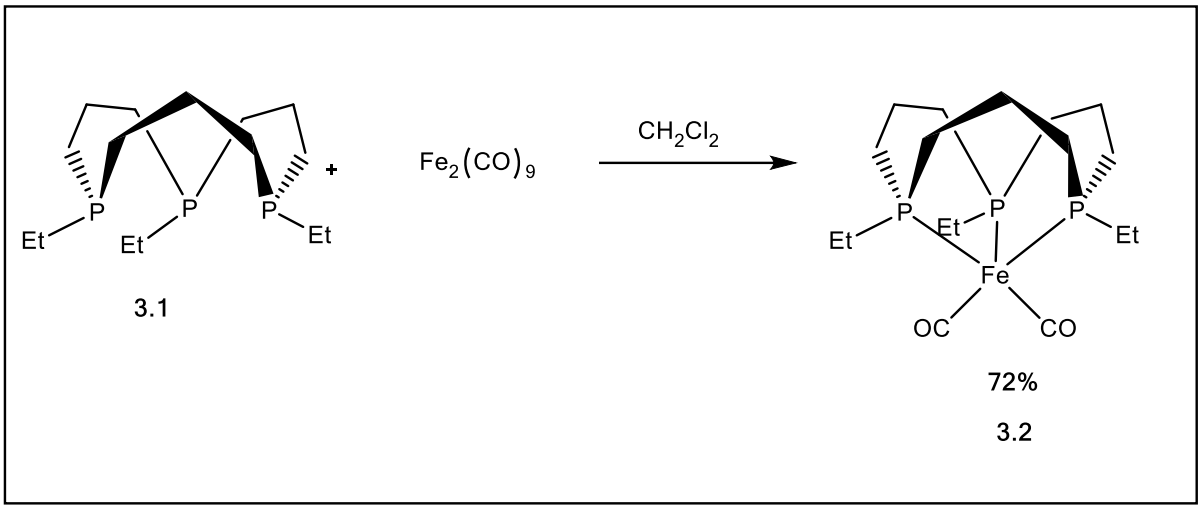

Scheme 3.1: Preparation of (dicarbonyl)fac-(η^3 -1,5,9-triethyl-1,5,9-triphosphacyclododecane) iron(0), (3.2)

Scheme 3.1 indicates the reaction of [12]-ane-$P_3(Et)_3$ with diiron nonocarbonyl to give the 18 electron compound, (dicarbonyl)fac-(η^3-1,5,9-triethyl-1,5,9-triphosphacyclododecane) iron(0), (3.2) in CH_2Cl_2 at room temperature. There was an immediate colour change upon addition of the ligand to the iron precursor. After further stirring for 30 minutes, the solvent was removed *in vacuo* and the microcrystalline solid of complex 3.2 was obtained by recrystallising from hot toluene.

This crystalline solid was characterised by $^{31}P\{^1H\}$, ^1H and $^{13}C\{^1H\}$ NMR spectroscopy, mass spectrometry, IR spectroscopy and elemental analysis.

3.2.2. Synthesis of (dicarbonyl) fac-(η^3 -1,5,9-triisopropyl-1,5,9-triphosphacyclododecane) iron(0)

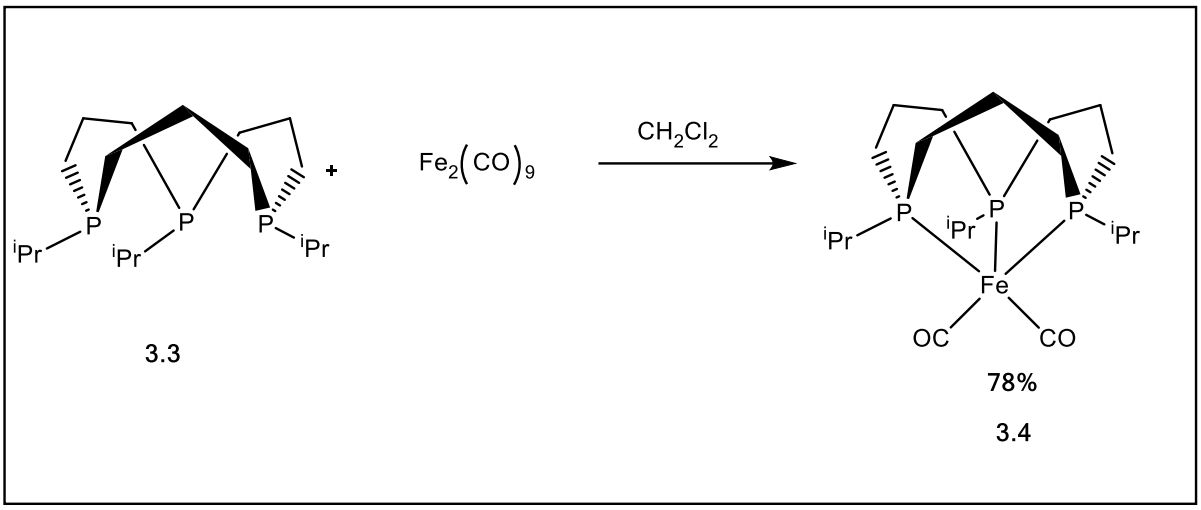

3.3

3.4

Scheme 3.2: Preparation of (dicarbonyl)fac-(η^3 -1,5,9-triisopropyl-1,5,9-triphosphacyclododecane) iron(0), (3.4)

The similar reaction of [12]-ane-$P_3(^iPr)_3$ with diiron nonocarbonyl gave an instantaneous colour change from yellow to blue-green. After 30 minutes of stirring the solvent was removed *in vacuo* and the complex was recrystallised from toluene. These complexes have been confirmed by analytical data.

Both reactions stated above (Scheme 3.1 and scheme 3.2) were straightforward and proceeded rapidly at room temperature. The light green colour microcrystalline solids have been obtained with in 72% and 78% yields respectively for 3.2 and 3.4 complexes. Similarly, the reaction of [12]-ane-P_3Et_3 with group 5 carbonylvanadium $[V(CO)_6]^-$, gave the oxidised neutral 17 electron mononuclear complex of *fac*-([12]-ane-$P_3Et_3V(CO)_3$.[9] In the presence of excess macrocycle,

there is no evidence of alternative species such as the bis-macrocycle complexes in contrast to the behaviour noted for the cobalt carbonyl complexes with [12]-ane-P_3R_3.

In solution, the phosphorus atoms are equivalent, showing one signal at δ 37.43 ppm and δ 37.70 ppm in the $^{31}P\{^1H\}$ NMR spectra for 3.2 and 3.4 respectively, corresponding to the co-ordinated phosphines. The ^1H NMR spectra of complexes 3.2 and 3.4 give rise to four resonances assignable to four different proton environments relevant to the [12]-ane-P_3R_3 macrocycle complexes similar to the spectra observed for the molybdenum(0) and (II) precursors. The $^{13}C\{^1H\}$ NMR spectra show five resonances of which four are due to the coordinated macrocycle and ethyl or isopropyl groups, with only broadened singlets at δ 224 ppm and δ 215 ppm for carbonyl carbons for the complexes 3.2 and 3.4 correspondingly. Similarly, in *fac*-[(12-[ane]-P_3Et_3)$V(CO)_3]^-$ complex the $^{13}C\{^1H\}$ NMR spectrum shows only a broadened singlet at δ 220 ppm for the carbonyl carbons.[9]

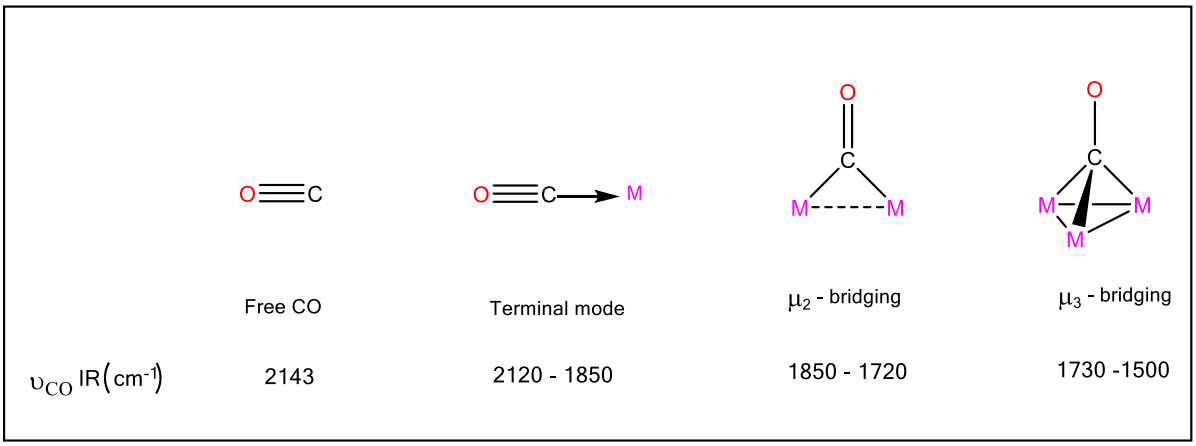

Figure 3.1: The CO stretching frequencies for neutral metal complexes

The terminal v(C-O) stretching absorption frequencies in the IR spectra of complexes 3.2 and 3.4 are observed at 2014 cm^1, 1985 cm^{-1} and 2016 cm^{-1}, 1941 cm^{-1} respectively as expected for

a complex of this nature. The carbonyl stretching frequencies are in the same range as previously reported triphosphine complexes and are also close to the isoelectronic chromium and molybdenum macrocycle complexes (Table 3.1).[9]

Complex	v(C=O) / cm^{-1}	Medium	Ref.
$[Et_4N][(12[ane]P_3Et_3)V(CO)_3]$	1894, 1857	THF	9
Mer-$[V(CO)_3(pp_3]^{-a}$	1910, 1815, 1680	THF	10
$12[ane]P_3Et_3Cr(CO)_3$	1911, 1813	Nujol	11
$12[ane]P_3Et_3Mo(CO)_3$	1918, 1815	Nujol	11
$(\eta^1\text{-}12[ane]P_3Et_3)(Cp)V(CO)_3$	1844, 1765	Toluene	9
$CpV(CO)_3(dppm)$	1950, 1872, 1845	THF	12
$CpV(CO)_2(dppm)$	1871, 1808	THF	9

Table 3.1: IR spectroscopic data for metal carbonyl complexes for comparison purposes.

$^a pp_3 = P[(CH_2)_3PEt_2]_3$

These two [12]-ane-P_3R_3 $[Fe(CO)_2]$ complexes (3.2 and 3.4) have 18 valence electrons with 8 valence electrons on Fe and five pairs of electrons provided by the CO and [12]-ane-P_3R_3 ligands. Reflecting their D_{3h} symmetrical structures and charge neutrality, they may have been shown to exhibit fluxional behaviour, which is the exchange, occurred in a pair-wise fashion, with two axial atoms exchanging with two equatorial atoms in a process which did not involve any bond breaking or bond reforming that requires a low potential energy (e. g. about ΔE = ~3.6 kcal/mol in PF_5[13]). Figure 3.2 shows the exchange of the trigonal bipyramidal and square pyramidal structures with the Fe atoms surrounded by five ligands: three in equatorial positions

and two axially bound. This mechanism was described by Berry in 1960,[13] and has become famously known as the Berry pseudorotation mechanism for XY_5 trigonal bipyramidal molecules, with D_{3h} symmetry (e.g. PF_5, VF_5, $Fe(CO)_5$, etc).

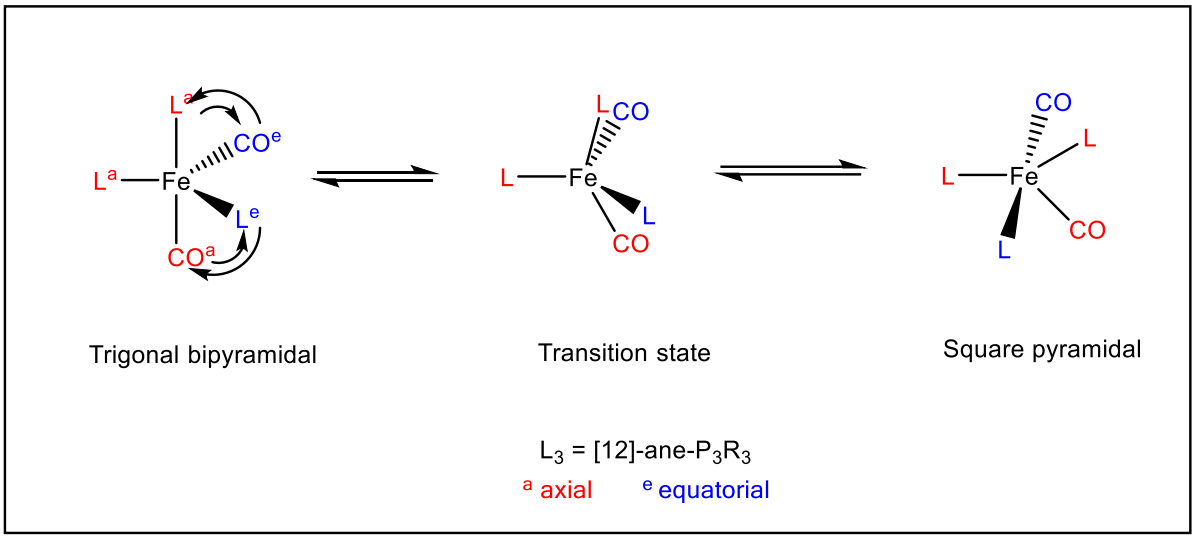

Figure 3.2: Potential diagram for the transposition of axial and equatorial atoms via a transition state.

Herein, we also attempted to synthesise and characterise the dihydrogen metal complexes of 3.2 and 3.4 due to the interest in hydrogenation reactions in homogeneous catalysis (Figure 3.3). Molecular dihydrogen ligands are coordinated in a side-on arrangement to the metal centre as σ-complexes. This denotation is due to the interaction between the electron donating σ-orbital of the H_2 bond and the empty *d*-orbital at the metal centre and by the back donation of the metal's d-orbitals into the empty σ^*-orbital of the hydrogen molecule. This type of bonding is also considered non-classical due to its 3-centre-2-electron (3c-2e) bonding character.[14,15] There are various molybdenum, tungsten and ruthenium based molecular dihydrogen complexes known.[16,17]

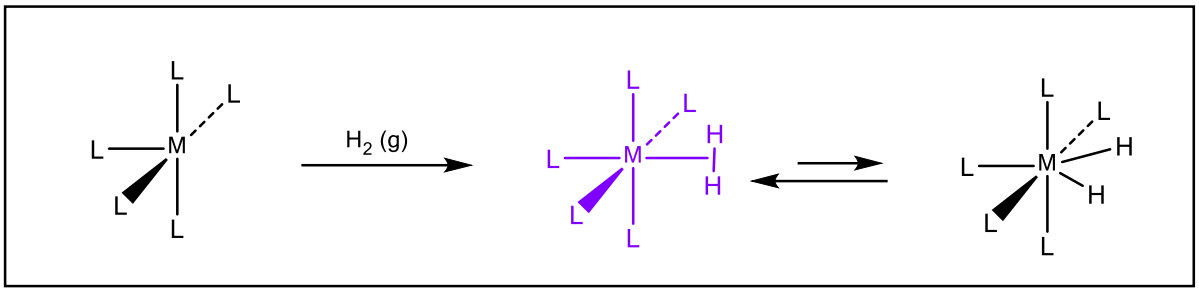

Figure 3.3: Schematic presentation of formation and equilibrium structures of metal dihydrogen and dihydride complexes; (L = ligand)

A typical one-pot direct synthetic protocol was used in the attempted synthesis of the dihydrogen complexes.[18] In an argon flushed fisher-porter bottle, diiron nonocarbonyl was added to the [12]-ane-P_3R_3 in Toluene. After the fisher-porter bottle was filled with H_2 gas to 5 bar pressure at room temperature, the reaction mixture was stirred for 48 hrs at room temperature. The fisher-porter bottle was then depressurised and flushed with argon. The solvent was removed *in vacuo* and the product was washed with petroleum ether and recrystallised from diethyl ether. The resultant microcrystalline solid was characterised analytically. The ^{31}P $\{^1H\}$, ^1H and ^{13}C $\{^1H\}$ NMR spectroscopy, mass spectrometry, IR spectroscopy and elemental analysis results confirmed only the formation of complexes 3.2 and 3.4. Attempts to hydrogenate [12]-ane-P_3R_3 $[Fe(CO)_2]$ complexes (3.2 and 3.4) did not yield the desired products, which may be due to the low pressure (5 bar).

3.3. Results and Discussion - New Cobalt Chemistry

3.3.1. Synthesis of (dicarbonyl)bis-fac-(η^3 -1,5,9-triethyl-1,5,9-triphosphacyclododeca- ne) bis(μ-cobalt(0)), 3.5

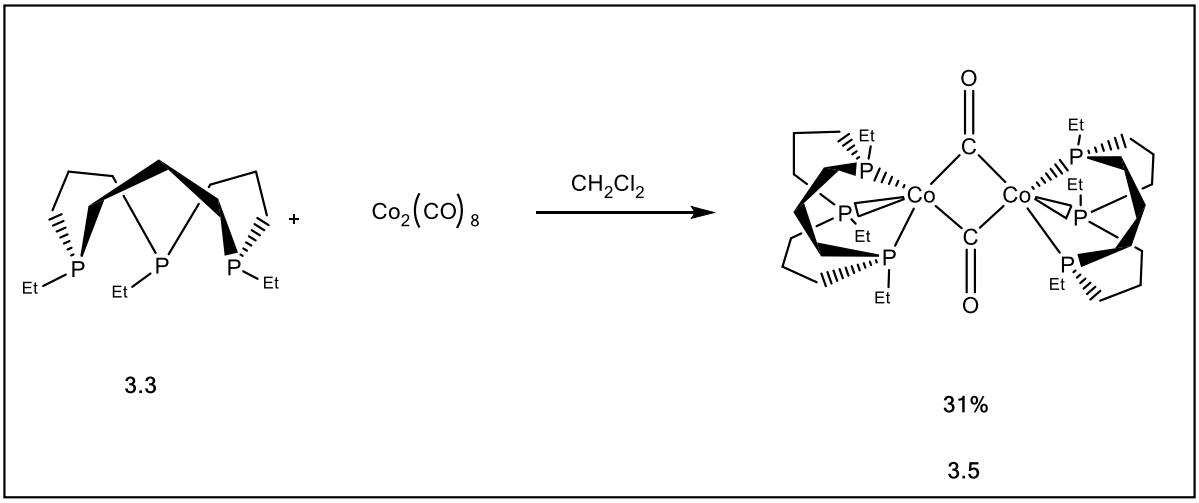

Scheme 3.3: Preparation of (dicarbonyl)bis-fac-(η^3 -1,5,9-triethyl-1,5,9-triphosphacyclododecane) bis(μ-cobalt(0)), 3.5

Addition of [12]-ane-$P_3(Et)_3$ to the $Co_2(CO)_8$ in CH_2Cl_2 in a 2:1 molar ratio resulted the formation of the neutral bimetallic species, 3.5. The product was obtained as a yellow microcrystalline solid when recrystallised from hot toluene. The crystalline solid was characterised by mass spectrometry, IR spectroscopy and elemental analysis and the attempt to analysed 3.5 using NMR spectroscopies have failed.

3.2.2. Synthesis of (dicarbonyl)bis-fac-(η^3 -1,5,9-triisopropyl-1,5,9-triphosphacyclodo-decane) bis(μ-cobalt(0)), 3.6

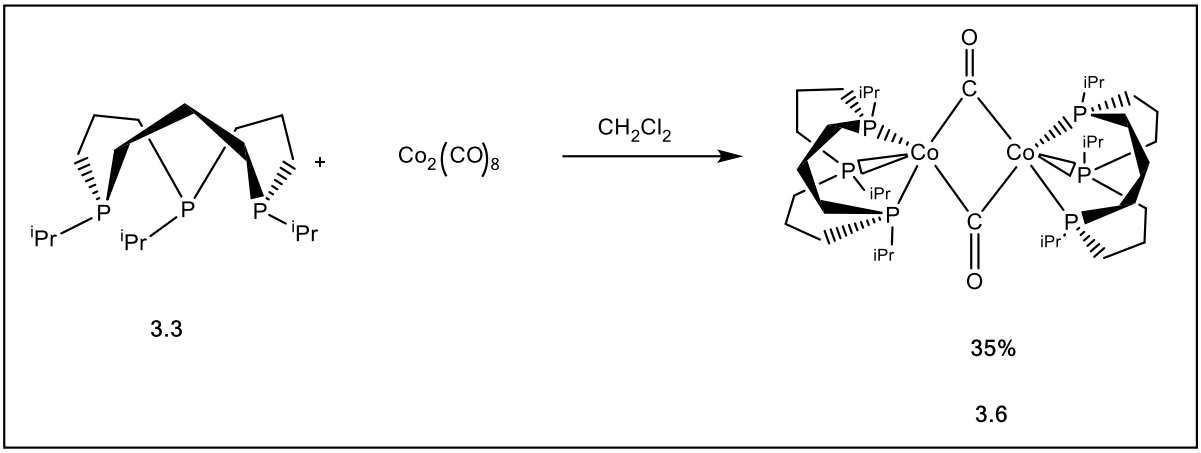

Scheme 3.4: Preparation of (dicarbonyl)bis-fac-(η^3 -1,5,9-triisopropyl-1,5,9-triphosphacyclodo- decane) bis(μ-cobalt(0)), 3.6

Analogously, the reaction with 2 equivalents of [12]-ane-$P_3(^iPr)_3$ with $Co_2(CO)_8$ in CH_2Cl_2, followed by evaporation of the solvent and recrystallisation from hot toluene, resulted a formation of a bimetallic complex, 3.6 in 55% yield. The characterisation using NMR spectroscopies of this complex is failed, but the crystalline solid was identified using mass spectrometry, IR spectroscopy and elemental analysis.

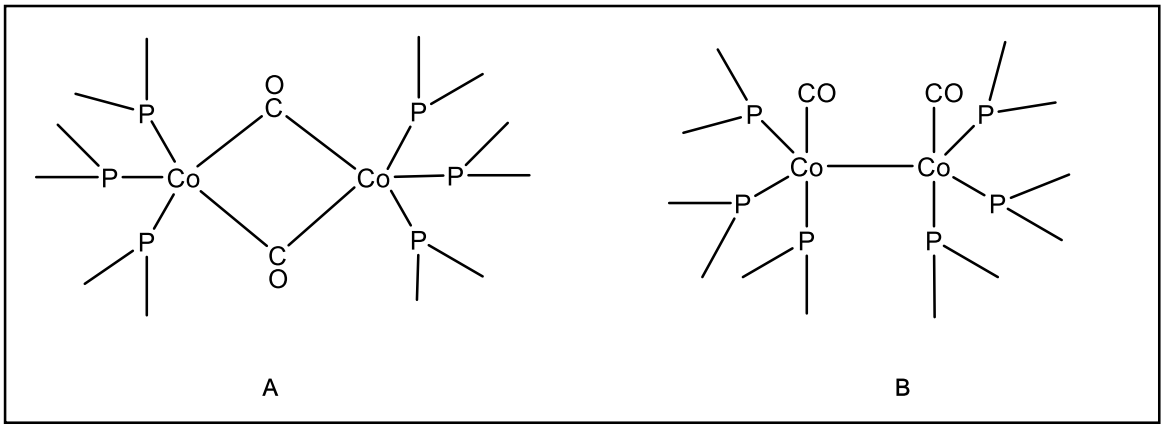

Figure 3.4: Schematic diagram of possible structures for complexes 3.5 and 3.6

The IR spectra of $Co_2(CO)_8$ shows three bands at 2053 cm^{-1} and a single band at 1876 cm^{-1} assigned to the terminal and bridging carbonyl groups, and two strong bands at 641 cm^{-1} and 531 cm^{-1} for Co-C stretching and Co-C-O bending respectively. The presence of CO bound to the metal centre was confirmed by the IR spectroscopy in complexes 3.5 and 3.6. The CO region of the IR spectra of Complexes 3.5 and 3.6 consist of two strong bands, which can be assignable to the terminal CO group at 2053 cm^{-1} and 2067 cm^{-1} and at 635 cm^{-1} and 648 cm^{-1} for Co-C stretching. Similar interactions have been observed for related systems. The absence of the high carbonyl frequency confirmed the [12]-ane-P_3R_3(Co-Co)[12]-ane-P_3R_3 structure (Figure 3.4 – (A)), with bridging CO ligands, instead of a direct Co–Co bond and two terminal CO ligands and two [12]-ane-P_3R_3 ligands, one on each Co atom.

The structure which can assigned to the complexes 3.5 and 3.6 are a combination of two trigonal bipyramids joined at an edge with a carbonyl and a phosphine ligands in the axial positions and two phosphine ligands in the equatorial positions with a D_{3d} symmetry.

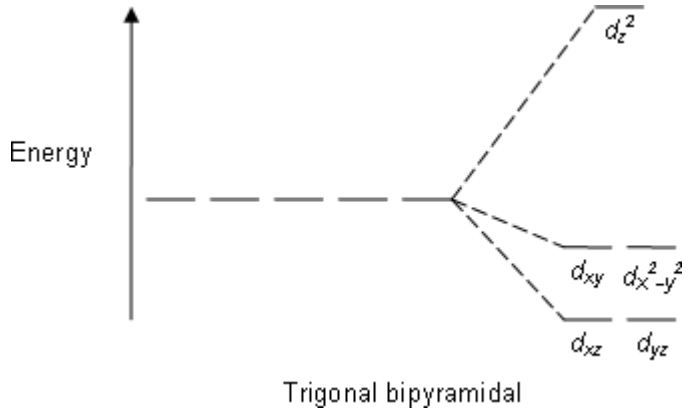

Figure 3.5: Low Spin Crystal Field Splitting Diagram of trigonal bipyramidal complexes

Complexes 3.5 and 3.6 have mass spectra showing the molecular ion [$(M)^+$, 786, 100%] and [$(M)^+$, 858, 100%] correspondingly and confirmed the complexes.

3.4. Attempted Reactions

Scheme 3.5 below gives a simplified graphical representation of some attempted syntheses of various rhodium- based complexes. They are not listed in the 'experimental' or results or discussion part of this chapter, due to either of the following reasons, (a) the reaction failed to work, (b) characterisation was minimal, (c) insufficient compound stability to obtain reasonable characterisation, or (d) low compound purity, which could not be increased by the usual purification methods.

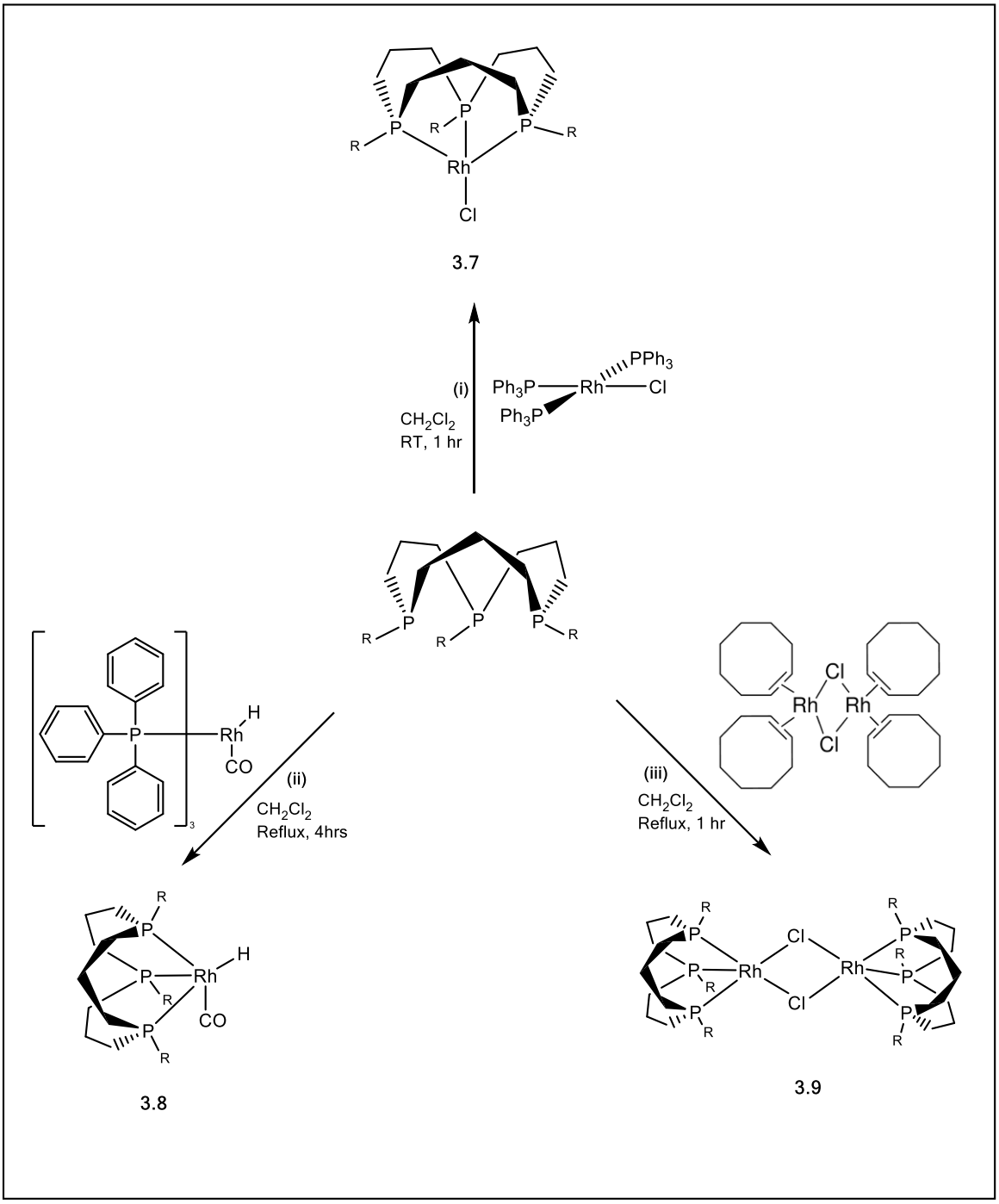

Scheme 3.5: Attempted syntheses of various rhodium-based complexes

3.4.1. Discussion

Scheme 3.5(i) shows the reaction of [12]-ane-P_3R_3 with $RhCl(PPh_3)_3$ in CH_2Cl_2 at room temperature resulting a mixture of compounds. The reaction characterisation did not prove the desired product and the recrystallisation of the product gave the crystal structure (Figure 3.6) of dimetallic $RhCl(PPh_3)_3$ complex, which indicates a disfavouration of the reaction. The altered reaction conditions did not improved the reaction towards the desired product.

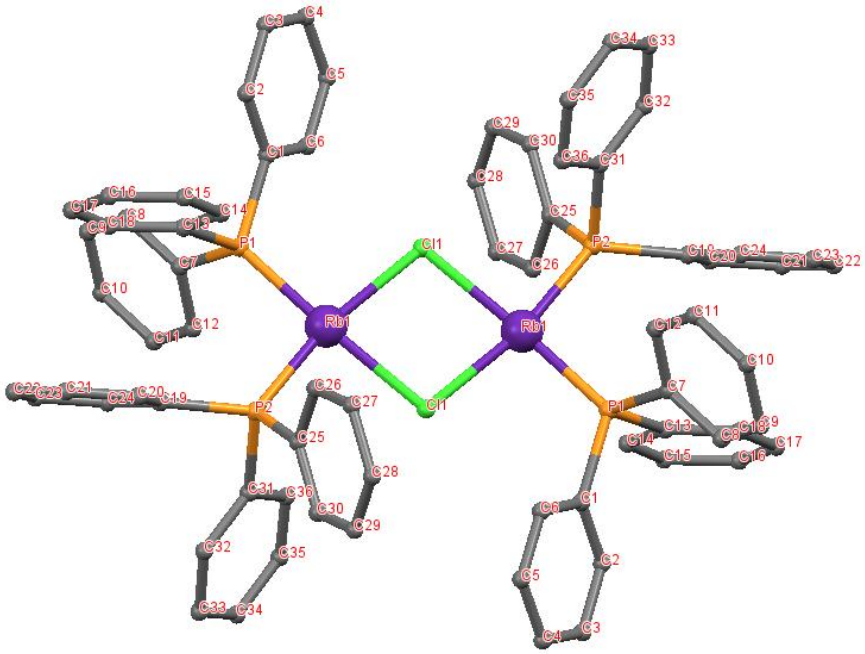

Figure 3.6: Molecular structure of the product obtained from the reaction in scheme 3.5 (i). For clarity, hydrogens have been omitted.

(ii) The attempted synthesis of complex 3.8, from the reaction between [12]-ane-$P_3(R)_3$ and $Rh(PPh_3)_3(CO)H$ in CH_2Cl_2 by refluxing for 4 hrs was not given the desired product. Extended heating and alteration of experimental conditions yielded no better results.

The only product isolated from the reaction arose from abstraction of halide from the solvent (Figure 3.7).

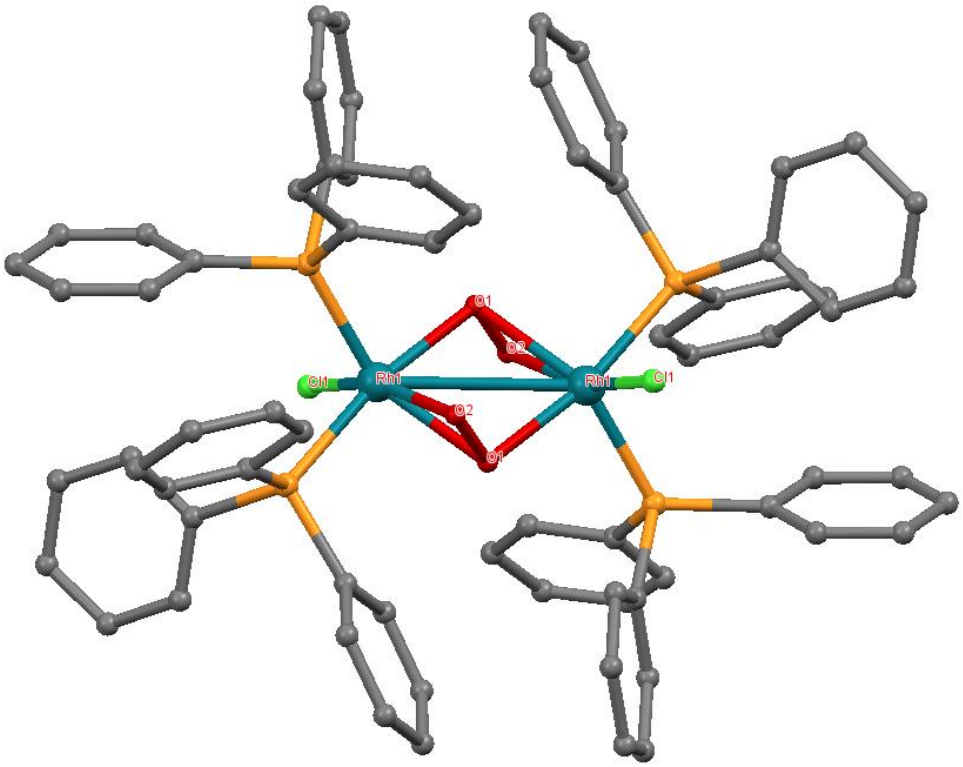

Figure 3.7: Molecular structure of the product obtained from the reaction in scheme 3.5 (ii). For clarity, hydrogens have been omitted.

(iii) Reaction of [12]-ane-P_3R_3 with $[RhCl(COE)_2]_2$ (Scheme 3.5(iii)) in CH_2Cl_2 was refluxed for 1 hr. A reaction was observed both visually and spectroscopically, but, no significant diagnostic data was obtained. Several attempts with different reaction conditions yielded a range of inseparable mixture of complexes without resulting the desired complex 3.9, where purification proved ineffectual.

3.5. Conclusion

The reactions of [12]-ane-$P_3(R)_3$ with groups 8 and 9 metals with the electronic configuration of d^8 and d^9 rapidly give rise to facially coordinated tris(phosphine) complexes with the other coordinated ligands are restricted to a mutually *cis* orientation environment.

Due to the failed hydrogenation reactions with Fe and Co, no catalytic tests were performed on any of the metal complexes obtained, but, future work on any such systems should engage this. Such complexes are known to be catalytically active, for example in alkene and acetylene hydrogenation,[19] hydroformylation[20] and numerous other processes.

3.6. Experimental

3.6.1. General

Techniques and Instruments*:* All reactions were carried out in an atmosphere of dry argon. All solvents were dried by boiling under reflux over standard drying agents. The compounds allylphosphine, *syn,syn*-1,5,9-triethyl-1,5,9-triphosphacyclododecane, [12]-ane-$P_3(Et)_3$ were prepared by literature methods. All other reagents including iron and cobalt starting materials were obtained from the Aldrich Chemical Company and, where appropriate, were degassed before use. The NMR spectra were recorded on a Bruker DPX-500 instrument at 500 MHz (^1H),

and 125.75MHz (^{13}C), Bruker DPX-400 instrument at 400 MHz and 100 MHz (^{13}C), Jeol Lamda Eclipse 300 at 121.65 MHz (^{31}P), 75.57 MHz (^{13}C). ^{1}H and ^{13}C chemical shifts are quoted in ppm relative to residual solvent peaks, and ^{31}P NMR chemical shifts quoted in ppm (δ) relative to 85% external H_3PO_4 (δ = 0ppm) . The infra-red spectra were recorded on a Nicolet 510 FT-IR spectrometer and the samples were prepared under Argon atmosphere as a KBr disk. Mass spectra of all the samples have been measured by direct injection into a Waters Low Resolution ZQ Mass Spectrometer fitted with ESCI source. Elemental analysis was performed by Warwick University Analytical Service.

X-Ray Crystallography*:* Data collections were carried out on a Bruker Kappa CCD diffractometer at 150(2) K with Mo $K\alpha$ irradiation (graphite monochromator). Empirical absorption corrections were performed using equivalent reflections. For the solution and refinement of the structures, the program package SHELXL 97 was employed. H atoms were placed into calculated positions and included in the last cycles of refinement. Crystal structure and refinement data are collected in Appendix A.

3.6.2. Synthesis of (dicarbonyl) fac-(η^3 -1,5,9-triethyl-1,5,9-triphosphacyclododecane) iron(0), 3.2.

A solution of [12]-ane-P_3Et_3 (0.326 mmol, 100 mg) in dichloromethane(15 ml) was added drop wise to a solution of diiron nonocarbonyl (0.326 mmol, 119 mg) in dichloromethane (15 ml) and an immediate colour change was obtained. Then it was stirred for further 30 minutes and the solvent was removed *in vacuo*, followed by recrystallisation of the yellow solid from hot toluene gave 3.2 as a blue-green microcrystalline solid (0.172 mmol, 71.9 mg, 72.0%). Analysis found (calculated): C, 49.52 (48.82); H, 7.87 (7.95). MS(ES), *m/z*: 418 (100%, $[M]^+$). NMR

($CDCl_3$): $^{31}P\{^1H\}$, δ 37.43 ppm (s). ^1H NMR (360 MHz, 27 ºC), δ (ppm): 1.68 (br m, PC*H*$_2$); 1.19 (br m, PC*H*$_2$C*H*$_2$); 1.05 (br m, PC*H*$_2$CH$_3$); 1.70 (br m, PCH$_2$C*H*$_3$). $^{13}C\{^1H\}$ NMR (90 MHz, 27 ºC), δ (ppm): 224 (br s, *C*O); 26.60 (d, $^1J_{(P\text{-}C)}$ 17Hz, P*C*H$_2$); 18.15 (br s, PCH$_2$*C*H$_2$); 25.7 (d, $^1J_{(P\text{-}C)}$, 50Hz, P*C*H$_2$CH$_3$); 15.01 (br s, PCH$_2$*C*H$_3$. IR/cm^{-1} (Nujol): ν(C-O) 2014 cm^{-1} (br) and 1985 cm^{-1} (br).

3.6.3. Synthesis of (dicarbonyl) fac-(η^3-1,5,9-triisopropyl-1,5,9-triphosphacyclododecane) iron(0), 3.4

A solution of [12]-ane-$P_3(^iPr)_3$ (0.200 mmol, 69.7 mg) dissolved in dichloromethane(15 ml) was added to a solution of diiron nonocarbonyl (0.200 mmol, 72.8 mg) in dichloromethane (15 ml) and was stirred for 30 minutes at room temperature. The solvent was removed *in vacuo*, followed by recrystallisation of the solid from hot toluene gave 3.4 as a blue-green solid (0.05 mmol, 23.0 mg, 78.0%). Analysis found (calculated): C, 51.52 (52.18); H, 8.96 (8.54). MS(ES), *m/z*: 460 (100%, ([M]$^+$), NMR ($CDCl_3$): $^{31}P\{^1H\}$, δ 37.70 ppm (s). ^1H NMR (360 MHz, 27 ºC), δ (ppm): 1.75 (br m, PCH$_2$C*H*$_2$); 1.45 (br m, PC*H* and PC*H*$_2$); 1.05(br s, C*H*). $^{13}C\{^1H\}$ NMR, δ (ppm): 31.5 (br, m, P*C*H$_2$); 21.5 (m, PCH$_2$*C*H$_2$); 18.5 (m, P*C*H); 17.5(s, *C*H$_3$).; 215 (s, *C*O). IR/cm^{-1} (Nujol): ν(C-O) 2016 cm^{-1} (br) and 1941 cm^{-1} (br).

3.6.4. Preparation of (dicarbonyl)bis-fac-(η^3-1,5,9-triethyl-1,5,9-triphosphacyclododecane) bis(μ-cobalt(0)), 3.5

A solution of [12]-ane-P_3Et_3 (0.326 mmol, 100 mg) in dichloromethane(15 ml) was added drop wise to a solution of dicobalt octacarbonyl (0.163 mmol, 55.7 mg) in dichloromethane (15 ml) and an immediate colour change was obtained. Then it was stirred for further 30 minutes and the solvent was removed *in vacuo*, followed by recrystallisation of the yellow solid from hot toluene gave 3.2 as a blue-green microcrystalline solid (0.172 mmol, 119 mg, 31.0%). Analysis found (calculated): C, 48.52 (48.86); H, 8.87 (8.45). MS(ES), *m/z*: 786 (100%, $[M]^+$). IR/cm^{-1} (Nujol): ν(C-O) 2053 cm^{-1} (sh) and ν(Co-C) 635 cm^{-1} (sh).

3.6.5. Synthesis of (dicarbonyl)bis-fac-(η^3 -1,5,9-triisopropyl-1,5,9-triphosphacyclododecane) bis(μ-cobalt(0)), 3.6

A solution of [12]-ane-$P_3(^iPr)_3$ (0.112 mmol, 39 mg) in dichloromethane (15 cm^3) was added dropwise to a solution of dicobalt octacarbonyl (0.56 mmol, 19.1 mg) in dichloromethane (15 cm^3) and the resultant mixture stirred for 2h at room temperature. Evaporation to dryness *in vacuo* gave a yellow colour residue which was recrystallised from CH_2Cl_2/petrol to give 3.6 as light yellow colour microcrystalline solid. (0.52 mmol, 40.4 mg, 35%) Analysis found (calculated): C, 51.47 (50.34); H, 9.48 (10.56), MS(ES), *m/z*: 858 [50%, (M^+)]. IR/cm^{-1} (Nujol): ν(C-O) 2067 cm^{-1} (sh) and ν(Co-C) 648 cm^{-1} (sh).

3.7. Reference

1. Greenwood, N. N., Earnshaw, A., 1984, *Chemistry of the Elements*. Oxford Pergamon Press, pp. 1282–86.

2. Laszlo, P., Hoffmann, R., 2000, *Angewandte Chemie (International ed. in English)* **39** (1), 123–124.

3. Wilkinson, G., Cotton, F. A., *Advanced Inorganic Chemistry*, 4th Ed., 1311.

4. Frankel, E. N., Peters, H. M., Jones, E. P., Dutton, H. J., *J. Am. Oil Chem. Soc.,* 1964, 41,186.

5. Petrucci et al., *General Chemistry: Principles & Modern Applications*, 9th Edition. New Jersey, Pearson Education, Inc., 2007.

6. Hieber, W., Ernst, W., *Berichte,* 1964, 97,1037.

7. Franke, U., Weiss, E., *J. Organomet. Chem.,* 1979, 172, 341.

8. Bechtold, H. C., Rehder, D., *Z. Naturforsch. B.,*1981, 36, 451.

9. Baker, R. J., Edwards, P. G., Farley, R. D., Murphy, D. M., Platts, J. A., Voss, K. E., *Dalton trans.,* 2003, 944 - 948.

10. Sussmilch, F., Glockner, W., Rehder, D., *Organomet. Chem.,* 1990, 388, 95.

11. Edwards, P. G., Fleming, J. S., Liyanage, S. S., *J. Chem. Soc., Dalton Trans.,* 1997, 193.

12. Ellis, J. E., Faltynek, R. A., Rochfort, G. L., Stevens, R. E., Zank, G. A., *Inorg. Chem.,* 1980, 19, 1082.

13. Berry, R.S., *J. Chem. Physics*, 1960, 32, 933-938.

14. Crabtree, R. H., Lavin, M., *J. Am. Chem. Soc.,* 1985, 23, 1661-1662.

15. Hamilton, D. G., Crabtree, R. H., *J. Am. Chem. Soc.,* 1988, 110, 4126-4133.

16. Gauri, Y., Castellanos, A., Sabo-Eienne, S., Chaudret, B., *J. Mol. Catal. A:Chem.,* 2004, 212, 77-82.

17. Kubas, G. J., *J. Organomet. Chem.,* 2001, 635, 37-68.

18. Choi, J-H., Schloerer, N. E., Berger, J., Prechtl, H. G., *Dalton Trans.,* 2014, **43**, 290.

19. Osborn, J. A., Jardine, F. H., Young, J. F., Wilkinson G., *J. Chem. Soc. (A),***1966**, 1711.

20. Evans, D., Osborn, J. A., Wilkinson, G., *J. Chem. Soc. (A),***1968**, 3133.

CHAPTER 4

Coordination Chemistry of [12]-ane-P_3R_3 with Group 8 Metal Ru(II) and Catalysis

4.1. Introduction and Background Chemistry

The group 8 metal Ruthenium, is very rare in the earth's crust. The metal is isolated commercially by a complex chemical process, the final stage of which is the hydrogen reduction of ammonium ruthenium chloride, which yields a powder. The powder is consolidated by powder metallurgy techniques or by argon-arc welding.[1]

Ruthenium in the metallic state can be considered to be a noble metallic element, which has its own expansive chemistry. Ruthenium is known to exist in a multitude of different oxidation states, from (-II) through to (VIII). Even though the (-II) state is rare, it occurs in the carbonyl ion $[Ru(CO)_4]^{2-}$. The known Ru(0) compounds are available in the carbonyl series as such, $Ru(CO)_5$, $Ru_3(CO)_{12}$, and $Ru(CO)_3(PPh_3)_2$. The low oxidation states tend to demand that the compounds be stable 18-electron species, with some few exceptions; 16 electron complex $Ru(CO)_2(MeP^tBu_2)_2$.[2] The cyclopentadienylruthenium dicarbonyl dimer, $[C_pRu(CO)_2]_2$, is a complex with Ru(I) oxidation state, which is analogous to Fe(I) system. Ru(II) and Ru(III) are the most common oxidation states for the metal compounds to be found in and some examples are $[Ru(H_2O)_6]^{2+}$ and $[Ru(H_2O)_6]^{3+}$.

Ligands such as CO and phosphines, that are capable of back bonding with Ru(II) and Ru(III) produce the immense range of complexes that are in existence. A mass of other electron-density donors, such as the cyclopentadienyl and a number of main group containing ligands form complexes with ruthenium in these oxidation states. Ru(IV) species are rare, but consisting basically of simple halogen-containing moieties (e.g. K_2RuCl_6), oxo compounds (e.g. RuO_2) and organometallic compounds such as tetra(cyclohexyl)ruthenium. Ru(V), Ru(VI), Ru(VII) and Ru(VIII) are entirely prepared as oxo and halogen compounds, hardly ever containing any classical ligands, such as phosphines and amines.

4.2. Ruthenium in Organometallic Chemistry

Ruthenium has a well-known coordination and organometallic chemistry; in particular ruthenium-phosphine chemistry is comprehensively prominent, with a diverse range of known complexes, mainly concerning complexes of Ru(II) oxidation state, including the Grubbs catalysts (Figure 4.1).[10] They are used in various catalytic applications such as hydrogenolysis,[4] hydrogenation[5], hydroformylation[6] and well known ring opening methathesis polymerisation (ROMP), Cross metathesis and Ring closing metathesis (RCM).[7-9]

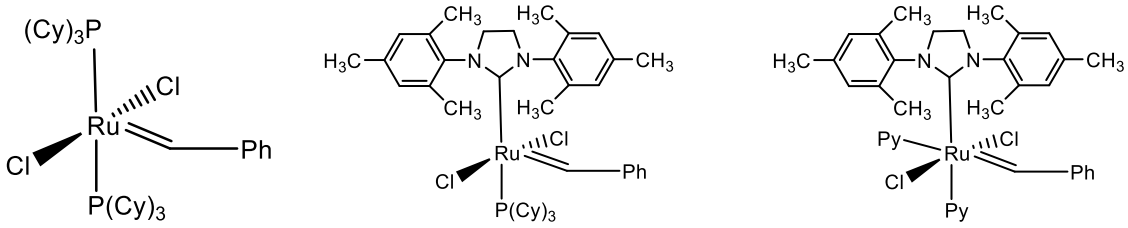

1st Generation 2.32 | 2nd Generation 2.33 | 3rd Generation 2.34

Figure 4.1: Grubbs Ru(II) catalysts

Studies on Ruthenium P_3 12-membered macrocycles are very limited and therefore investigation of this area will be of potential importance in the study of reactivity especially in catalysis, as the higher stability of the macrocyclic ligand complexes in comparison to cyclic and monodentate analogues, which may lead to more robust catalysts. This in turn should lead to prolonged existence. In addition, the rigid facially capping (*cis*) arrangement of P-ligands, might direct to mechanistic differentiations and thus novel reactivity.

4.3. Results and Discussion – New Ruthenium Chemistry

4.3.1. Synthesis of dichloro(dimethyl sulphoxide) [*fac*-η^3-*cis,cis*-1,5,9-triethyl-1,5,9-triphospha cyclododecane] ruthenium(II), 4.2.

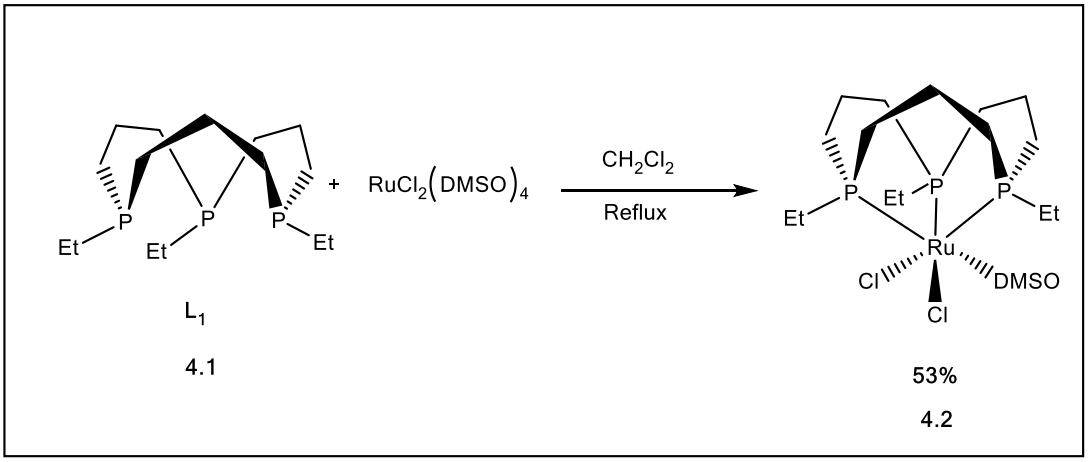

L_1

4.1

53%

4.2

Scheme 4.1: Synthesis of dichloro(dimethyl sulphoxide) [*fac*-η^3-*cis,cis*-1,5,9-triethyl-1,5,9-triphospha cyclododecane] ruthenium(II), 4.2

When the reaction of L_1 with dichlorotetra(dimethyl sulphoxide)ruthenium(II) in CH_2Cl_2 was carried out for 4 hrs at room temperature, a mixture of partially substituted products was resulted. Subsequent reflux for another one hour gave the desired product 4.2 as a yellow solid with 53% yield (Scheme 4.1).

4.3.2. Synthesis of dichloro(dimethyl sulphoxide) [*fac*-η^3-*cis,cis*-1,5,9-triisopropyl-1,5,9-triphospha cyclododecane] ruthenium(II), 4.3.

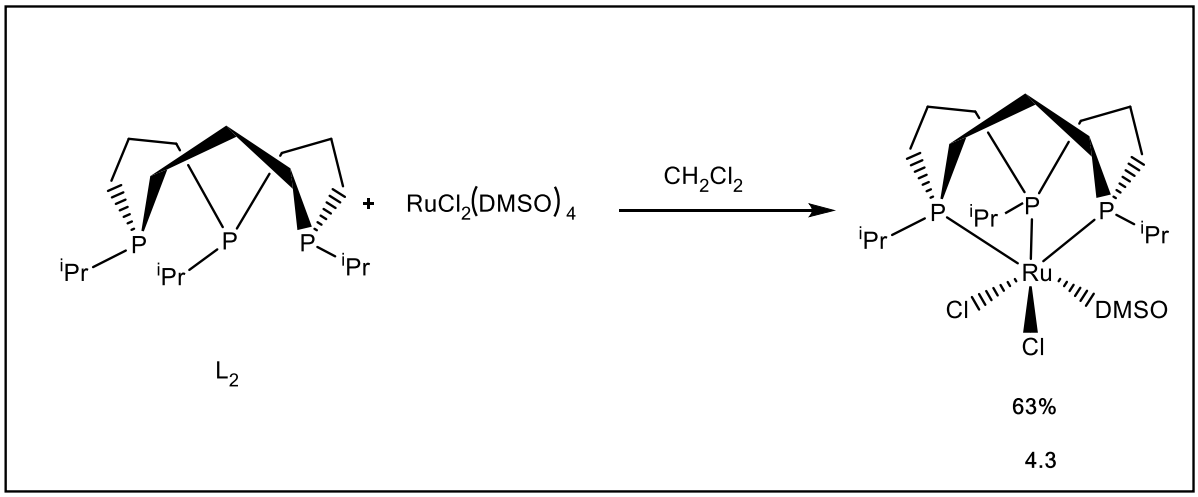

Scheme 4.2: Synthesis of dichloro(dimethyl sulphoxide) [*fac*-η^3-*cis,cis*-1,5,9-triisopropyl-1,5,9-triphospha cyclododecane] ruthenium(II), 4.3

Analogously, the tris-isopropyl macrocycle is formed (4.3) by the reaction of L_2 with dichlorotetra(dimethyl sulphoxide) ruthenium(II) at room temperature (Scheme 4.2). The product 4.3 was obtained by stirring the reaction mixture for 4 hrs at room temperature which gave the yellow product with 63% yield.

The successful formation of the product 4.3 at room temperature shows the difference of the reactivity between the ethyl and isopropyl ligands. The complexes 4.2 and 4.3 have C_s symmetry and therefore, a doublet and a triplet, *i.e.* A_2B pattern are expected in $^{31}P\{^1H\}$ NMR spectrum, but only a singlet was observed in both cases at δ 36.36 ppm and δ 37.44 ppm

respectively. This unexpected behaviour for the unsymmetrical structures of 4.2 and 4.3 was explained may be due to the facile lability of DMSO in solution.[11]

In the ^{1}H NMR spectra of 4.2 and 4.3, the resonances attributable to the α and β ring protons are at δ 1.60 ppm, δ 1.29 ppm and δ 1.60 ppm, δ 1.72 ppm respectively. Resonances (4.2), due to the ethyl substituents occur at δ 1.08 ppm and δ 1.72 ppm arising from methyl and methylene groups respectively whereas, for isopropyl substituents (4.3), the resonances are at δ 1.08 ppm and δ 1.58 ppm for PCH*CH*$_3$ and PC*H* protons. Also, the resonances for the protons of DMSO (C*H*$_3$SOC*H*$_3$) appear at δ 2.87 ppm and δ 2.91 ppm for 4.2 and 4.3 complexes respectively.

The ν (Ru-Cl) bands of 4.2 were observed in the infra-red spectrum at 325 cm^{-1} and 302 cm^{-1} and for the ν (S-O), broad peaks appeared at 1150 cm^{-1} and 912 cm^{-1}. These values are about 5-10 cm^{-1} differ from those observed for 4.3.

These complexes also analysed with ^{13}C NMR, mass spectrometry, elemental analysis (See experimental section). However, attempts to recrystallise these (4.2 and 4.3) complexes were not successful.

4.3.3. Synthesis of tris(μ-chloro)bis-fac-(η^3 -1,5,9-triethyl-1,5,9-triphosphacyclodo-decane)bis(ruthenium(II)), 4.4.

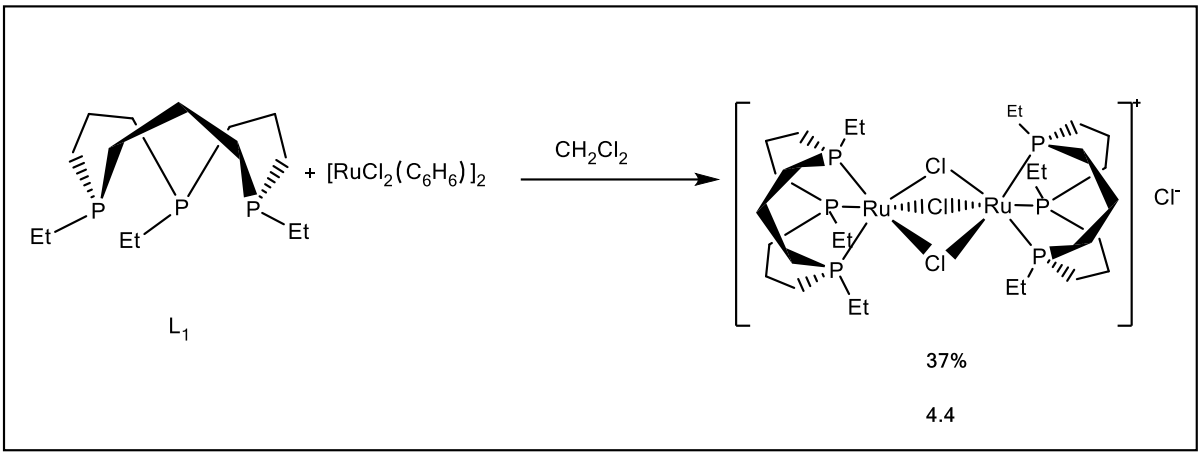

Scheme 4.3: Preparation of tris(μ-chloro)bis-fac-(η^3 -1,5,9-triethyl-1,5,9-triphosphacyclodo-decane) bis(ruthenium(II)), 4.4

The complex 4.4, tris(μ-chloro)bis-fac-(η^3-1,5,9-triethyl-1,5,9-triphosphacyclododecane)bis (ruthenium(II)) chloride was formed instantaneously upon the addition of 2 equivalents of [12]-ane-P_3Et_3 into a $[RuCl_2(C_6H_6)]_2$ in CH_2Cl_2 at room temperature. This bi-metallic bridging complex was crystallized with 40/60 petroleum ether into CH_2Cl_2 and red-yellow colour microcrystalline solid was obtained with 37% yield.

4.3.4. Synthesis of tris(μ-chloro)bis-fac-(η^3-1,5,9-triisopropyl-1,5,9- triphosphacyclodo-decane)bis(ruthenium(II), 4.5.

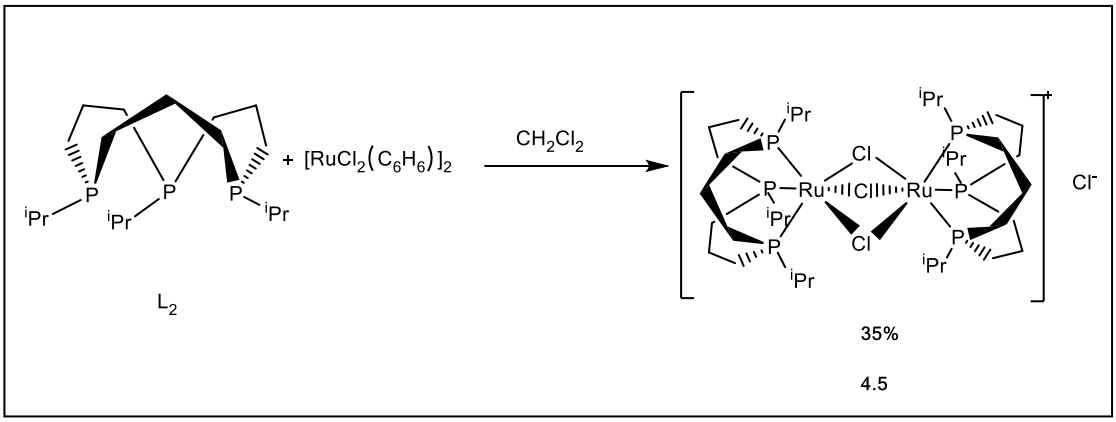

Scheme 4.4: Preparation of tris(μ-chloro)bis-fac-(η^3 -1,5,9-triisopropyl-1,5,9-triphosphacyclododecane)bis(ruthenium(II)), 4.5

The complex 4.5, was formed upon the reaction of $[RuCl_2(C_6H_6)]_2$ with 2 equivalents of L_2 in CH_2Cl_2 at room temperature by the displacement of the arene from the metal centre to afford the red-orange material. This bi-metallic bridging complex was crystallized by slow diffusion of 40/60 petroleum ether into CH_2Cl_2 producing crystals with 39% yield.

In complexes 4.4 and 4.5, both ruthenium atoms are symmetrical and all phosphorus atoms magnetically equivalent giving rise to the singlets observed in the ^{31}P $\{^1H\}$ NMR spectra at δ 23.59 ppm and δ 25.4 ppm for complexes 4.4 and 4.5 respectively, suggesting the coordination of free macrocyclic ligand to the metal centre. The ^1H NMR and ^{13}C $\{^1H\}$ NMR spectra consist of

four resonances assignable to the four different proton and carbon environments relevant to the macrocycles similarly (In experimental section).

The symmetric triply halide-bridged bi-octahedral architecture is a recurring structure of remarkable stability and conceptual interest in ruthenium chemistry. The work of Geoffrey Wilkinson has provided the understanding of tertiary phosphine complexes of ruthenium(II).[12] Among these reported analogous halide-bridged ruthenium phosphorus complexes, not many structures have been characterised crystallographically.[13a] Of the few, tris-μ-chloro-bis[tris(trimethylphosphine)ruthenium(II)] tetrafluoroborate is a good example.[12] A more complex example, using the 'tripod' analogue [tripod = $MeC(CH_2Eph_2)_3$, E = P (triphos)], namely 'triphos', gives the co-facile bi-octahedral species.[13b]

4.4. Ruthenium Complexes and Catalysis

Ru-carbene and Ru-vinylidene complexes have been proven to be highly efficient catalysts for a variety of olefin transformations. During the last decade, the chemistry of metal vinylidene complexes has been the object of significant development due to the discovery of general synthetic methods and their use to generate new material carbenes.[17] Mono-substituted vinylidene complexes, arising from the (η^2-alkyne)metal to (η^1-vinylidene)metal tautomerism, have been at the basis of innovation, because this process constitutes the first step of terminal alkyne metal activation and provides an electrophilic activation, due to the heteroallene nature of the M=C=CHR moiety. These mono-substituted vinylidenes are excellent precursors and they have been recognised as active species in selective homogeneous catalytic

transformations. The Ru=C=CHR moiety has been shown to be the effective catalytic species for many catalytic applications.[18] Olefin-metathesis reactions catalysed by transition metal complexes have attracted a great deal of attention owing to their versatility in organic and polymer syntheses.[19]

This rapid progress in recent years has been triggered off by the discovery of the Grubbs catalyst in mid 1990s'.[20,21] It has been demonstrated that the single component alkylideneruthenium complexes $RuCl_2(=CHR)(PCy_3)_2$, where (R=Ph, $CH=Ph_2$) exhibit extremely high catalytic activity and excellent tolerance towards polar functional groups. The latter feature, which is the principle advantage of the ruthenium catalysts over the conventional early transition metal based ones, has brought about a remarkable extension of the scope of applications of olefin-metathesis reactions.[22]

Olefin metathesis reactions have proven to be a powerful technique for the formation of C-C bonds.[23] The development of ruthenium complexes bearing sterically demanding phosphines such as the well-defined, neutral 16-electron complex $RuCl_2(=C(H)Ph)(PCy_3)_2$ as an efficient catalyst system has allowed significant progress in the field of olefin metathesis.[24] Since at elevated temperatures phosphines suffer from significant P-C degradation,[25] the development of sterically demanding ligands that can mimic the phosphine behaviour and at the same time show stability at higher temperatures would prove useful.[26] Imidazolylidene ligands with sterically demanding groups substituted in the 1 and 3 positions of the five-membered ring have been used to generate very effective catalysts for Suzuki crosscoupling[27] and ring-closing metathesis reactions.[28,29]

Recent studies have shown that complexes of unsaturated "C_α" ligands other than the alkylidenes, such as allenylidenes, are also efficient catalyst precursors in the olefin metathesis reactions.[30]

The changes in the ligand sphere can also have profound and largely unpredictable effects on catalytic activity, stability and selectivity.[31-36] Several examples are illustrated in Figure 4.4: in comparison to $(PCy_3)_2(Cl)_2Ru=CHPh$ or $(PCy_3)_2(Cl)_2Ru=CHCH=CPh_2$, the diiodide derivative exhibits enhanced initiation properties,[37] the N-heterocyclic carbene derivative displays increased catalytic propagation rates,[38,39] and the Schiff-base derivative displays greater thermal stability.[40]

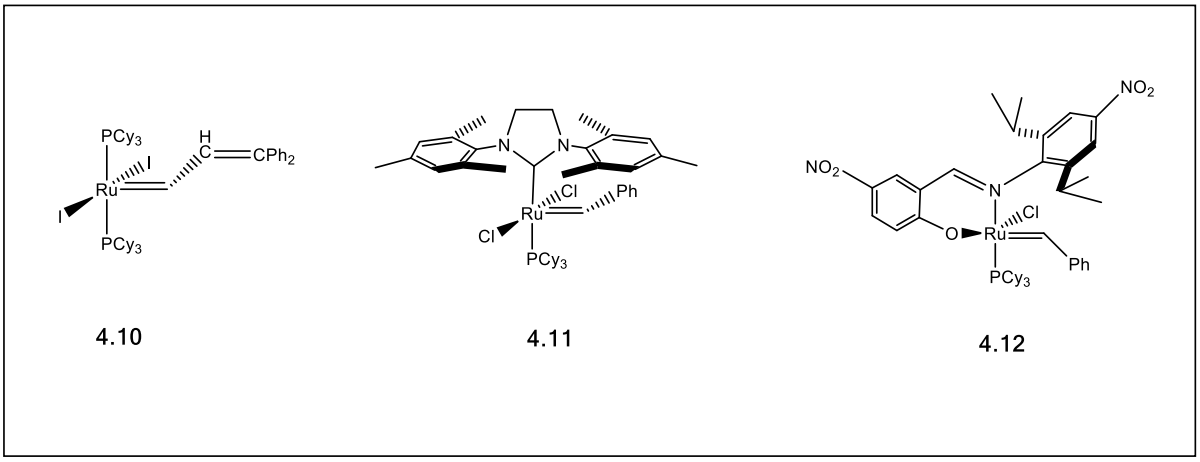

4.10 4.11 4.12

Figure 4.4: Variations in the ligand sphere of ruthenium alkylidene olefin metathesis catalysts

4.4.1. Catalytic Testing: Ring Closing Metathesis of Diethyl diallylmalonate

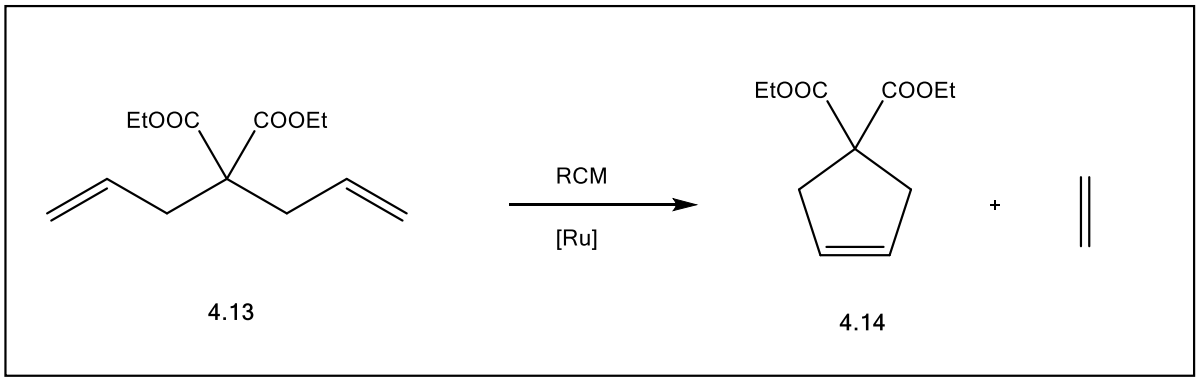

4.13 4.14

Scheme 4.5: Ring Closing Metathesis of Diethyl diallylmalonate

Scheme 4.6 is a schematic representation of the ideal ring closing metathesis reaction that would occur in diethyl diallylmalonate to substituted cycloolefin, in the presence of the ruthenium-based catalyst. Depending on the catalyst and the conditions employed, catalytic reactivity and selectivity will vary significantly.

Complex	Temperature (ºC)	Time (min)	Yield (%)[a]	Reference
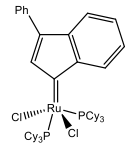 4.15	RT	25	84	41
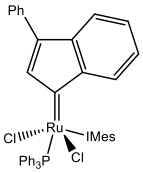 4.16	40	25	65	41
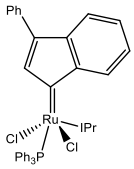 4.17	40	25	56	41
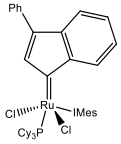 4.18	RT	25	88	41
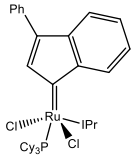 4.19	RT	25	75	41

Table: 4.3: Ring Closing Metathesis results using previously reported catalysts. [a] Determined by ^{1}H NMR.

Complex	Temperature (ºC)	Time (min)	Yield (%)[a]	Reference
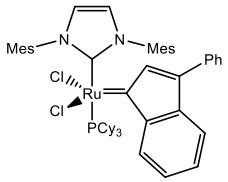 4.20	RT	25	88	43
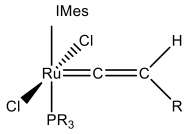 R = Ph, tBu, Me_3Si 4.21	RT	25	86	42
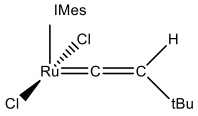 4.22	RT	25	95	42
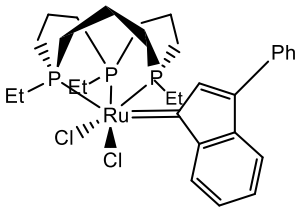 4.9	60	25	64	This Study

Table 4.3: Ring Closing Metathesis Results using previously reported catalysts.

[a] Determined by ^{1}H NMR.

The indenylidene complex 4.22 is shown to be good catalyst precursor with a 95% yield in the RCM of sterically unhindered diethyl diallylmalonate substrate, comparable to the complexes 4.15 – 4.21. Indeed, the catalytic activity of the above mentioned complexes proved to be better-quality, supporting the concept of a higher degree of unsaturation in the coordination sphere of the metal promoting catalysis. Detailed mechanistic investigations of the ruthenium-catalysed metathesis chemistry strongly indicated that increased ligand dissociation (that is of phosphane) is necessary to accelerate initiation and thereby increased the catalytic activity in this type of reactions.[43]

4.4.2. Results and Discussion - New Catalytic Activity

4.4.2.1. Synthesis of Ruthenium Indenylidene complex –

Dichloro(3-phenyl indenylidene)[*fac*-η^3-*cis,cis*-1,5,9-triethyl-1,5,9-triphosphacyclododecane] ruthenium(II), (4.9)

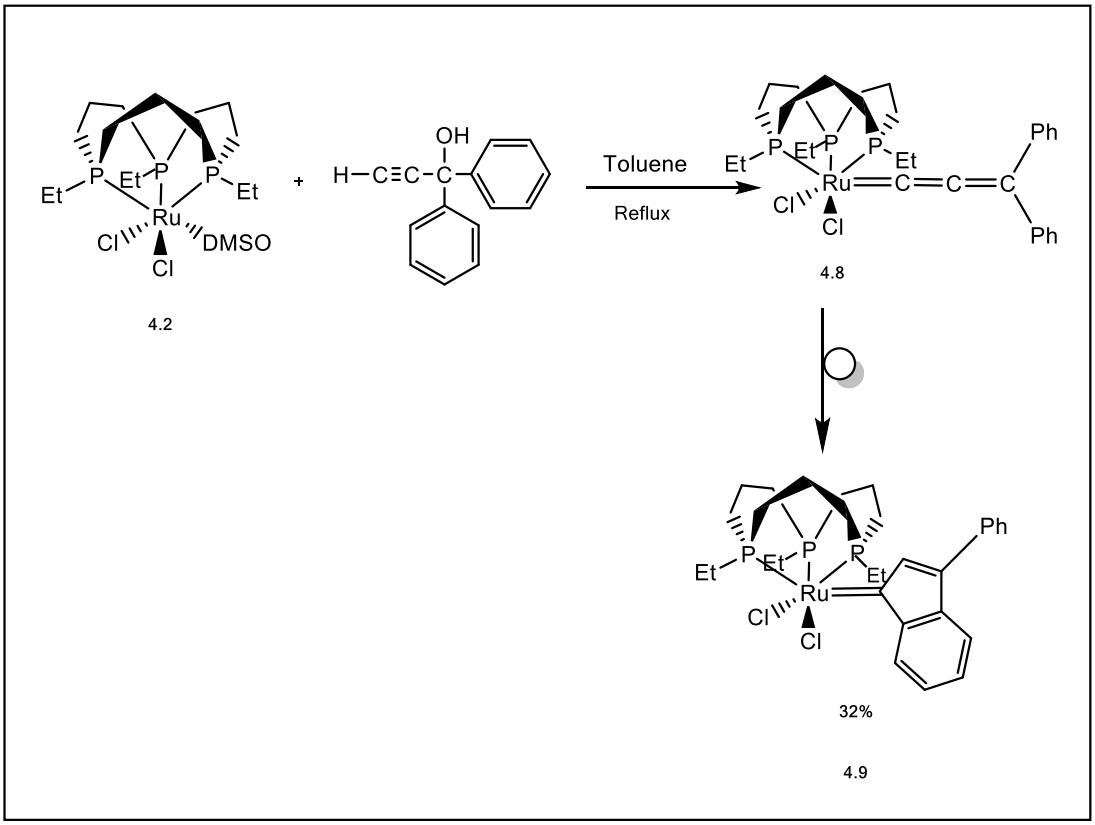

Scheme 4.6: Synthesis of dichloro(3-phenyl indenylidene) [*fac*-η^3-*cis,cis*-1,5,9-triethyl-1,5,9-triphospha cyclododecane] ruthenium(II), (4.9)

Complex 4.2 was reacted with an excess of 1,1-diphenylprop-2-yn-1-ol in toluene and refluxed for a period of 2hrs. The solvent was removed in *vacuo* and a bright orange-yellow oily product was obtained, which was recrystallised from hot 40/60 petroleum ether into CH_2Cl_2 and the resultant microcrystalline solid was obtained in 32% yield for which the analytical data indicate the formula 4.9. The initially formed ruthenium allenylidene complex 4.8, leads by an intramolecular rearrangement to the more stable indenylidene complex 4.9. This complex was characterised by $^{31}P\{^1H\}$, ^1H and $^{13}C\{^1H\}$ NMR spectroscopies, mass spectrometry, IR spectroscopy, and elemental analysis. This intramolecular rearrangement has been proved before unequivocally for a similar reaction of $[RuCl_2(PPh_3)_3]$ with 1,1-diphenylprop-2-yn-1-ol which resulted $(IMes)(PPh_3)Cl_2Ru$(3-phenylindenylid-1-ene).[15]

A singlet was observed in $^{31}P\{^1H\}$ NMR spectrum for the product 4.9, at δ 39.79 ppm where a 3 ppm downfield shift from the parent 4.2 complex. The singlet may be unexpected for the unsymmetrical structure of 4.9, but, this type of behaviour is precedented for tripodal arsine ligands,[16] and previously reported complexes 4.2 and 4.3. In the ^1H NMR spectrum, the signal for the single proton on C_β of indenylidene appears as a singlet at δ 7.34 ppm while the resonances attributed to the phenyl ring protons of appear in the region of δ 6.8 - 7.4 ppm along with the four resonances assignable to the four different proton environments relevant to the macrocycle similar to the spectra observed for complex 4.2 (In experimental section). Similarly, $^{31}P\{^1H\}$ NMR spectra of $(IMes)(PPh_3)Cl_2Ru$(3-phenylindenylid-1-ene) and $(IPr)(PPh_3)Cl_2Ru$(3-phenylindenylid-1-ene) complexes show singlets at δ 29.0 ppm δ 30.51 ppm and the signal for the single proton on C_β of indenylidene appears as a singlet at δ 7.49 ppm and δ 7.33 ppm in their ^1H NMR spectra respectively.[15]

Complex 4.9 shows bands in the IR spectrum at 320 and 302 cm^{-1} which are assigned to the terminal ν(Ru-Cl) absorbances consistent with 4.9 having a mononuclear structure. Furthermore, the analytical data is consistent with the formulation and a strong molecular ion peak (*m/z*= 668) is observed in the mass spectrum. Attempts to recrystallise the complex 4.9 was unsuccessful.

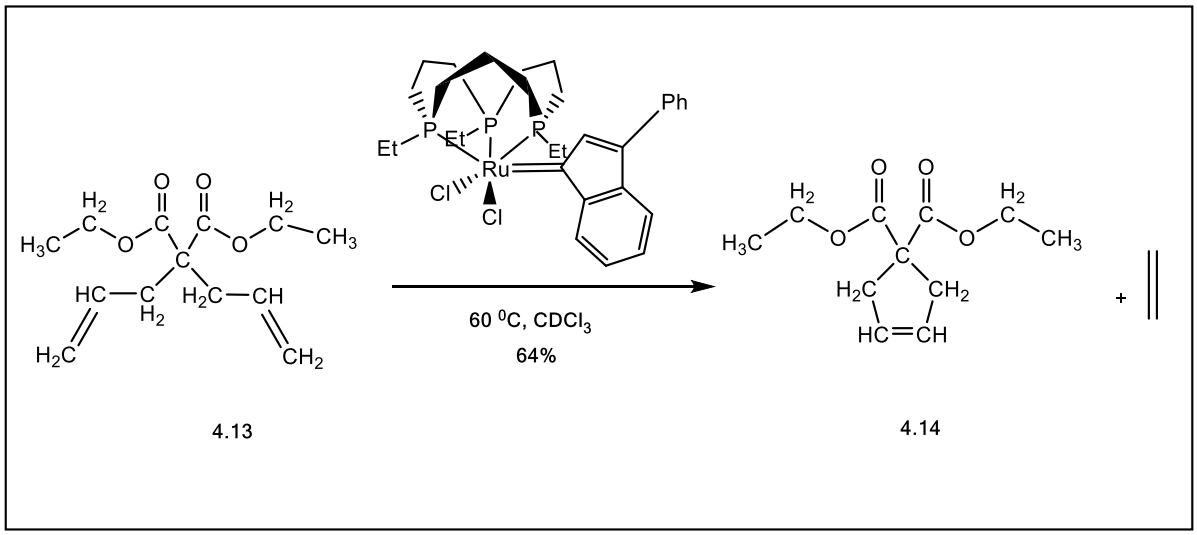

Scheme 4.7: RCM of Diethyl diallylmalonate in the presence complex 4.9

The role of complex 4.9 as a catalyst precursor in the ring-closing metathesis reaction was investigated. The diethyl diallylmalonate was chosen as the substrate for two reasons; it has been observed that ring-closing metathesis to the corresponding cyclopentene diester is quantitative and relatively facile, and the rates of ring-closing are slow enough to be followed by ^{1}H NMR but fast enough to be experimentally feasible[44].

Addition of 25 mol % equivalents of diethyl diallylmalonate to a room-temperature solution of 4.9 in $CDCl_3$ in an NMR tube under a nitrogen atmosphere did not cause a colour change.

Therefore the mixture was heated to 60 ºC and the colour started changing from orange-red to yellow after 20 minutes.

Product formation and diene disappearance were monitored by integrating the allylic methylene peaks in the ^{1}H NMR spectra; the results are presented in Figures 4.5, 4.6 and 4.7, and the catalytic transformation is depicted in Scheme 4.7.

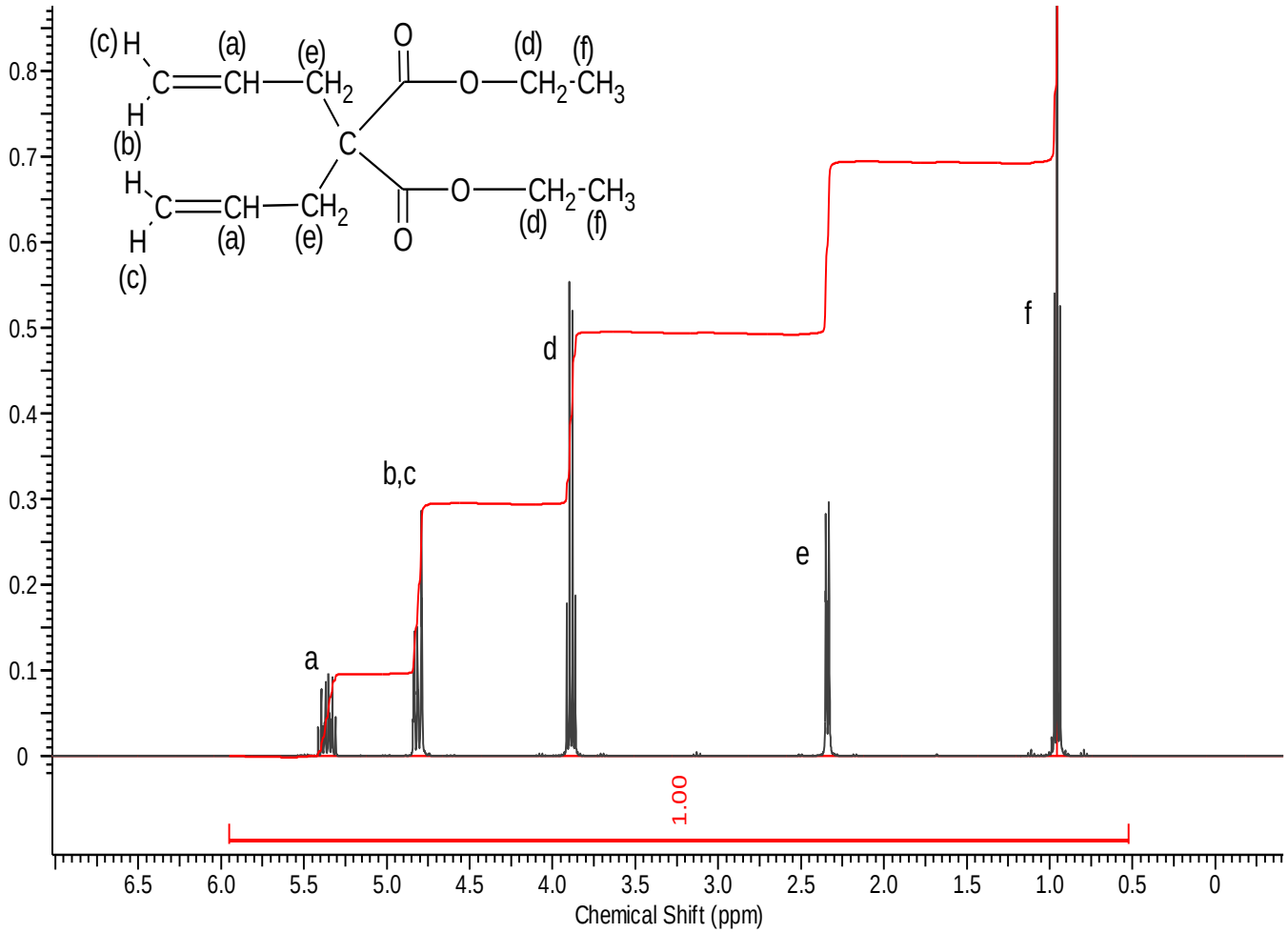

Figure 4.5: ^{1}NMR spectrum of Diethyl diallylmalonate in $CDCl_3$ at room temperature

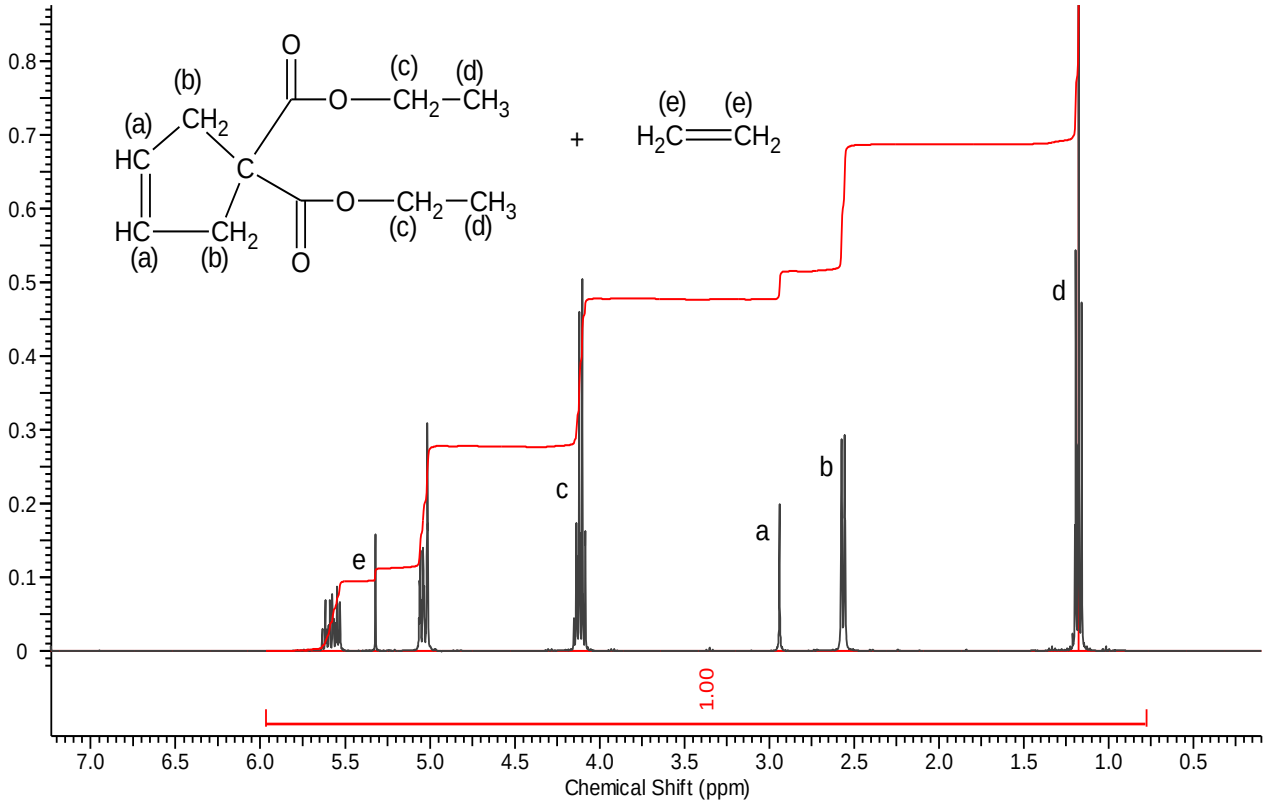

Figure 4.6: ^{1}H NMR spectrum of Diethyl diallylmalonate, Diethyl 3-Cyclopentene-1,1-dicarboxylate and ethane 2 hours after the initiation of RCM in $CDCl_3$

This complex suffered from a lack of initiation efficiency and proved active only at elevated temperatures. This complex proceeds to an 85% conversion after 5 hrs that was confirmed by the GC-mass spectrum. The conversion was remained after 24 hours which confirmed by the GC-mass spectrum that indicates a longer life time of the complex 4.9. Full conversion could not be attained due to the low initiation rate and the lack of selectivity which may be rationalized by the catalyst.

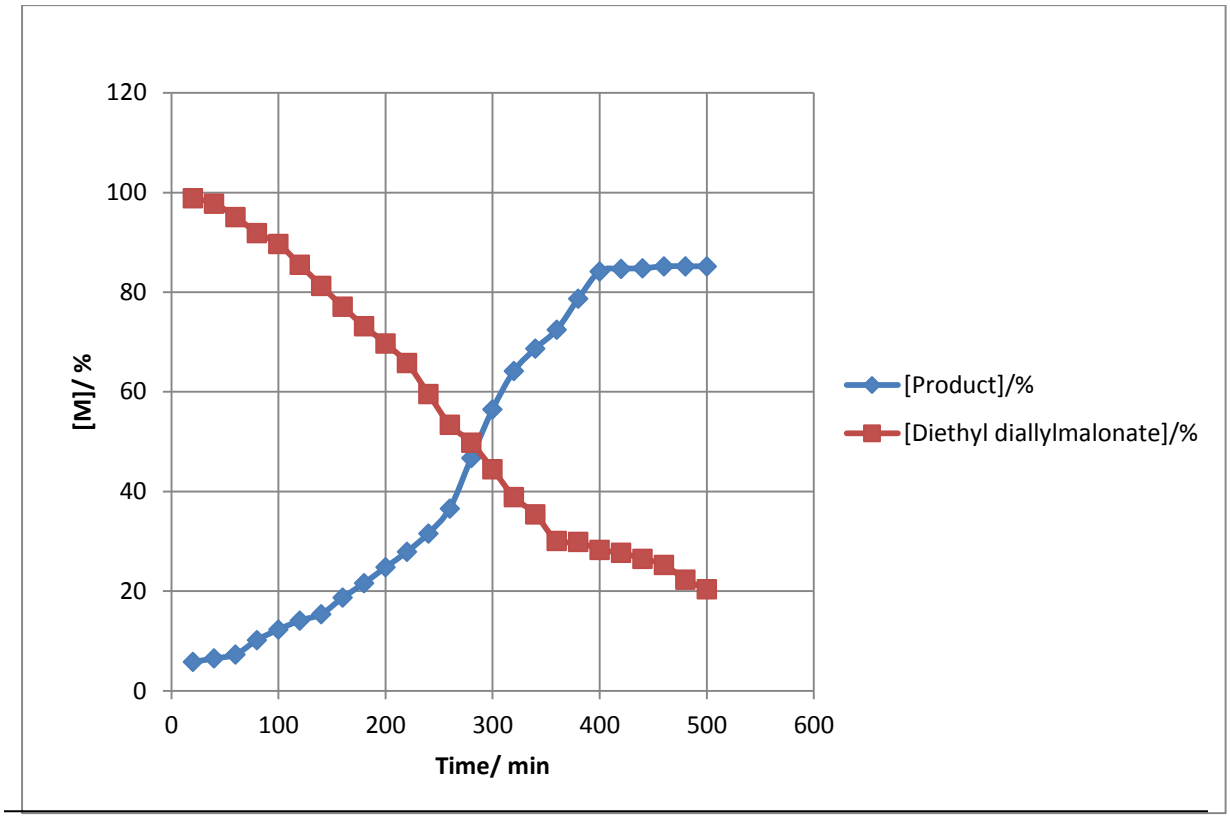

Figure 4.7: Representation plot of Diethyl diallylmalonate and its corresponding cyclopentene diester concentrations vs time. The filled diamonds are the data points.

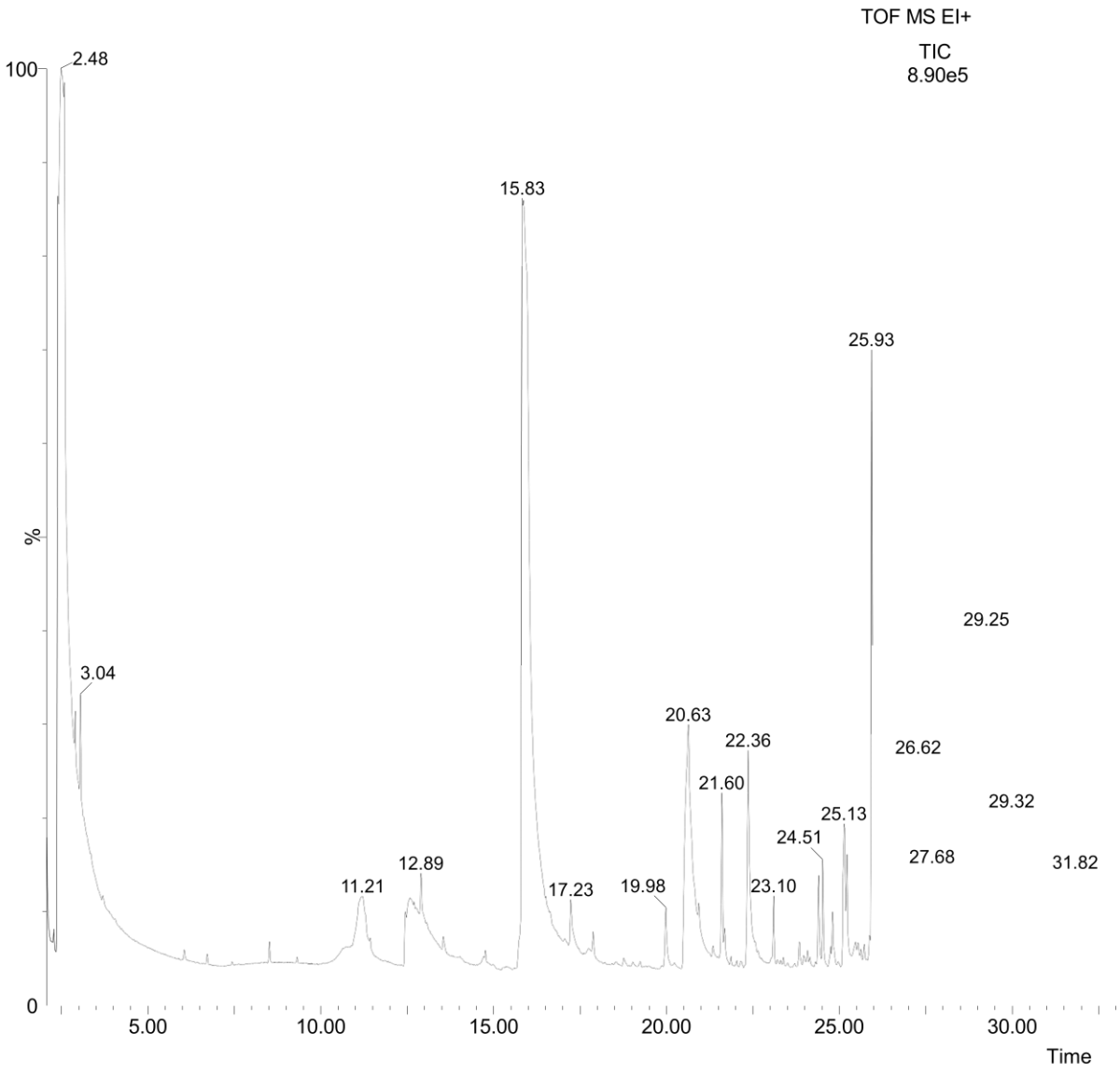

Figure 4.8: GC trace obtained from the RCM reaction of Diethyl diallylmalonate with complex 4.9

The information obtained from the above experiment can be summarised as follows; where,

Pk = Peak assignment number,

RT = Retention time of product on column / mins,

Pr = Product assignment to peak in question,

EIMS = Electron impact mass spectrum of product, *m/z*

[a] = *m/z,*

[b] = Relative intensities.

Obviously one cannot assign all peaks, but below is a compressed summation of data attained.

Pk 1 with an *RT* of 15.83 although somewhat broadened gives the expected *Pr* corresponding to the ring closed cycloolefin product 4.14 with its correct *EIMS* assignment, which is (M^+, 212[a], 100%) (Figure 4.8). *Pk* 2 with an *RT* of 20.63 gives a *Pr* analogous to the diethyl diallylmalonate 4.13 with *EIMS* giving (M^+, 240[a], 100%) (Figure 4.9). *Pk* 3 with an *RT* of 24.51 represents the ruthenium pre catalyst 4.9 used in this experiment, giving an *EIMS* of (M^+, 668[a], 17%).

Most of the remaining peaks in the GC trace in question can be put down to (a) minor impurities, and (b) mostly unidentifiable, which bear resemblance to possible metathesis products.

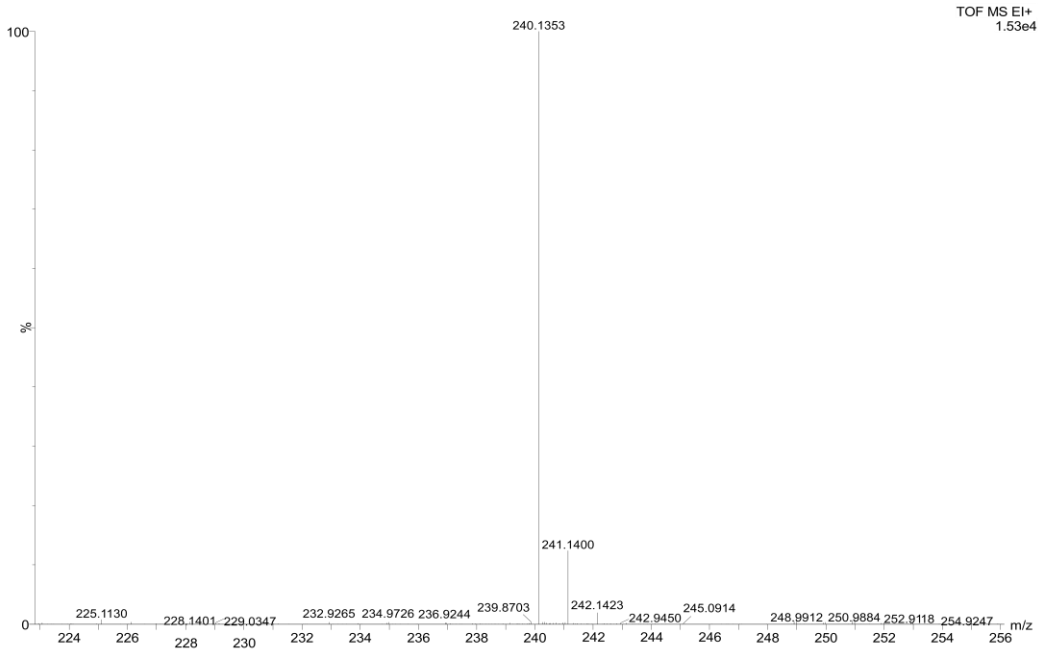

Figure 4.9: MS of Diethyl diallylmalonate

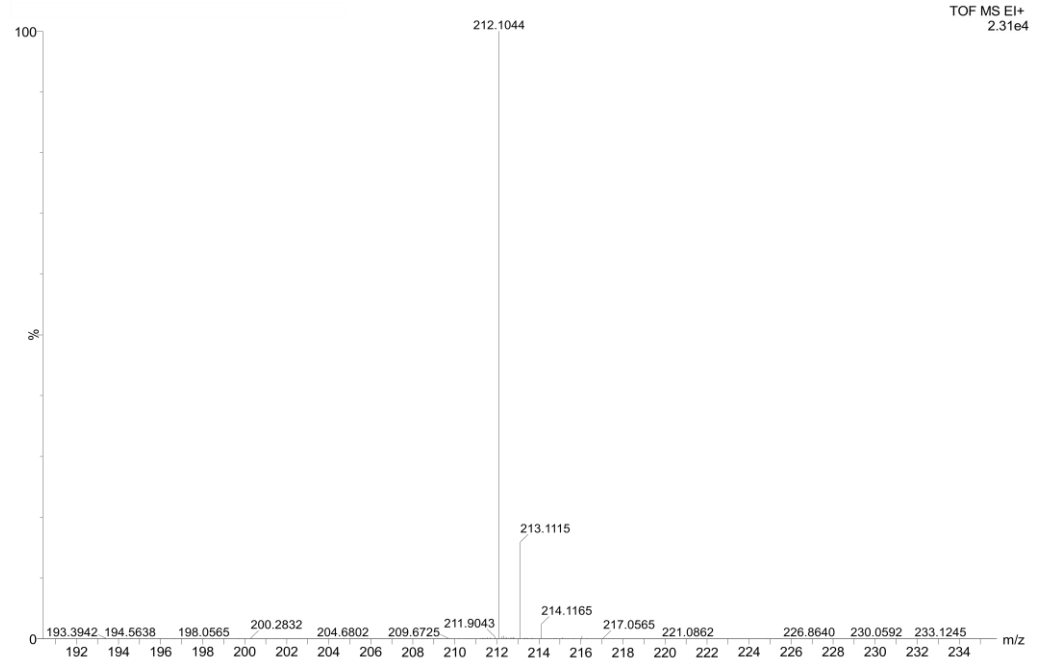

Figure 4.10: MS of the ring closed product of Diethyl diallylmalonate in the presence of the Ruthenium pre-catalyst 4.9

4.5. Attempted Reactions

Scheme 4.8 below gives a simplified graphical representation of some attempted reactions of dichloro(3-phenyl indenylidene) [*fac*-η^3-*cis,cis*-1,5,9-triethyl-1,5,9-triphospha cyclododecane] ruthenium(II), (4.9) with AgOTf and $AgBF_4$ in 1:1 and 1:2 molar ratios with $CDCl_3$ and CD_3CN solvents. The purpose of these reactions is to obtain the cationic compound of complex 4.9 to check the differences in reactivities between different catalysts.

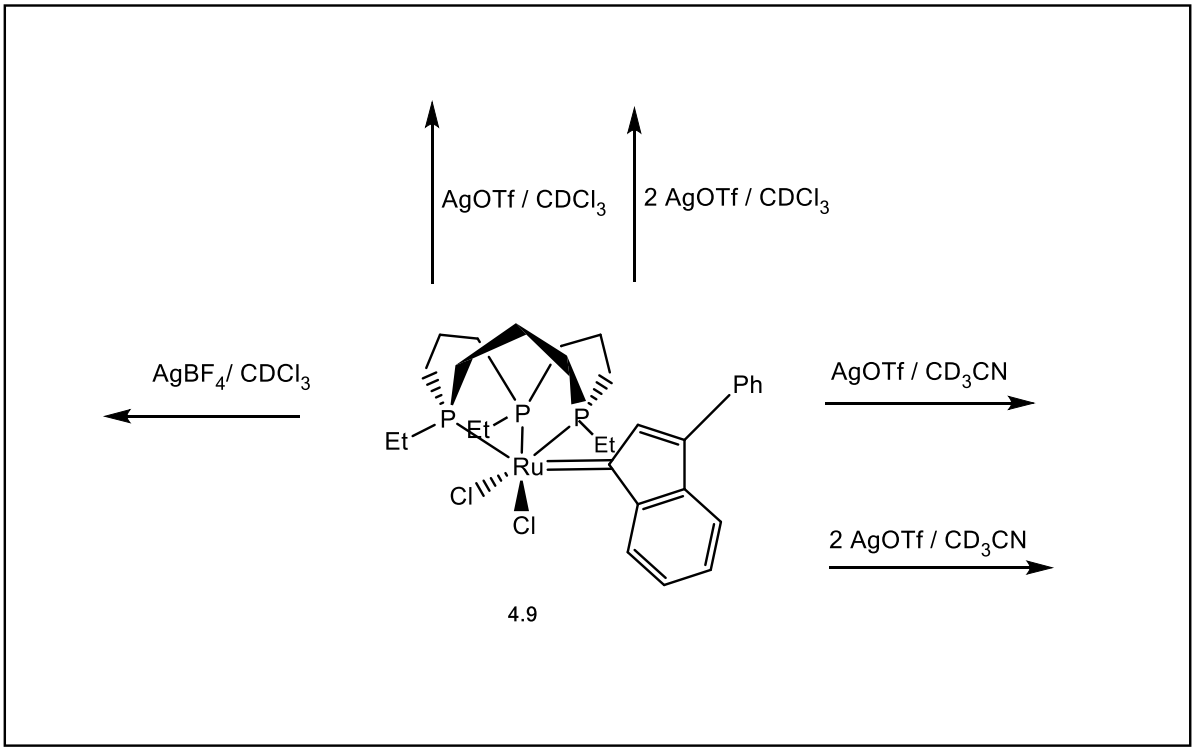

Scheme 4.8: Attempted reactions in order to prepare cationic compounds of complex 4.9.

4.5.1. Discussion

The reaction characterisation in Scheme 4.9 did not prove the desired product and the altered reaction conditions did not improved the reactions towards the desired product. The failure of these reactions may either be one or more reasons listed below; (a) the reaction failed to work, (b) characterisation was minimal, (c) insufficient compound stability to obtain reasonable characterisation, (d) acetonitrile might have shut the reaction down by competing for coordination or (e) low compound purity, which could not be increased by the usual purification methods.

4.6. Conclusion

The reactions of [12]-ane-P_3 ligands with d^6 Ru(II) precursor complexes readily gave rise to facially co-ordinated complexes in which other anionic or neutral ligands are restricted to a mutually *cis* coordination environment. Also, these Ru(II) complexes are significantly more kinetically inert than similar complexes with linear tridentate ligands.

Due to the particular steric and electronic environment, provided by the ligands the vinylidene ruthenium complexes exhibit some interesting activity and selectivity. Combining vinylidene ligands with other specific ligands, in the coordination sphere of the ruthenium core, allows further access to efficient ruthenium metathesis pre-catalysts.

The prepared ruthenium indenylidene complex (4.9), emerge as a quite efficient and versatile ring closing metathesis pre-catalyst. This complex has proved to be rather robust, stable upon heating and even left to stand for extended periods without decomposition.

4.7. Experimental

4.7.1. General

Techniques and Instruments*:* All reactions were carried out in an atmosphere of dry argon. All solvents were dried by boiling under reflux over standard drying agents. The compounds allylphosphine, [12]-ane-$P_3(Et)_3$, [12]-ane-$P_3(^iPr)_3$, dichlorotetra(dimethylsulphoxide) ruthenium(II) and di-μ-chloro-(η^4-cycloocta-1,5-diene)ruthenium(II) were prepared by literature methods. All other reagents including Ruthenium starting materials and diethyl diallylmalonate were obtained from the Aldrich Chemical Company and, where appropriate, were degassed before use. The NMR spectra were recorded on a Bruker DPX-500 instrument at 500 MHz (^{1}H), and 125.75MHz (^{13}C), Bruker DPX-400 instrument at 400 MHz and 100 MHz (^{13}C), Jeol Lamda Eclipse 300 at 121.65 MHz (^{31}P), 75.57 MHz (^{13}C). ^{1}H and ^{13}C chemical shifts are quoted in ppm relative to residual solvent peaks, and ^{31}P NMR chemical shifts quoted in ppm (δ) relative to 85% external H_3PO_4 (δ = 0ppm) . The infra-red spectra were recorded on a Nicolet 510 FT-IR spectrometer and the samples were prepared under Argon atmosphere as a KBr disk. Mass spectra of all the samples have been measured by direct injection into a Waters Low Resolution ZQ Mass Spectrometer fitted with ESCI source. Elemental analysis was performed by Warwick University Analytical Service.

X-Ray Crystallography*:* Data collections were carried out on a Bruker Kappa CCD diffractometer at 150(2) K with Mo $K\alpha$ irradiation (graphite monochromator). Empirical absorption corrections were performed using equivalent reflections. For the solution and refinement of the structures, the program package SHELXL 97 was employed. H atoms were placed into calculated positions and included in the last cycles of refinement. Crystal structure and refinement data are collected in Appendix A.

4.7.2. Preparation of dichloro(dimethyl sulphoxide) [*fac-η³-cis,cis*-1,5,9-triethyl-1,5,9-triphosphacyclododecane]ruthenium(II), 4.2

A solution of [12]-ane-$P_3(Et)_3$ (0.326 mmol, 100 mg) in dichloromethane(15 ml) was added drop wise to a solution of dichlorotetra(dimethyl sulphoxide)ruthenium(II) (0.326 mmol, 158 mg) in dichloromethane (15 ml) and was gently refluxed for 1 hour. The solvent was removed *in vacuo*, followed by recrystallisation of the oily residue from hot toluene gave 4.2 as a yellow microcrystalline solid (0.172 mmol, 126 mg, 63.0%). Analysis found (calculated): C, 39.72 (40.13); H, 7.82 (7.53). MS(ES), *m/z*: 478 (6%, $[M\text{-}DMSO]^+$). NMR ($CDCl_3$): $^{31}P\{^1H\}$, δ 36.36 ppm (s). ^1H NMR (360 MHz, 27 ºC), δ (ppm): 1.60 (br m, PCH_2); 1.29 (br m, PCH_2CH_2); 1.08 (br m, PCH_2CH_3); 1.72 (br m, PCH_2CH_3); 2.87 (s, CH_3SOCH_3). $^{13}C\{^1H\}$ NMR (90 MHz, 27 ºC), δ (ppm): 27.60 (d, $^1J_{(P\text{-}C)}$ 17Hz, PCH_2); 18.10 (br s, PCH_2CH_2); 25.9 (d, $^1J_{(P\text{-}C)}$, 50Hz, PCH_2CH_3); 15.11 (br s, PCH_2CH_3); 46.8 (s, CH_3SOCH_3). IR/cm^{-1} (KBr): ν(S-O) 1150 cm^{-1} (br) and 912 cm^{-1} (br); ν(Ru-Cl) 325 cm^{-1} (weak) and 302 cm^{-1} (weak).

4.7.3. Preparation of dichloro(dimethyl sulphoxide) [*fac-η³-cis,cis*-1,5,9-triisopropyl-1,5,9-triphosphacyclododecane]ruthenium(II), 4.3

A solution of [12]-ane-$P_3(iPr)_3$ (0.20 mmol, 69.7 mg) dissolved in dichloromethane(15 ml) was added to a solution of dichlorotetra(dimethyl sulphoxide)ruthenium(II) (0.20 mmol, 96.9 mg) in dichloromethane (15 ml) and was stirred for 4 hrs at room temperature. The solvent was removed *in vacuo*, followed by recrystallisation of the oily residue from hot toluene gave 4.3 as a yellow solid (0.05 mmol, 57 mg, 63.0%). Analysis found (calculated): C, 36.52 (36.69); H, 6.96 (7.06). MS(ES), *m/z*: 520 (7%, ($[M\text{-}DMSO]^+$), NMR ($CDCl_3$): $^{31}P\{^1H\}$, δ 37.44 ppm (s). ^1H NMR

(360 MHz, 27 ºC), δ (ppm): 1.72 (br m, PCH_2CH_2); 1.60 (br m, PC*H* and PCH_2); 1.08 (br S, C*H*); 2.91 (s, CH_3SOCH_3). $^{13}C\{^1H\}$ NMR, δ (ppm): 32.5 (br, m, PCH_2); 21.5 (m, PCH_2CH_2); 22.5 (m, PCH); 18.5(s, CH_3); 46.8 (s, CH_3SOCH_3).). IR/cm^{-1} (KBr): ν(S-O) 1155 cm^{-1} (br) and 920 cm^{-1} (br); ν(Ru-Cl) 320 cm^{-1} (weak) and 307 cm^{-1} (weak).

2.7.4. Preparation of tris(μ-chloro)bis-fac-(η³-1,5,9-triethyl-1,5,9-triphosphacyclododecane)(ruthenium(II)) chloride, 4.4:

A solution of [12]-ane-$P_3(Et)_3$ (30.6 mg, 0.10 mmol) in dichloromethane (15 cm^3) was added drop wise to a solution of di-μ-chloro-(η⁴-cycloocta-1,5-diene)ruthenium(II) (25.0 mg, 0.05 mmol) in dichloromethane (15 cm^3) and the resultant mixture was stirred for 2h at room temperature. Solvent was removed *in vacuo* followed by recrystallisation from CH_2Cl_2/petrol to give 4.4 as a yellow microcrystalline solid. (35 mg, 37%) Analysis found (calculated): C, 39.81 (39.11); H, 7.95 (7.22), MS(ES), *m/z*: 921 [50 %, (M^+-H)]. NMR ($CDCl_3$): $^{31}P\{^1H\}$, δ 23.59 ppm (s, cation). ^1H NMR (360 MHz, 27 ºC), δ (ppm): 1.70 (br m, PCH_2); 1.89 (br m, PCH_2CH_2); 1.10 (br m, PCH_2CH_3); 1.28 (br m, PCH_2CH_3). $^{13}C\{^1H\}$ NMR (90 MHz, 27 ºC), δ (ppm): 25.60 (d, $^1J_{(P-C)}$ 50 Hz, PCH_2); 23.40 (m, PCH_2CH_2); 25.9 (d, $^1J_{(P-C),}$ 50Hz, PCH_2CH_3); 18.11 (br s, PCH_2CH_3). IR/cm^{-1} (KBr): ν(Ru-Cl) 275 cm^{-1} (vw).

2.7.5. Preparation of tris(μ-chloro)bis-fac-(η³ -1,5,9-triisopropyl-1,5,9-triphosphacyclododecane)(ruthenium(II)) chloride, 4.5:

A solution of [12]-ane-$P_3(^iPr)_3$ (34.8 mg, 0.10 mmol) in dichloromethane (15 cm^3) was added dropwise to a solution of di-μ-chloro-(η⁴-cycloocta-1,5-diene)ruthenium(II) (25.0 mg, 0.05 mmol)

in dichloromethane (15 cm^3) and the resultant mixture stirred for 2h at room temperature. Evaporation to dryness *in vacuo* gave a yellow colour residue which was recrystallised from CH_2Cl_2/petrol to give 4.5 as light yellow colour crystals (41 mg, 35%). Analysis found (calculated): C, 41.47 (41.54); H, 7.48 (7.50), MS(ES), *m/z*: 1004.14 [45%, (M^+-H)]. NMR ($CDCl_3$): $^{31}P\{^1H\}$ NMR, δ (ppm): 25.4 (*s*, cation). ^1H NMR (360 MHz, 27 ºC), δ(ppm): 1.75 (br m, PCH_2CH_2); 1.45 (br m, PC*H* and PCH_2); 1.05(br s, C*H*);. $^{13}C\{^1H\}$ NMR (90 MHz, 27 ºC), δ (ppm): 31.5 (br m, PCH_2); 21.5 (m, PCH_2CH_2); 18.5 (m, PCH); 17.5(s, CH_3); IR/cm^{-1} (KBr): ν(Ru-Cl) 270 cm^{-1} (vw).

4.7.6. Preparation of Dichloro(3-phenyl indenylidene)[*fac-η³-cis,cis*-1,5,9-triethyl-1,5,9-triphosphacyclododecane]ruthenium(II), 4.9

A solution of 4.2 (0.209 mmol, 100 mg) in toluene (10 ml) was added drop wise to a solution of 1,1-diphenylprop-2-yn-1-ol (0.313 mmol, 65 mg) in toluene (10 ml) and was gently refluxed for 2 hours. The solvent was removed in *vacuo* and a bright orange-yellow oily product was obtained. It was then followed by recrystallisation from hot petrol, where 4.9 was obtained as a yellow microcrystalline solid (0.117 mmol, 92 mg, 32.0%). Analysis found (calculated): C, 54.12 (53.89); H, 6.82 (6.48). MS(ES), *m/z*: 668 (50%, $[M]^+$). NMR ($CDCl_3$): $^{31}P\{^1H\}$, δ 39.79 ppm (s). ^1H NMR (360 MHz, 27 ºC), δ (ppm): 7.34 (s, Ru=CCH); 6.03 – 6.38 (m, 4 H); 6.8 – 7.4 (m, 6 H); 1.60 (br m, PCH_2); 1.29 (br m, PCH_2CH_2); 1.08 (br m, PCH_2CH_3); 1.72 (br m, PCH_2CH_3). $^{13}C\{^1H\}$ NMR (90 MHz, 27 ºC), δ (ppm): 27.60 (d, $^1J_{(P-C)}$ 17Hz, PCH_2); 18.10 (br s, PCH_2CH_2); 25.9 (d, $^1J_{(P-C)}$, 50Hz, PCH_2CH_3); 15.11 (br s, PCH_2CH_3); 46.8 (s, CH_3SOCH_3). IR/cm^{-1} (KBr): ν(Ru-Cl) 328 cm^{-1} (weak) and 300 cm^{-1} (weak).

4.7.7. General Procedure for Ring Closing Metathesis Catalytic testing

The general procedure followed was similar to that of Nolan *et al*[41] An example of the methodology follows:

In a dry box, the catalyst precursor, Dichloro(3-phenyl indenylidene)[*fac*-η^3-*cis,cis*-1,5,9-triethyl-1,5,9-triphosphacyclododecane] ruthenium(II) (4.9), (25 mol %) was accurately weighed in a screw-capped NMR tube and was dissolved in CD_2Cl_2 (0.4 ml). Diethyldiallyl malonate was then added to the solution, and the NMR tube was heated under Ar to 60 ºC. Product formation and diene disappearance were monitored by integrating the allylic methylene peaks in the ^{1}H NMR and a sample of this was used for the GC-MS analysis.

4.8. References

1. Tellmann, K., Humphries, M., Gibson, V., Rzepa, H., *Organometallics*, 2004, **23**, 5503.

2. Ogasawara, M., Macgregor, S. S., Streib, W. E., Folting, K., Eisenstein, O., Caulton, K., *J. Am. Chem. Soc.,***1995,** 117, 8869.

3. Treichel,P., Wong,W., *Inorg. Chim. Acta.*, 1979, **33**, 171.

4. Bianchini, C., Meli, A., Moneti, S., Vizza, F., *Organometallics,* **1998**, 17, 2636**.**

5. Hallman, P. S., McGarvey, B. R., Wilkinson, G., *J. Chem. Soc. (A),* **1968**, 3143.

6. Sanchez-Delgado, R. A., Bradley, J. S., Wilkinson, G., *J. Chem. Soc., Dalton Trans.,* **1976**, 399.

7. Ivin, K.J., *Olefin Metathesis,* Academic Press, London, 1983.

8. (a) Grubbs, R. H., *Comprehensive Organometallic Chemistry,* Wilkinson, G., ed., Pergamon Press Ltd., New York, **1982**, Vol. 8, pp. 499-551. (b) Grubbs, R. H., Tumas, W., *Science,* **1989**, 243, 907-915.

9. (a) Fu, G. C., Grubbs, R. H., *J. Am. Chem. Soc.,* **1992**, 114, 5426-5427. (b) Fu, G. C., Grubbs, R. H., *J. Am. Chem. Soc.,* **1992**, 114, 7324-7325. (c) Fu, G. C., Grubbs, R. H., *J. Am. Chem. Soc.,* **1993**, 115, 3800-3801.

10. Frenzel,U., Weskamp, F. , Kohl, W., Schattenmann, O., Nuyken, W. ,Herrmann,W., *J. Organomet. Chem.*, 1999, **586**, 263.

11. Davies, S. G., Simpson, S. J., Felkin, H., Fillebeen-Khan, T., *Organometallics,* 1983, **2,** 539.

12. J. A. Statler, G. Wilkinson, *J. Chem. Soc., Dalton Trans*., 1984, 1731.

13. (a) P. W. Armit, T. A. Stephenson**,** *J. Organomet. Chem.*, 1973, **57**, 80. (b) Rhodes, L. F., Sorato, C., Venanzi, L. M., Bachechi, F., *Inorg. Chem.,* **1988**, 27,604. (c) Edwards, P. G., Fleming, J. S., Coles, S. J., Hursthouse, M. B., *J. Chem. Soc., Dalton. Trans.,***1995**, 1139.

14. (a) Pothupitiya, T. K., *Doctoral Thesis*, 2010, Cardiff University. (b) Edwards, P. G., Fleming, J. S., Coles, S. J., Hursthouse, M. B., *J. Chem. Soc., Dalton. Trans.,***1997**, 3201-3206.

15. Jafarpour, L., Schanz, H. J., Stevens, E. D., Nolan S. P., *Organometllics,* **1999**, 18, 5416.

16. Davies, S. G., Simpson, S. J., Felkin, H., Khan, T. F., *Organometallics,* 1983, **2**, 539.

17. Bruce, M. I., Swincer, A. G., *Adv. Organomet. Chem.* **1983**, 22, 59.

18. Agadec, R. L., Roman, E., Toupet, L., Muller, U.,Dixneuf, P. H., *Organometallics,***1994**, 13, 5030-5039.

19. Dorwald, F. Z., *Metal Carbenes in Organic synthesis,* Wiley VCH, Weinheim, 1999.

20. Schwab, P., Grubbs, R. H., Ziller, J. W., *J. Chem. Soc.,* 118, 1996, 100.

21. Nguyen, S. B., Grubbs, R. H., Ziller, J. W., *J. Am. Chem. Soc.,* 115, 1993, 9858.

22. Katayama, H., Urushima, H., Ozawa, F., *Organometallics,* 606, 2000, 16-25.

23. Schwab, P., France, M. B., Ziller, J. W., Grubbs, R. H., *Angew. Chem., Int. Ed. Engl.* **1995**, *34*, 2039-2041. (b) Schwab, P., Grubbs, R. H., Ziller, J. W., *J. Am. Chem. Soc.* **1996**, *118*, 100-110. (c) Dias, E. L., Nguyen, S. T., Grubbs, R. H., *J. Am. Chem. Soc.* **1997**, *119*, 3887- 3897.

24. Collman, J. P., Hegedus, L. S., Norton, J. R., Finke, R. J. *Principles and Application of Organotransition Metal Chemistry*, 2nd ed., University Science, Mill Valley, CA, 1987.

25. Huang, J., Stevens, E. D., Nolan, S. P. *J. Am. Chem. Soc.,* **1999**, *121*, 2674-2678. (b) Huang, J., Schanz, H. -J., Stevens, E. D., Nolan, S. P., *Organometallics* **1999**, *18*, 2370-2375. (c) Wanzlick, H.-W., *Angew. Chem., Int. Ed. Engl.* **1962**, *1*, 75-80. (d) Arduengo, A. J., Krafczyk, R., *Chem. Z.* **1998**, *32*, 6-14. (e) Arduengo, A. J., Krafczyk, R. Marshall, W. J., *Angew. Chem.* **1998**, *110*, 2062-2064.

26. Arduengo, A. J., Harlow, R. L., Kline, M. J., *J. Am. Chem. Soc.* **1991**, *113*, 361-363.

27. Zhang. C., Huang, J., Trudell, M. L., Nolan, S. P., *J. Org. Chem.*,**1999**, *64*, 3804-3805.

28. (a) Jafarpour, L., Huang, J., Stevens, E. D., Nolan, S. P., *Organometallics* **1999**, *18*, 3760-3763. (b) Scholl, M., Trnka, T. M., Morgan, J. P., Grubbs, R. H., *Tetrahedron Lett.* **1999**, *40*, 2247-2250. (c) Weskamp, T., Schattenmann, W. C., Spiegler, M., Hermann, W. A., *Angew. Chem., Int. Ed.* **1998**, *37*, 2490-2493. (c) Weskamp, T., Schattenmann, W. C., Spiegler, M., Hermann, W. A., *Angew. Chem., Int. Ed.* **1999**, *38*, 262. (d) Ackermann, L., Fu¨ rstner, A., Weskamp, T.,Kohl, F., Herrmann, W. A., *Tetrahedron Lett.* **1999**, *40*, 4787-4790.

29. Fu¨ rstner, A., Picquet, M., Bruneau, C., Dixneuf, P. H., *Chem.Commun.* **1998**, 1315-1316.

30. Fu¨ rstner, A., Hill, A. F., Liebl, M., Wilton-Ely, J. D. E. T., *Chem. Commun.* **1999**, 601-602.

31. Love, J. A., Morgan, J. P., Tranka, T. M., Grubbs, R. H., *Angew. Chem Int. Ed.,* **2002**, 41, 4035.

32. Nguyen, S. T., Johnson, L. K., Grubbs, R. H., Ziller, J. W., *J. Am. Chem. Soc.,* **1992**, 114, 3974.

33. (a) De Clercq, B., Verpoort, F., *Adv. Synth. Catal.,* **2002**, 344, 639. (b) Garber, S. B., Kingsbury, J. S., Gray, B. L., Hoveyda, A. H., *J. Am. Chem. Soc.,* **2000**, 122, 8168.

34. Denk, K., Fridgen, J., Herrmann, W. A., *Adv. Synth. Catal.,* **2002**, 344, 666.

35. Van der Schaaf, P. A., Kolly, R., Kirner, H.-J., Rime, F., Muhlebach, A., Hafner, A., *J. Organomet. Chem.,* **2000**, 606, 65.

36. (a) Herndon, J. W.,*Coord. Chem Rev.,***2002**, 227, 1. (b) Trnka, T. M., Grubbs, R. H., *Acc. Chem. Res.,* **2001**, 34, 18. (c) Jafarpour, L., Nolan, S. P., *J. Organomet. Chem.,* **2001**, 617,17.

37. Dias, E. L., Nguyen, S. T., Grubbs, R. H., *J. Am. Chem. Soc.,* **1997**, 119, 3887.

38. Scholl, M., Ding, S., Lee, C. W., Grubbs, R. H., *Org. Lett.,* **1999**, 1, 953.

39. (a) Sanford, M. S., Ulman, M., Grubbs, R. H., *J. Am. Chem. Soc.,* **2001**, 123, 749. (b) Sanford, M. S., Love, J. A., Grubbs, R. H., *J. Am. Chem. Soc.,* **2001**, 123, 6543.

40. Cheng, S., Jones, L., Wang, C., Henling, L. M., Grubbs, R. H., *Organometallics,* **1998**, 17, 3460.

41. Jafarpour, L., Schanz, H-J., Stevens, E. D., Nolan, S. P., *Organometallics* **1999**, *18,* 5416-5419.

42. Dragutan, V., Dragutan, I., *Platinum Metals Rev.,* 2004, **48**, (4), 148-153.

43. Dragutan, V., Dragutan, I., *Platinum Metals Rev.,* 2005, **49**, (1), 33-40

Appendix I

Crystal data and structure refinement for [12]-ane-P_3Et_3[Cu(μ-Cl)(CuCl)] (2.28).

Table 1

Identification code	shelx	
Empirical formula	C15 H33 Cl2 Cu2 P3	
Formula weight	504.30	
Temperature	150(2) K	
Wavelength	0.71073 Å	
Crystal system	Orthorhombic	
Space group	P b c a	
Unit cell dimensions	a = 8.59020(10) Å	□= 90°.
	b = 15.6586(3) Å	□= 90°.
	c = 32.0807(5) Å	□ = 90°.
Volume	4315.19(12) $Å^3$	
Z	8	
Density (calculated)	1.552 Mg/m^3	
Absorption coefficient	2.436 mm^{-1}	
F(000)	2080	
Crystal size	0.250 x 0.200 x 0.150 mm^3	
Theta range for data collection	2.988 to 27.484°.	
Index ranges	-11<=h<=11, -20<=k<=20, -41<=l<=41	
Reflections collected	9299	
Independent reflections	4940 [R(int) = 0.0355]	
Completeness to theta = 25.242°	99.7 %	
Refinement method	Full-matrix least-squares on F^2	
Data / restraints / parameters	4940 / 110 / 231	
Goodness-of-fit on F^2	1.019	
Final R indices [I>2sigma(I)]	R1 = 0.0436, wR2 = 0.0958	
R indices (all data)	R1 = 0.0671, wR2 = 0.1065	
Extinction coefficient	0.00108(18)	
Largest diff. peak and hole	0.762 and -0.900 $e.Å^{-3}$	

Table 2: Atomic coordinates (x 10^4) and equivalent isotropic displacement parameters ($Å^2$x 10^3) for [12]-ane-P_3Et_3[Cu(μ-Cl)(CuCl)]. U(eq) is defined as one third of the trace of the orthogonalized U^{ij} tensor.

	x	y	z	U(eq)
C(1)	198(11)	3666(5)	4033(2)	46(2)
C(2)	534(7)	3283(4)	4453(2)	35(1)
C(3)	-311(7)	2477(3)	4598(2)	34(1)
C(4)	-1005(5)	781(4)	4492(2)	61(1)
C(5)	-2394(5)	810(3)	4200(1)	57(1)
C(6)	-2177(5)	414(3)	3777(1)	52(1)
C(7)	-2314(4)	1719(3)	3131(1)	42(1)
C(8)	-2434(5)	2624(3)	3299(1)	50(1)
C(9)	-1065(5)	3207(3)	3216(1)	45(1)
C(10)	2084(6)	3730(3)	3297(1)	49(1)
C(11)	2696(6)	3338(3)	2897(1)	62(1)
C(12)	2094(5)	1206(2)	4750(1)	38(1)
C(13)	2909(5)	393(3)	4622(1)	45(1)
C(14)	-731(5)	150(3)	3004(1)	41(1)
C(15)	251(5)	422(3)	2636(1)	47(1)
P(1)	642(1)	3051(1)	3554(1)	34(1)
P(2)	600(1)	1533(1)	4376(1)	37(1)
P(3)	-961(1)	986(1)	3397(1)	31(1)
Cl(1)	3535(1)	1120(1)	3460(1)	39(1)
Cl(2)	4944(1)	3183(1)	4229(1)	46(1)
Cu(1)	1068(1)	1665(1)	3691(1)	25(1)
Cu(2)	4085(1)	2165(1)	3862(1)	36(1)
C(1A)	-260(20)	3668(11)	3978(3)	39(3)
C(2A)	-285(19)	3356(8)	4386(4)	37(2)
C(3A)	497(18)	2670(6)	4597(4)	40(3)

Table 3: Bond lengths [Å] and angles [°] for [12]-ane-P_3Et_3[Cu(μ-Cl)(CuCl)]

C(1)-C(2)	1.503(6)	C(14)-C(15)	1.513(6)
C(1)-P(1)	1.853(6)	C(14)-P(3)	1.827(4)
C(1)-H(1A)	0.9900	C(14)-H(14A)	0.9900
C(1)-H(1B)	0.9900	C(14)-H(14B)	0.9900
C(2)-C(3)	1.528(6)	C(15)-H(15A)	0.9800
C(2)-H(2A)	0.9900	C(15)-H(15B)	0.9800
C(2)-H(2B)	0.9900	C(15)-H(15C)	0.9800
C(3)-P(2)	1.818(5)	P(1)-C(1A)	1.841(9)
C(3)-H(3A)	0.9900	P(1)-Cu(1)	2.2444(10)
C(3)-H(3B)	0.9900	P(2)-C(3A)	1.918(8)
C(4)-C(5)	1.519(6)	P(2)-Cu(1)	2.2441(10)
C(4)-P(2)	1.851(5)	P(3)-Cu(1)	2.2492(10)
C(4)-H(4A)	0.9900	Cl(1)-Cu(2)	2.1368(10)
C(4)-H(4B)	0.9900	Cl(1)-Cu(1)	2.4024(9)
C(5)-C(6)	1.502(6)	Cl(2)-Cu(2)	2.1142(11)
C(5)-H(5A)	0.9900	Cu(1)-Cu(2)	2.7627(6)
C(5)-H(5B)	0.9900	C(1A)-C(2A)	1.397(8)
C(6)-P(3)	1.839(4)	C(1A)-H(1A1)	0.9900
C(6)-H(6A)	0.9900	C(1A)-H(1A2)	0.9900
C(6)-H(6B)	0.9900	C(2A)-C(3A)	1.435(8)
C(7)-C(8)	1.520(6)	C(2A)-H(2A1)	0.9900
C(7)-P(3)	1.843(4)	C(2A)-H(2A2)	0.9900
C(7)-H(7A)	0.9900	C(3A)-H(3A1)	0.9900
C(7)-H(7B)	0.9900	C(3A)-H(3A2)	0.9900
C(8)-C(9)	1.513(6)		
C(8)-H(8A)	0.9900	C(2)-C(1)-P(1)	119.8(5)
C(8)-H(8B)	0.9900	C(2)-C(1)-H(1A)	107.4
C(9)-P(1)	1.840(4)	P(1)-C(1)-H(1A)	107.4
C(9)-H(9A)	0.9900	C(2)-C(1)-H(1B)	107.4
C(9)-H(9B)	0.9900	P(1)-C(1)-H(1B)	107.4
C(10)-C(11)	1.518(6)	H(1A)-C(1)-H(1B)	106.9
C(10)-P(1)	1.829(4)	C(1)-C(2)-C(3)	120.7(6)
C(10)-H(10A)	0.9900	C(1)-C(2)-H(2A)	107.1
C(10)-H(10B)	0.9900	C(3)-C(2)-H(2A)	107.1
C(11)-H(11A)	0.9800	C(1)-C(2)-H(2B)	107.1
C(11)-H(11B)	0.9800	C(3)-C(2)-H(2B)	107.1
C(11)-H(11C)	0.9800	H(2A)-C(2)-H(2B)	106.8
C(12)-C(13)	1.510(5)	C(2)-C(3)-P(2)	110.4(4)
C(12)-P(2)	1.829(4)	C(2)-C(3)-H(3A)	109.6
C(12)-H(12A)	0.9900	P(2)-C(3)-H(3A)	109.6
C(12)-H(12B)	0.9900	C(2)-C(3)-H(3B)	109.6
C(13)-H(13A)	0.9800	P(2)-C(3)-H(3B)	109.6
C(13)-H(13B)	0.9800	H(3A)-C(3)-H(3B)	108.1
C(13)-H(13C)	0.9800	C(5)-C(4)-P(2)	116.2(3)

C(5)-C(4)-H(4A)	108.2	H(11B)-C(11)-H(11C)	109.5
P(2)-C(4)-H(4A)	108.2	C(13)-C(12)-P(2)	112.5(3)
C(5)-C(4)-H(4B)	108.2	C(13)-C(12)-H(12A)	109.1
P(2)-C(4)-H(4B)	108.2	P(2)-C(12)-H(12A)	109.1
H(4A)-C(4)-H(4B)	107.4	C(13)-C(12)-H(12B)	109.1
C(6)-C(5)-C(4)	116.6(4)	P(2)-C(12)-H(12B)	109.1
C(6)-C(5)-H(5A)	108.1	H(12A)-C(12)-H(12B)	107.8
C(4)-C(5)-H(5A)	108.1	C(12)-C(13)-H(13A)	109.5
C(6)-C(5)-H(5B)	108.1	C(12)-C(13)-H(13B)	109.5
C(4)-C(5)-H(5B)	108.1	H(13A)-C(13)-H(13B)	109.5
H(5A)-C(5)-H(5B)	107.3	C(12)-C(13)-H(13C)	109.5
C(5)-C(6)-P(3)	118.0(3)	H(13A)-C(13)-H(13C)	109.5
C(5)-C(6)-H(6A)	107.8	H(13B)-C(13)-H(13C)	109.5
P(3)-C(6)-H(6A)	107.8	C(15)-C(14)-P(3)	113.4(3)
C(5)-C(6)-H(6B)	107.8	C(15)-C(14)-H(14A)	108.9
P(3)-C(6)-H(6B)	107.8	P(3)-C(14)-H(14A)	108.9
H(6A)-C(6)-H(6B)	107.1	C(15)-C(14)-H(14B)	108.9
C(8)-C(7)-P(3)	117.4(3)	P(3)-C(14)-H(14B)	108.9
C(8)-C(7)-H(7A)	108.0	H(14A)-C(14)-H(14B)	107.7
P(3)-C(7)-H(7A)	108.0	C(14)-C(15)-H(15A)	109.5
C(8)-C(7)-H(7B)	108.0	C(14)-C(15)-H(15B)	109.5
P(3)-C(7)-H(7B)	108.0	H(15A)-C(15)-H(15B)	109.5
H(7A)-C(7)-H(7B)	107.2	C(14)-C(15)-H(15C)	109.5
C(9)-C(8)-C(7)	116.6(4)	H(15A)-C(15)-H(15C)	109.5
C(9)-C(8)-H(8A)	108.2	H(15B)-C(15)-H(15C)	109.5
C(7)-C(8)-H(8A)	108.1	C(10)-P(1)-C(9)	101.3(2)
C(9)-C(8)-H(8B)	108.1	C(10)-P(1)-C(1A)	108.3(6)
C(7)-C(8)-H(8B)	108.2	C(9)-P(1)-C(1A)	91.6(5)
H(8A)-C(8)-H(8B)	107.3	C(10)-P(1)-C(1)	102.2(3)
C(8)-C(9)-P(1)	115.8(3)	C(9)-P(1)-C(1)	104.8(3)
C(8)-C(9)-H(9A)	108.3	C(1A)-P(1)-C(1)	13.5(6)
P(1)-C(9)-H(9A)	108.3	C(10)-P(1)-Cu(1)	122.69(16)
C(8)-C(9)-H(9B)	108.3	C(9)-P(1)-Cu(1)	111.94(14)
P(1)-C(9)-H(9B)	108.3	C(1A)-P(1)-Cu(1)	115.6(5)
H(9A)-C(9)-H(9B)	107.4	C(1)-P(1)-Cu(1)	111.9(2)
C(11)-C(10)-P(1)	112.4(3)	C(3)-P(2)-C(12)	105.8(2)
C(11)-C(10)-H(10A)	109.1	C(3)-P(2)-C(4)	96.8(3)
P(1)-C(10)-H(10A)	109.1	C(12)-P(2)-C(4)	102.3(2)
C(11)-C(10)-H(10B)	109.1	C(3)-P(2)-C(3A)	23.2(4)
P(1)-C(10)-H(10B)	109.1	C(12)-P(2)-C(3A)	92.9(4)
H(10A)-C(10)-H(10B)	107.9	C(4)-P(2)-C(3A)	118.8(5)
C(10)-C(11)-H(11A)	109.5	C(3)-P(2)-Cu(1)	112.69(19)
C(10)-C(11)-H(11B)	109.5	C(12)-P(2)-Cu(1)	122.82(14)
H(11A)-C(11)-H(11B)	109.5	C(4)-P(2)-Cu(1)	112.91(16)
C(10)-C(11)-H(11C)	109.5	C(3A)-P(2)-Cu(1)	106.5(4)
H(11A)-C(11)-H(11C)	109.5	C(14)-P(3)-C(6)	99.8(2)

C(14)-P(3)-C(7)	101.27(19)	C(2A)-C(1A)-P(1)	120.9(10)
C(6)-P(3)-C(7)	104.6(2)	C(2A)-C(1A)-H(1A1)	107.1
C(14)-P(3)-Cu(1)	122.98(13)	P(1)-C(1A)-H(1A1)	107.1
C(6)-P(3)-Cu(1)	113.02(15)	C(2A)-C(1A)-H(1A2)	107.1
C(7)-P(3)-Cu(1)	112.84(14)	P(1)-C(1A)-H(1A2)	107.1
Cu(2)-Cl(1)-Cu(1)	74.72(3)	H(1A1)-C(1A)-H(1A2)	106.8
P(2)-Cu(1)-P(1)	104.56(4)	C(1A)-C(2A)-C(3A)	134.1(13)
P(2)-Cu(1)-P(3)	103.24(4)	C(1A)-C(2A)-H(2A1)	103.7
P(1)-Cu(1)-P(3)	104.41(4)	C(3A)-C(2A)-H(2A1)	103.7
P(2)-Cu(1)-Cl(1)	115.33(4)	C(1A)-C(2A)-H(2A2)	103.7
P(1)-Cu(1)-Cl(1)	115.28(4)	C(3A)-C(2A)-H(2A2)	103.7
P(3)-Cu(1)-Cl(1)	112.69(4)	H(2A1)-C(2A)-H(2A2)	105.3
P(2)-Cu(1)-Cu(2)	89.99(3)	C(2A)-C(3A)-P(2)	122.9(9)
P(1)-Cu(1)-Cu(2)	85.27(3)	C(2A)-C(3A)-H(3A1)	106.6
P(3)-Cu(1)-Cu(2)	160.76(3)	P(2)-C(3A)-H(3A1)	106.6
Cl(1)-Cu(1)-Cu(2)	48.26(3)	C(2A)-C(3A)-H(3A2)	106.6
Cl(2)-Cu(2)-Cl(1)	172.17(4)	P(2)-C(3A)-H(3A2)	106.6
Cl(2)-Cu(2)-Cu(1)	130.65(4)	H(3A1)-C(3A)-H(3A2)	106.6
Cl(1)-Cu(2)-Cu(1)	57.02(3)		

Symmetry transformations used to generate equivalent atoms:

Table 4: Anisotropic displacement parameters ($Å^2 x\ 10^3$) for [12]-ane-P_3Et_3[Cu(μ-Cl)(CuCl)]. The anisotropic displacement factor exponent takes the form: $-2\pi^2[\ h^2 a^{*2} U^{11} + ... + 2\ h\ k\ a^*\ b^*\ U^{12}\ ]$

	U^{11}	U^{22}	U^{33}	U^{23}	U^{13}	U^{12}
C(1)	65(4)	35(3)	37(3)	-9(2)	-22(3)	32(3)
C(2)	35(3)	35(3)	35(3)	-13(2)	3(2)	6(2)
C(3)	29(3)	37(3)	35(3)	-4(2)	10(2)	6(2)
C(4)	40(2)	101(4)	43(3)	25(3)	10(2)	6(3)
C(5)	37(2)	80(3)	52(3)	13(3)	13(2)	-4(2)
C(6)	30(2)	69(3)	57(3)	21(2)	5(2)	-9(2)
C(7)	27(2)	53(2)	46(2)	1(2)	-6(2)	3(2)
C(8)	40(2)	57(3)	52(3)	3(2)	-6(2)	19(2)
C(9)	50(2)	40(2)	44(2)	8(2)	-10(2)	10(2)
C(10)	63(3)	32(2)	53(3)	7(2)	-11(2)	-14(2)
C(11)	73(3)	58(3)	54(3)	8(2)	9(3)	-21(3)
C(12)	48(2)	36(2)	31(2)	0(2)	-5(2)	5(2)
C(13)	50(2)	42(2)	44(2)	6(2)	-7(2)	13(2)
C(14)	37(2)	33(2)	51(2)	1(2)	-9(2)	-5(2)
C(15)	49(3)	48(2)	43(2)	-9(2)	0(2)	3(2)
P(1)	45(1)	27(1)	29(1)	-3(1)	-5(1)	6(1)
P(2)	40(1)	47(1)	25(1)	4(1)	5(1)	17(1)
P(3)	21(1)	36(1)	34(1)	5(1)	0(1)	-3(1)
Cl(1)	25(1)	41(1)	51(1)	-16(1)	7(1)	2(1)
Cl(2)	38(1)	57(1)	43(1)	-16(1)	-2(1)	-9(1)
Cu(1)	23(1)	27(1)	25(1)	-1(1)	2(1)	2(1)
Cu(2)	29(1)	41(1)	37(1)	-7(1)	1(1)	-2(1)
C(1A)	36(5)	42(4)	39(5)	-6(4)	-8(4)	16(4)
C(2A)	42(4)	36(4)	33(4)	-8(3)	9(4)	10(4)
C(3A)	43(5)	42(5)	36(4)	2(4)	10(4)	15(4)

Table 5: Hydrogen coordinates (x 10^4) and isotropic displacement parameters (Å^{2}x 10^3) for [12]-ane-P_3Et_3[Cu(μ-Cl)(CuCl)].

	x	y	z	U(eq)
H(1A)	777	4211	4016	55
H(1B)	-924	3810	4026	55
H(2A)	331	3731	4664	42
H(2B)	1663	3159	4463	42
H(3A)	-1415	2503	4511	41
H(3B)	-280	2443	4906	41
H(4A)	-577	193	4489	73
H(4B)	-1379	896	4779	73
H(5A)	-3278	519	4338	68
H(5B)	-2693	1415	4160	68
H(6A)	-3220	334	3652	63
H(6B)	-1722	-161	3818	63
H(7A)	-2002	1754	2834	50
H(7B)	-3365	1461	3139	50
H(8A)	-3376	2892	3179	60
H(8B)	-2590	2591	3605	60
H(9A)	-1420	3806	3246	54
H(9B)	-734	3128	2923	54
H(10A)	1606	4291	3234	59
H(10B)	2965	3830	3490	59
H(11A)	3089	2762	2954	92
H(11B)	3541	3692	2786	92
H(11C)	1853	3305	2692	92
H(12A)	2874	1669	4777	46
H(12B)	1606	1122	5026	46
H(13A)	2140	-64	4589	68
H(13B)	3664	231	4837	68
H(13C)	3451	484	4357	68
H(14A)	-245	-355	3136	49
H(14B)	-1773	-22	2902	49
H(15A)	-232	916	2500	70
H(15B)	324	-51	2436	70
H(15C)	1296	576	2732	70
H(1A1)	258	4231	3986	47
H(1A2)	-1360	3773	3896	47
H(2A1)	-1401	3240	4439	44
H(2A2)	-32	3863	4557	44
H(3A1)	17	2624	4876	48
H(3A2)	1584	2859	4641	48

Crystal data and structure refinement for [12]-ane-P_3Et_3[CuBr] (2.29)

Table 1

Identification code	pge1319c	
Empirical formula	C15 H33 Br Cu P3	
Formula weight	449.77	
Temperature	150(2) K	
Wavelength	1.54184 Å	
Crystal system	Monoclinic	
Space group	P 21/c	
Unit cell dimensions	a = 13.4480(3) Å	□= 90°.
	b = 10.6233(3) Å	□= 92.123(3)°.
	c = 13.7607(5) Å	□ = 90°.
Volume	1964.53(10) $Å^3$	
Z	4	
Density (calculated)	1.521 Mg/m^3	
Absorption coefficient	6.165 mm^{-1}	
F(000)	928	
Crystal size	0.292 x 0.097 x 0.061 mm^3	
Theta range for data collection	3.289 to 73.389°.	
Index ranges	-16<=h<=16, -13<=k<=13, -15<=l<=16	
Reflections collected	6042	
Independent reflections	6042 [R(int) = ?]	
Completeness to theta = 67.684°	100.0 %	
Refinement method	Full-matrix least-squares on F^2	
Data / restraints / parameters	6042 / 0 / 184	
Goodness-of-fit on F^2	1.200	
Final R indices [I>2sigma(I)]	R1 = 0.0584, wR2 = 0.1763	
R indices (all data)	R1 = 0.0622, wR2 = 0.1785	
Extinction coefficient	n/a	
Largest diff. peak and hole	1.168 and -0.627 e.$Å^{-3}$	

Table 2: Atomic coordinates (x 10^4) and equivalent isotropic displacement parameters ($Å^2$x 10^3) for [12]-ane-P_3Et_3[CuBr]. U(eq) is defined as one third of the trace of the orthogonalized U^{ij} tensor.

	x	y	z	U(eq)
C(1)	9592(5)	-396(7)	2908(5)	26(1)
C(2)	8967(5)	371(7)	2160(5)	27(1)
C(3)	8612(5)	1644(7)	2526(5)	29(2)
C(4)	6476(5)	1817(7)	2627(5)	28(2)
C(5)	6036(5)	587(7)	2187(5)	27(1)
C(6)	5427(5)	-197(7)	2885(5)	26(1)
C(7)	6524(5)	-2486(7)	2993(5)	26(1)
C(8)	7454(5)	-3230(6)	3324(5)	26(1)
C(9)	8427(5)	-2609(7)	3044(5)	27(1)
C(10)	7787(6)	3233(7)	3901(5)	34(2)
C(11)	7049(7)	3609(8)	4652(7)	47(2)
C(12)	5287(5)	-1780(7)	4562(5)	27(1)
C(13)	5752(6)	-2750(9)	5254(6)	38(2)
C(14)	9784(5)	-1931(7)	4622(5)	27(1)
C(15)	9309(6)	-2857(8)	5320(6)	37(2)
Br(1)	7571(1)	259(1)	6080(1)	31(1)
Cu(1)	7569(1)	-97(1)	4336(1)	19(1)
P(1)	8840(1)	-1240(2)	3784(1)	21(1)
P(2)	7602(1)	1642(1)	3407(1)	22(1)
P(3)	6208(1)	-1122(2)	3753(1)	20(1)

Table 3: Bond lengths [Å] and angles [°] for [12]-ane-P_3Et_3[CuBr].

C(1)-C(2)	1.538(9)	C(14)-C(15)	1.530(10)
C(1)-P(1)	1.835(7)	C(14)-P(1)	1.837(7)
C(1)-H(1A)	0.9900	C(14)-H(14A)	0.9900
C(1)-H(1B)	0.9900	C(14)-H(14B)	0.9900
C(2)-C(3)	1.527(10)	C(15)-H(15A)	0.9800
C(2)-H(2A)	0.9900	C(15)-H(15B)	0.9800
C(2)-H(2B)	0.9900	C(15)-H(15C)	0.9800
C(3)-P(2)	1.853(7)	Br(1)-Cu(1)	2.4300(10)
C(3)-H(3A)	0.9900	Cu(1)-P(2)	2.2476(17)
C(3)-H(3B)	0.9900	Cu(1)-P(3)	2.2509(18)
C(4)-C(5)	1.548(10)	Cu(1)-P(1)	2.2521(18)
C(4)-P(2)	1.833(7)		
C(4)-H(4A)	0.9900	C(2)-C(1)-P(1)	113.4(5)
C(4)-H(4B)	0.9900	C(2)-C(1)-H(1A)	108.9
C(5)-C(6)	1.531(9)	P(1)-C(1)-H(1A)	108.9
C(5)-H(5A)	0.9900	C(2)-C(1)-H(1B)	108.9
C(5)-H(5B)	0.9900	P(1)-C(1)-H(1B)	108.9
C(6)-P(3)	1.845(7)	H(1A)-C(1)-H(1B)	107.7
C(6)-H(6A)	0.9900	C(3)-C(2)-C(1)	114.7(6)
C(6)-H(6B)	0.9900	C(3)-C(2)-H(2A)	108.6
C(7)-C(8)	1.534(10)	C(1)-C(2)-H(2A)	108.6
C(7)-P(3)	1.846(7)	C(3)-C(2)-H(2B)	108.6
C(7)-H(7A)	0.9900	C(1)-C(2)-H(2B)	108.6
C(7)-H(7B)	0.9900	H(2A)-C(2)-H(2B)	107.6
C(8)-C(9)	1.527(10)	C(2)-C(3)-P(2)	117.4(5)
C(8)-H(8A)	0.9900	C(2)-C(3)-H(3A)	107.9
C(8)-H(8B)	0.9900	P(2)-C(3)-H(3A)	107.9
C(9)-P(1)	1.849(7)	C(2)-C(3)-H(3B)	107.9
C(9)-H(9A)	0.9900	P(2)-C(3)-H(3B)	107.9
C(9)-H(9B)	0.9900	H(3A)-C(3)-H(3B)	107.2
C(10)-C(11)	1.513(10)	C(5)-C(4)-P(2)	116.0(5)
C(10)-P(2)	1.834(7)	C(5)-C(4)-H(4A)	108.3
C(10)-H(10A)	0.9900	P(2)-C(4)-H(4A)	108.3
C(10)-H(10B)	0.9900	C(5)-C(4)-H(4B)	108.3
C(11)-H(11A)	0.9800	P(2)-C(4)-H(4B)	108.3
C(11)-H(11B)	0.9800	H(4A)-C(4)-H(4B)	107.4
C(11)-H(11C)	0.9800	C(6)-C(5)-C(4)	114.8(6)
C(12)-C(13)	1.521(10)	C(6)-C(5)-H(5A)	108.6
C(12)-P(3)	1.834(7)	C(4)-C(5)-H(5A)	108.6
C(12)-H(12A)	0.9900	C(6)-C(5)-H(5B)	108.6
C(12)-H(12B)	0.9900	C(4)-C(5)-H(5B)	108.6
C(13)-H(13A)	0.9800	H(5A)-C(5)-H(5B)	107.5
C(13)-H(13B)	0.9800	C(5)-C(6)-P(3)	113.0(5)
C(13)-H(13C)	0.9800	C(5)-C(6)-H(6A)	109.0

P(3)-C(6)-H(6A)	109.0	C(12)-C(13)-H(13B)	109.5
C(5)-C(6)-H(6B)	109.0	H(13A)-C(13)-H(13B)	109.5
P(3)-C(6)-H(6B)	109.0	C(12)-C(13)-H(13C)	109.5
H(6A)-C(6)-H(6B)	107.8	H(13A)-C(13)-H(13C)	109.5
C(8)-C(7)-P(3)	116.0(4)	H(13B)-C(13)-H(13C)	109.5
C(8)-C(7)-H(7A)	108.3	C(15)-C(14)-P(1)	110.8(5)
P(3)-C(7)-H(7A)	108.3	C(15)-C(14)-H(14A)	109.5
C(8)-C(7)-H(7B)	108.3	P(1)-C(14)-H(14A)	109.5
P(3)-C(7)-H(7B)	108.3	C(15)-C(14)-H(14B)	109.5
H(7A)-C(7)-H(7B)	107.4	P(1)-C(14)-H(14B)	109.5
C(9)-C(8)-C(7)	113.5(5)	H(14A)-C(14)-H(14B)	108.1
C(9)-C(8)-H(8A)	108.9	C(14)-C(15)-H(15A)	109.5
C(7)-C(8)-H(8A)	108.9	C(14)-C(15)-H(15B)	109.5
C(9)-C(8)-H(8B)	108.9	H(15A)-C(15)-H(15B)	109.5
C(7)-C(8)-H(8B)	108.9	C(14)-C(15)-H(15C)	109.5
H(8A)-C(8)-H(8B)	107.7	H(15A)-C(15)-H(15C)	109.5
C(8)-C(9)-P(1)	116.3(4)	H(15B)-C(15)-H(15C)	109.5
C(8)-C(9)-H(9A)	108.2	P(2)-Cu(1)-P(3)	103.20(7)
P(1)-C(9)-H(9A)	108.2	P(2)-Cu(1)-P(1)	102.72(7)
C(8)-C(9)-H(9B)	108.2	P(3)-Cu(1)-P(1)	103.64(7)
P(1)-C(9)-H(9B)	108.2	P(2)-Cu(1)-Br(1)	115.77(5)
H(9A)-C(9)-H(9B)	107.4	P(3)-Cu(1)-Br(1)	113.46(6)
C(11)-C(10)-P(2)	114.4(6)	P(1)-Cu(1)-Br(1)	116.35(6)
C(11)-C(10)-H(10A)	108.7	C(1)-P(1)-C(14)	102.9(3)
P(2)-C(10)-H(10A)	108.7	C(1)-P(1)-C(9)	100.6(3)
C(11)-C(10)-H(10B)	108.7	C(14)-P(1)-C(9)	102.6(3)
P(2)-C(10)-H(10B)	108.7	C(1)-P(1)-Cu(1)	113.7(2)
H(10A)-C(10)-H(10B)	107.6	C(14)-P(1)-Cu(1)	121.3(2)
C(10)-C(11)-H(11A)	109.5	C(9)-P(1)-Cu(1)	113.2(2)
C(10)-C(11)-H(11B)	109.5	C(4)-P(2)-C(10)	102.8(4)
H(11A)-C(11)-H(11B)	109.5	C(4)-P(2)-C(3)	103.1(3)
C(10)-C(11)-H(11C)	109.5	C(10)-P(2)-C(3)	98.5(3)
H(11A)-C(11)-H(11C)	109.5	C(4)-P(2)-Cu(1)	112.5(2)
H(11B)-C(11)-H(11C)	109.5	C(10)-P(2)-Cu(1)	123.5(2)
C(13)-C(12)-P(3)	111.5(5)	C(3)-P(2)-Cu(1)	113.8(2)
C(13)-C(12)-H(12A)	109.3	C(12)-P(3)-C(6)	102.4(3)
P(3)-C(12)-H(12A)	109.3	C(12)-P(3)-C(7)	102.7(3)
C(13)-C(12)-H(12B)	109.3	C(6)-P(3)-C(7)	100.9(3)
P(3)-C(12)-H(12B)	109.3	C(12)-P(3)-Cu(1)	121.8(2)
H(12A)-C(12)-H(12B)	108.0	C(6)-P(3)-Cu(1)	114.1(2)
C(12)-C(13)-H(13A)	109.5	C(7)-P(3)-Cu(1)	112.4(2)

Symmetry transformations used to generate equivalent atoms:

Table 4: Anisotropic displacement parameters ($Å^2 x\ 10^3$) for [12]-ane-P_3Et_3[CuBr]. The anisotropic displacement factor exponent takes the form: $-2\pi^2[\ h^2 a^{*2} U^{11} + ... + 2\ h\ k\ a^*\ b^*\ U^{12}\ ]$

	U^{11}	U^{22}	U^{33}	U^{23}	U^{13}	U^{12}
C(1)	27(4)	25(3)	27(3)	0(3)	4(2)	1(3)
C(2)	29(4)	29(4)	23(3)	5(3)	6(2)	-1(3)
C(3)	30(4)	24(4)	32(4)	9(3)	3(3)	-1(3)
C(4)	30(4)	21(3)	34(4)	11(3)	2(3)	7(3)
C(5)	27(4)	32(4)	22(3)	6(3)	-2(2)	3(3)
C(6)	27(3)	28(4)	24(3)	3(3)	-4(2)	-1(3)
C(7)	30(4)	24(3)	25(3)	-6(3)	-2(2)	-4(3)
C(8)	38(4)	16(3)	23(3)	-3(2)	5(3)	1(3)
C(9)	31(4)	26(3)	24(3)	-6(3)	4(2)	3(3)
C(10)	43(4)	20(3)	39(4)	-1(3)	6(3)	1(3)
C(11)	62(6)	30(4)	50(5)	-9(4)	16(4)	4(4)
C(12)	29(4)	24(3)	27(3)	3(3)	4(3)	-3(3)
C(13)	37(4)	47(5)	31(4)	13(4)	4(3)	-4(3)
C(14)	28(4)	27(4)	27(3)	2(3)	0(2)	5(3)
C(15)	35(4)	43(5)	34(4)	13(3)	-2(3)	3(3)
Br(1)	42(1)	31(1)	19(1)	-4(1)	1(1)	1(1)
Cu(1)	24(1)	15(1)	18(1)	0(1)	1(1)	0(1)
P(1)	25(1)	19(1)	20(1)	0(1)	3(1)	2(1)
P(2)	30(1)	14(1)	22(1)	2(1)	2(1)	0(1)
P(3)	24(1)	18(1)	19(1)	0(1)	0(1)	-1(1)

Table 5: Hydrogen coordinates (x 10^4) and isotropic displacement parameters ($Å^2$x 10^3) for [12]-ane-P_3Et_3[CuBr].

	x	y	z	U(eq)
H(1A)	10053	179	3268	31
H(1B)	9999	-1013	2559	31
H(2A)	9368	511	1581	32
H(2B)	8378	-134	1951	32
H(3A)	8385	2148	1955	34
H(3B)	9192	2086	2831	34
H(4A)	5959	2228	3011	34
H(4B)	6628	2392	2086	34
H(5A)	5605	805	1613	33
H(5B)	6589	62	1959	33
H(6A)	4991	-777	2502	31
H(6B)	4996	373	3253	31
H(7A)	5949	-3069	2969	31
H(7B)	6618	-2183	2322	31
H(8A)	7457	-3328	4039	31
H(8B)	7417	-4082	3033	31
H(9A)	8354	-2337	2357	32
H(9B)	8959	-3253	3082	32
H(10A)	8467	3289	4199	41
H(10B)	7742	3843	3357	41
H(11A)	6396	3753	4331	71
H(11B)	7276	4383	4978	71
H(11C)	6997	2934	5133	71
H(12A)	4994	-1092	4943	32
H(12B)	4744	-2180	4166	32
H(13A)	5977	-3476	4881	57
H(13B)	5257	-3026	5714	57
H(13C)	6321	-2373	5612	57
H(14A)	10289	-2375	4245	33
H(14B)	10123	-1253	5000	33
H(15A)	8765	-2439	5647	56
H(15B)	9810	-3142	5805	56
H(15C)	9047	-3583	4953	56

Crystal data and structure refinement for [12]-aneP_3Et_3[Cu(μ-Br)CuBr] (2.30)

Table 1

Identification code	pge1319d	
Empirical formula	C15 H33 Br2 Cu2 P3	
Formula weight	593.22	
Temperature	293(2) K	
Wavelength	1.54184 Å	
Crystal system	Orthorhombic	
Space group	P212121	
Unit cell dimensions	a = 8.7892(4) Å	□= 90°.
	b = 12.9061(6) Å	□= 90°.
	c = 19.9507(9) Å	□ = 90°.
Volume	2263.09(18) $Å^3$	
Z	4	
Density (calculated)	1.741 Mg/m^3	
Absorption coefficient	8.404 mm^{-1}	
F(000)	1184	
Crystal size	0.08 x 0.05 x 0.04 mm^3	
Theta range for data collection	4.08 to 73.32°.	
Index ranges	-9<=h<=10, -15<=k<=15, -12<=l<=24	
Reflections collected	5785	
Independent reflections	3741 [R(int) = 0.0174]	
Completeness to theta = 73.32°	96.3 %	
Max. and min. transmission	0.7298 and 0.5529	
Refinement method	Full-matrix least-squares on F^2	
Data / restraints / parameters	3741 / 0 / 203	
Goodness-of-fit on F^2	1.049	
Final R indices [I>2sigma(I)]	R1 = 0.0351, wR2 = 0.0939	
R indices (all data)	R1 = 0.0376, wR2 = 0.0967	
Absolute structure parameter	0.46(4)	
Largest diff. peak and hole	0.751 and -0.589 e.$Å^{-3}$	

Table 2: Atomic coordinates (x 10^4) and equivalent isotropic displacement parameters ($Å^2$x 10^3) for [12]-aneP_3Et_3[Cu(μ-Br)CuBr]. U(eq) is defined as one third of the trace of the orthogonalized U^{ij} tensor.

	x	y	z	U(eq)
C(1)	-1910(7)	12345(4)	896(3)	51(1)
C(2)	-2843(7)	12436(4)	1530(3)	57(1)
C(3)	-2006(8)	12150(5)	2180(3)	60(2)
C(4)	-3339(8)	10318(6)	2813(3)	70(2)
C(5)	-4719(8)	9982(7)	2418(4)	73(2)
C(6)	-4633(7)	8932(5)	2085(4)	62(2)
C(7)	-4733(7)	9244(6)	659(4)	64(2)
C(8)	-4187(17)	9853(11)	124(6)	170(8)
C(9)	-3496(7)	10819(6)	100(4)	64(2)
C(10)	-237(8)	10857(5)	2999(3)	56(1)
C(11)	410(11)	9823(6)	3221(3)	74(2)
C(12)	-3299(8)	7437(5)	1230(4)	64(2)
C(13)	-2398(11)	7134(6)	603(5)	87(2)
C(14)	-310(7)	11228(5)	-107(3)	53(1)
C(15)	70(11)	10242(7)	-483(3)	78(2)
Cu(1)	-1370(1)	9845(1)	1379(1)	32(1)
Cu(2)	1529(1)	10483(1)	1397(1)	51(1)
Br(1)	1027(1)	8775(1)	1278(1)	54(1)
Br(2)	2461(1)	12085(1)	1498(1)	70(1)
P(1)	-1695(1)	11027(1)	560(1)	39(1)
P(2)	-1657(2)	10761(1)	2333(1)	43(1)
P(3)	-3445(1)	8840(1)	1333(1)	44(1)

Table 3: Bond lengths [Å] and angles [°] for [12]-aneP_3Et_3[Cu(μ-Br)CuBr]

C(1)-C(2)	1.513(9)	C(14)-C(15)	1.514(10)
C(1)-P(1)	1.838(6)	C(14)-P(1)	1.822(6)
C(1)-H(1A)	0.9700	C(14)-H(14A)	0.9700
C(1)-H(1B)	0.9700	C(14)-H(14B)	0.9700
C(2)-C(3)	1.536(9)	C(15)-H(15A)	0.9600
C(2)-H(2A)	0.9700	C(15)-H(15B)	0.9600
C(2)-H(2B)	0.9700	C(15)-H(15C)	0.9600
C(3)-P(2)	1.844(6)	Cu(1)-P(3)	2.2397(13)
C(3)-H(3A)	0.9700	Cu(1)-P(1)	2.2536(13)
C(3)-H(3B)	0.9700	Cu(1)-P(2)	2.2560(14)
C(4)-C(5)	1.510(11)	Cu(1)-Br(1)	2.5265(8)
C(4)-P(2)	1.852(7)	Cu(1)-Cu(2)	2.6779(10)
C(4)-H(4A)	0.9700	Cu(2)-Br(2)	2.2337(10)
C(4)-H(4B)	0.9700	Cu(2)-Br(1)	2.2598(10)
C(5)-C(6)	1.511(11)	C(2)-C(1)-P(1)	115.7(4)
C(5)-H(5A)	0.9700	C(2)-C(1)-H(1A)	108.4
C(5)-H(5B)	0.9700	P(1)-C(1)-H(1A)	108.4
C(6)-P(3)	1.832(6)	C(2)-C(1)-H(1B)	108.4
C(6)-H(6A)	0.9700	P(1)-C(1)-H(1B)	108.4
C(6)-H(6B)	0.9700	H(1A)-C(1)-H(1B)	107.4
C(7)-C(8)	1.410(12)	C(1)-C(2)-C(3)	115.3(5)
C(7)-P(3)	1.834(6)	C(1)-C(2)-H(2A)	108.4
C(7)-H(7A)	0.9700	C(3)-C(2)-H(2A)	108.4
C(7)-H(7B)	0.9700	C(1)-C(2)-H(2B)	108.4
C(8)-C(9)	1.388(12)	C(3)-C(2)-H(2B)	108.4
C(8)-H(8A)	0.9700	H(2A)-C(2)-H(2B)	107.5
C(8)-H(8B)	0.9700	C(2)-C(3)-P(2)	117.0(4)
C(9)-P(1)	1.850(6)	C(2)-C(3)-H(3A)	108.1
C(9)-H(9A)	0.9700	P(2)-C(3)-H(3A)	108.1
C(9)-H(9B)	0.9700	C(2)-C(3)-H(3B)	108.1
C(10)-C(11)	1.516(9)	P(2)-C(3)-H(3B)	108.1
C(10)-P(2)	1.827(6)	H(3A)-C(3)-H(3B)	107.3
C(10)-H(10A)	0.9700	C(5)-C(4)-P(2)	117.4(4)
C(10)-H(10B)	0.9700	C(5)-C(4)-H(4A)	107.9
C(11)-H(11A)	0.9600	P(2)-C(4)-H(4A)	107.9
C(11)-H(11B)	0.9600	C(5)-C(4)-H(4B)	107.9
C(11)-H(11C)	0.9600	P(2)-C(4)-H(4B)	107.9
C(12)-C(13)	1.531(11)	H(4A)-C(4)-H(4B)	107.2
C(12)-P(3)	1.827(6)	C(4)-C(5)-C(6)	116.5(6)
C(12)-H(12A)	0.9700	C(4)-C(5)-H(5A)	108.2
C(12)-H(12B)	0.9700	C(6)-C(5)-H(5A)	108.2
C(13)-H(13A)	0.9600	C(4)-C(5)-H(5B)	108.2
C(13)-H(13B)	0.9600	C(6)-C(5)-H(5B)	108.2
C(13)-H(13C)	0.9600	H(5A)-C(5)-H(5B)	107.3

C(5)-C(6)-P(3)	116.5(4)	H(13A)-C(13)-H(13C)	109.5
C(5)-C(6)-H(6A)	108.2	H(13B)-C(13)-H(13C)	109.5
P(3)-C(6)-H(6A)	108.2	C(15)-C(14)-P(1)	112.9(5)
C(5)-C(6)-H(6B)	108.2	C(15)-C(14)-H(14A)	109.0
P(3)-C(6)-H(6B)	108.2	P(1)-C(14)-H(14A)	109.0
H(6A)-C(6)-H(6B)	107.3	C(15)-C(14)-H(14B)	109.0
C(8)-C(7)-P(3)	120.3(6)	P(1)-C(14)-H(14B)	109.0
C(8)-C(7)-H(7A)	107.3	H(14A)-C(14)-H(14B)	107.8
P(3)-C(7)-H(7A)	107.3	C(14)-C(15)-H(15A)	109.5
C(8)-C(7)-H(7B)	107.3	C(14)-C(15)-H(15B)	109.5
P(3)-C(7)-H(7B)	107.3	H(15A)-C(15)-H(15B)	109.5
H(7A)-C(7)-H(7B)	106.9	C(14)-C(15)-H(15C)	109.5
C(9)-C(8)-C(7)	132.6(12)	H(15A)-C(15)-H(15C)	109.5
C(9)-C(8)-H(8A)	104.1	H(15B)-C(15)-H(15C)	109.5
C(7)-C(8)-H(8A)	104.1	P(3)-Cu(1)-P(1)	105.02(5)
C(9)-C(8)-H(8B)	104.1	P(3)-Cu(1)-P(2)	104.29(6)
C(7)-C(8)-H(8B)	104.1	P(1)-Cu(1)-P(2)	104.04(5)
H(8A)-C(8)-H(8B)	105.5	P(3)-Cu(1)-Br(1)	111.09(4)
C(8)-C(9)-P(1)	119.2(6)	P(1)-Cu(1)-Br(1)	114.70(4)
C(8)-C(9)-H(9A)	107.5	P(2)-Cu(1)-Br(1)	116.55(5)
P(1)-C(9)-H(9A)	107.5	P(3)-Cu(1)-Cu(2)	162.45(5)
C(8)-C(9)-H(9B)	107.5	P(1)-Cu(1)-Cu(2)	85.54(4)
P(1)-C(9)-H(9B)	107.5	P(2)-Cu(1)-Cu(2)	86.19(5)
H(9A)-C(9)-H(9B)	107.0	Br(1)-Cu(1)-Cu(2)	51.37(3)
C(11)-C(10)-P(2)	114.1(5)	Br(2)-Cu(2)-Br(1)	169.72(5)
C(11)-C(10)-H(10A)	108.7	Br(2)-Cu(2)-Cu(1)	129.42(4)
P(2)-C(10)-H(10A)	108.7	Br(1)-Cu(2)-Cu(1)	60.85(3)
C(11)-C(10)-H(10B)	108.7	Cu(2)-Br(1)-Cu(1)	67.78(3)
P(2)-C(10)-H(10B)	108.7	C(14)-P(1)-C(1)	101.7(3)
H(10A)-C(10)-H(10B)	107.6	C(14)-P(1)-C(9)	103.3(3)
C(10)-C(11)-H(11A)	109.5	C(1)-P(1)-C(9)	103.1(3)
C(10)-C(11)-H(11B)	109.5	C(14)-P(1)-Cu(1)	122.8(2)
H(11A)-C(11)-H(11B)	109.5	C(1)-P(1)-Cu(1)	112.06(19)
C(10)-C(11)-H(11C)	109.5	C(9)-P(1)-Cu(1)	111.7(2)
H(11A)-C(11)-H(11C)	109.5	C(10)-P(2)-C(3)	99.7(3)
H(11B)-C(11)-H(11C)	109.5	C(10)-P(2)-C(4)	101.0(3)
C(13)-C(12)-P(3)	112.5(5)	C(3)-P(2)-C(4)	104.7(3)
C(13)-C(12)-H(12A)	109.1	C(10)-P(2)-Cu(1)	124.9(2)
P(3)-C(12)-H(12A)	109.1	C(3)-P(2)-Cu(1)	112.8(2)
C(13)-C(12)-H(12B)	109.1	C(4)-P(2)-Cu(1)	111.3(2)
P(3)-C(12)-H(12B)	109.1	C(12)-P(3)-C(6)	101.3(3)
H(12A)-C(12)-H(12B)	107.8	C(12)-P(3)-C(7)	104.1(3)
C(12)-C(13)-H(13A)	109.5	C(6)-P(3)-C(7)	103.4(3)
C(12)-C(13)-H(13B)	109.5	C(12)-P(3)-Cu(1)	121.4(2)
H(13A)-C(13)-H(13B)	109.5	C(6)-P(3)-Cu(1)	113.1(2)
C(12)-C(13)-H(13C)	109.5	C(7)-P(3)-Cu(1)	111.6(2)

Table 4: Anisotropic displacement parameters ($Å^2 x\ 10^3$) for [12]-aneP_3Et_3[Cu(μ-Br)CuBr]. The anisotropic displacement factor exponent takes the form: $-2\pi^2[\ h^2 a^{*2} U^{11} + ... + 2\ h\ k\ a^*\ b^*\ U^{12}\ ]$

	U^{11}	U^{22}	U^{33}	U^{23}	U^{13}	U^{12}
C(1)	48(3)	37(2)	69(3)	13(2)	-9(3)	6(2)
C(2)	54(3)	43(3)	74(4)	4(3)	-4(3)	13(2)
C(3)	68(4)	48(3)	63(3)	-11(3)	-3(3)	19(3)
C(4)	70(4)	86(4)	52(3)	-6(3)	21(3)	5(4)
C(5)	48(3)	103(6)	68(4)	11(4)	28(3)	4(4)
C(6)	41(3)	73(4)	70(4)	13(3)	8(3)	-7(3)
C(7)	37(3)	81(4)	74(4)	17(4)	-13(3)	-16(3)
C(8)	171(12)	191(12)	148(9)	117(9)	-125(10)	-136(11)
C(9)	45(3)	76(4)	70(4)	26(3)	-19(3)	-7(3)
C(10)	71(4)	52(3)	46(3)	-8(3)	-9(3)	4(3)
C(11)	96(5)	75(4)	52(3)	-4(3)	-16(4)	25(4)
C(12)	58(3)	51(3)	82(4)	2(3)	-5(3)	-15(3)
C(13)	84(5)	69(4)	109(6)	-26(4)	8(5)	-13(4)
C(14)	49(3)	62(3)	48(3)	17(3)	4(2)	-3(3)
C(15)	102(6)	82(5)	48(3)	1(4)	19(4)	0(5)
Cu(1)	26(1)	36(1)	36(1)	2(1)	0(1)	-1(1)
Cu(2)	40(1)	50(1)	61(1)	6(1)	-3(1)	-3(1)
Br(1)	40(1)	52(1)	69(1)	2(1)	1(1)	8(1)
Br(2)	52(1)	61(1)	98(1)	11(1)	-10(1)	-12(1)
P(1)	33(1)	41(1)	43(1)	9(1)	-4(1)	0(1)
P(2)	44(1)	45(1)	40(1)	-5(1)	4(1)	7(1)
P(3)	31(1)	48(1)	54(1)	6(1)	-1(1)	-9(1)

Table 5: Hydrogen coordinates (x 10^4) and isotropic displacement parameters ($Å^2$x 10^3) for [12]-aneP_3Et_3[Cu(μ-Br)CuBr].

	x	y	z	U(eq)
H(1A)	-905	12624	983	62
H(1B)	-2377	12774	554	62
H(2A)	-3729	11993	1488	68
H(2B)	-3203	13144	1569	68
H(3A)	-2588	12420	2554	72
H(3B)	-1032	12503	2180	72
H(4A)	-3026	9742	3093	83
H(4B)	-3646	10876	3110	83
H(5A)	-4911	10497	2074	87
H(5B)	-5589	9983	2718	87
H(6A)	-5657	8721	1967	74
H(6B)	-4253	8438	2412	74
H(7A)	-5165	8620	466	76
H(7B)	-5564	9622	865	76
H(8A)	-3481	9401	-108	204
H(8B)	-5056	9921	-173	204
H(9A)	-4225	11323	263	76
H(9B)	-3308	10981	-368	76
H(10A)	591	11292	2844	68
H(10B)	-696	11195	3383	68
H(11A)	-408	9354	3318	112
H(11B)	1017	9921	3615	112
H(11C)	1030	9542	2869	112
H(12A)	-2806	7145	1622	76
H(12B)	-4313	7145	1202	76
H(13A)	-2941	7354	211	131
H(13B)	-2271	6395	592	131
H(13C)	-1418	7461	614	131
H(14A)	-709	11734	-421	64
H(14B)	616	11510	85	64
H(15A)	331	9707	-169	116
H(15B)	915	10366	-777	116
H(15C)	-796	10027	-741	116

Crystal data and structure refinement for [12]-aneP_3Et_3 [LCuI] (2.31)

Table 1

Identification code	shelx	
Empirical formula	C15 H33 Cu I P3	
Formula weight	496.76	
Temperature	150(2) K	
Wavelength	0.71073 Å	
Crystal system	Orthorhombic	
Space group	P n a 21	
Unit cell dimensions	a = 14.0792(6) Å	□= 90°.
	b = 10.7291(4) Å	□= 90°.
	c = 13.5869(4) Å	□ = 90°.
Volume	2052.40(13) $Å^3$	
Z	4	
Density (calculated)	1.608 Mg/m^3	
Absorption coefficient	2.793 mm^{-1}	
F(000)	1000	
Crystal size	0.300 x 0.100 x 0.030 mm^3	
Theta range for data collection	2.419 to 27.467°.	
Index ranges	?<=h<=?, ?<=k<=?, ?<=l<=?	
Reflections collected	?	
Independent reflections	4463 [R(int) = ?]	
Completeness to theta = 25.242°	99.8 %	
Refinement method	Full-matrix least-squares on F^2	
Data / restraints / parameters	4463 / 62 / 185	
Goodness-of-fit on F^2	1.051	
Final R indices [I>2sigma(I)]	R1 = 0.0493, wR2 = 0.0933	
R indices (all data)	R1 = 0.0910, wR2 = 0.1107	
Absolute structure parameter	0.43(14)	
Extinction coefficient	n/a	
Largest diff. peak and hole	0.953 and -0.682 $e.Å^{-3}$	

Table 2: Atomic coordinates (x 10^4) and equivalent isotropic displacement parameters ($Å^2$x 10^3) for [12]-aneP_3Et_3 [LCuI]. U(eq) is defined as one third of the trace of the orthogonalized U^{ij} tensor.

	x	y	z	U(eq)
C(1)	2550(20)	1590(30)	3950(20)	44(9)
C(2)	2190(20)	350(30)	4370(20)	29(7)
C(3)	2890(30)	-440(30)	4920(20)	49(9)
C(4)	3080(20)	-2680(30)	3840(20)	36(9)
C(5)	3394(6)	-3303(7)	2900(30)	38(2)
C(6)	3070(20)	-2650(30)	1950(20)	41(9)
C(7)	2890(20)	-390(30)	820(20)	31(8)
C(8)	2160(30)	340(30)	1460(30)	55(11)
C(9)	2560(20)	1580(40)	1830(20)	46(10)
C(10)	3844(9)	3105(11)	2604(9)	44(4)
C(11)	4518(11)	3533(12)	3391(10)	54(4)
C(12)	4595(18)	-1890(30)	5129(18)	35(8)
C(13)	5260(20)	-2790(30)	4680(20)	48(9)
C(14)	4580(20)	-1880(30)	676(19)	39(9)
C(15)	5310(20)	-2820(30)	1110(20)	48(11)
P(1)	3362(2)	1518(2)	2895(9)	37(1)
P(2)	3766(7)	-1271(8)	4208(3)	30(2)
P(3)	3765(7)	-1265(8)	1602(3)	30(2)
Cu(1)	4289(1)	-183(1)	2897(6)	27(1)
I(1)	6101(1)	254(1)	2899(4)	35(1)

Table 3: Bond lengths [Å] and angles [°] for [12]-aneP_3Et_3[LCuI]

C(1)-C(2)	1.54(4)	C(9)-C(8)-C(7)	113(3)
C(1)-P(1)	1.84(3)	C(8)-C(9)-P(1)	117(3)
C(2)-C(3)	1.51(4)	C(11)-C(10)-P(1)	110.9(9)
C(3)-P(2)	1.80(3)	C(13)-C(12)-P(2)	111.3(19)
C(4)-C(5)	1.51(4)	C(15)-C(14)-P(3)	113(2)
C(4)-P(2)	1.86(3)	C(1)-P(1)-C(9)	103.2(4)
C(5)-C(6)	1.54(4)	C(1)-P(1)-C(10)	110.4(12)
C(6)-P(3)	1.84(3)	C(9)-P(1)-C(10)	91.5(13)
C(7)-C(8)	1.55(5)	C(1)-P(1)-Cu(1)	113.4(11)
C(7)-P(3)	1.88(3)	C(9)-P(1)-Cu(1)	112.8(12)
C(8)-C(9)	1.52(5)	C(10)-P(1)-Cu(1)	121.9(4)
C(9)-P(1)	1.84(3)	C(3)-P(2)-C(12)	104.1(13)
C(10)-C(11)	1.501(15)	C(3)-P(2)-C(4)	101.0(16)
C(10)-P(1)	1.875(13)	C(12)-P(2)-C(4)	102.6(14)
C(12)-C(13)	1.48(2)	C(3)-P(2)-Cu(1)	113.2(11)
C(12)-P(2)	1.83(2)	C(12)-P(2)-Cu(1)	121.3(10)
C(14)-C(15)	1.550(13)	C(4)-P(2)-Cu(1)	112.3(10)
C(14)-P(3)	1.83(3)	C(14)-P(3)-C(6)	102.8(14)
P(1)-Cu(1)	2.243(2)	C(14)-P(3)-C(7)	101.8(13)
P(2)-Cu(1)	2.253(10)	C(6)-P(3)-C(7)	101.3(14)
P(3)-Cu(1)	2.233(11)	C(14)-P(3)-Cu(1)	121.4(10)
Cu(1)-I(1)	2.5944(10)	C(6)-P(3)-Cu(1)	113.1(10)
		C(7)-P(3)-Cu(1)	113.9(10)
C(2)-C(1)-P(1)	117(2)	P(3)-Cu(1)-P(1)	103.3(4)
C(3)-C(2)-C(1)	117(3)	P(3)-Cu(1)-P(2)	104.26(8)
C(2)-C(3)-P(2)	117(2)	P(1)-Cu(1)-P(2)	103.4(4)
C(5)-C(4)-P(2)	116(2)	P(3)-Cu(1)-I(1)	114.8(3)
C(4)-C(5)-C(6)	115.0(7)	P(1)-Cu(1)-I(1)	115.15(7)
C(5)-C(6)-P(3)	115.1(16)	P(2)-Cu(1)-I(1)	114.4(3)
C(8)-C(7)-P(3)	112(2)		

Symmetry transformations used to generate equivalent atoms:

Table 4: Anisotropic displacement parameters ($Å^2 x\ 10^3$) for [12]-aneP_3Et_3 [LCuI]. The anisotropic displacement factor exponent takes the form: $-2\pi^2[h^2 a^{*2} U^{11} + ... + 2 h k a^* b^* U^{12}]$

	U^{11}	U^{22}	U^{33}	U^{23}	U^{13}	U^{12}
C(1)	43(12)	45(12)	43(11)	-11(8)	-5(8)	16(8)
C(2)	19(9)	38(10)	30(9)	-4(7)	1(7)	8(7)
C(3)	53(17)	56(15)	39(12)	-2(10)	-5(11)	3(12)
C(4)	32(13)	37(14)	38(13)	4(10)	-14(10)	1(11)
C(5)	36(5)	28(4)	50(5)	2(12)	-6(12)	-2(3)
C(6)	32(12)	31(12)	59(15)	-9(10)	-15(10)	-5(10)
C(7)	24(12)	30(12)	39(12)	7(9)	-13(9)	4(10)
C(8)	49(15)	63(14)	52(14)	12(10)	-2(10)	14(10)
C(9)	45(14)	44(13)	49(13)	9(9)	3(9)	20(9)
C(10)	48(7)	32(6)	53(10)	1(5)	-14(6)	11(5)
C(11)	62(9)	32(7)	69(9)	-6(6)	-25(7)	-9(7)
C(12)	28(12)	41(13)	36(12)	9(10)	0(9)	16(10)
C(13)	46(16)	57(17)	39(13)	15(12)	-4(11)	4(13)
C(14)	46(17)	40(13)	32(13)	-2(11)	5(12)	-16(12)
C(15)	32(17)	48(18)	64(17)	9(13)	16(13)	24(14)
P(1)	30(1)	22(1)	59(2)	-4(6)	5(6)	3(1)
P(2)	26(6)	33(5)	32(4)	5(3)	-1(4)	-2(4)
P(3)	31(6)	24(5)	36(5)	4(3)	-5(4)	2(4)
Cu(1)	24(1)	22(1)	35(1)	-2(3)	-2(3)	0(1)
I(1)	26(1)	36(1)	43(1)	0(2)	2(2)	-5(1)

Table 5: Hydrogen coordinates (x 10^4) and isotropic displacement parameters ($Å^2$x 10^3) for [12]-aneP_3Et_3[LCuI].

	x	y	z	U(eq)
H(1A)	2876	2049	4488	52
H(1B)	1992	2097	3756	52
H(2A)	1649	526	4808	35
H(2B)	1944	-153	3810	35
H(3A)	2532	-1060	5315	59
H(3B)	3234	102	5395	59
H(4A)	3123	-3300	4382	43
H(4B)	2404	-2446	3774	43
H(5A)	3149	-4168	2897	45
H(5B)	4096	-3348	2899	45
H(6A)	2395	-2394	2032	49
H(6B)	3093	-3256	1404	49
H(7A)	3232	195	385	37
H(7B)	2541	-990	394	37
H(8A)	1585	507	1062	66
H(8B)	1975	-178	2027	66
H(9A)	2014	2118	2006	55
H(9B)	2898	1983	1282	55
H(10A)	4178	3080	1964	53
H(10B)	3312	3705	2549	53
H(11A)	4172	3637	4011	81
H(11B)	4801	4330	3197	81
H(11C)	5020	2910	3477	81
H(12A)	4958	-1192	5424	42
H(12B)	4232	-2301	5661	42
H(13A)	4941	-3595	4590	71
H(13B)	5811	-2908	5121	71
H(13C)	5482	-2479	4045	71
H(14A)	4214	-2302	153	47
H(14B)	4933	-1181	370	47
H(15A)	5681	-2411	1627	72
H(15B)	5739	-3105	587	72
H(15C)	4972	-3536	1387	72

Crystal data and structure refinement for 3.5(i)

Table 1.

Identification code	pge1311b	
Empirical formula	C74 H68 Cl6 O4 P4 Rh2	
Formula weight	1563.68	
Temperature	293(2) K	
Wavelength	1.54184 Å	
Crystal system	Triclinic	
Space group	P-1	
Unit cell dimensions	a = 11.3787(11) Å	α= 64.650(8)°.
	b = 13.5705(11) Å	β= 66.406(8)°.
	c = 13.5803(10) Å	γ = 73.887(8)°.
Volume	1722.3(3) $Å^3$	
Z	1	
Density (calculated)	1.508 Mg/m^3	
Absorption coefficient	7.285 mm^{-1}	
F(000)	796	
Crystal size	0.15 x 0.06 x 0.06 mm^3	

Table 1. Crystal data and structure refinement for pge1311b.

Identification code	pge1311b	
Empirical formula	C74 H68 Cl6 O4 P4 Rh2	
Formula weight	1563.68	
Temperature	293(2) K	
Wavelength	1.54184 Å	
Crystal system	Triclinic	
Space group	P-1	
Unit cell dimensions	a = 11.3787(11) Å	α= 64.650(8)°.
	b = 13.5705(11) Å	β= 66.406(8)°.
	c = 13.5803(10) Å	γ = 73.887(8)°.
Volume	1722.3(3) $Å^3$	
Z	1	
Density (calculated)	1.508 Mg/m^3	
Absorption coefficient	7.285 mm^{-1}	
F(000)	796	

Crystal size	0.15 x 0.06 x 0.06 mm^3
Theta range for data collection	3.63 to 73.58°.
Index ranges	-13<=h<=14, -16<=k<=16, -16<=l<=11
Reflections collected	11981
Independent reflections	6700 [R(int) = 0.0862]
Completeness to theta = 73.58°	96.6 %
Max. and min. transmission	0.6690 and 0.4079
Refinement method	Full-matrix least-squares on F^2
Data / restraints / parameters	6700 / 78 / 434
Goodness-of-fit on F^2	1.031
Final R indices [I>2sigma(I)]	R1 = 0.0833, wR2 = 0.2182
R indices (all data)	R1 = 0.0984, wR2 = 0.2405
Largest diff. peak and hole	3.505 and -1.983 e.$Å^{-3}$

Table 2. Atomic coordinates (x 10^4) and equivalent isotropic displacement parameters ($Å^2$x 10^3) for 3.5(i). U(eq) is defined as one third of the trace of the orthogonalized U^{ij} tensor.

	x	y	z	U(eq)
C(1)	4320(6)	2305(5)	3693(6)	35(1)
C(2)	3343(7)	1644(6)	4353(6)	39(1)
C(3)	2669(7)	1384(6)	3851(7)	47(2)
C(4)	2988(8)	1785(6)	2673(6)	44(2)
C(5)	3975(8)	2449(6)	1993(7)	46(2)
C(6)	4616(7)	2718(6)	2506(6)	42(1)
C(7)	4403(7)	1957(5)	5875(5)	36(1)
C(8)	3175(7)	2417(6)	6374(6)	42(2)
C(9)	2444(8)	1882(7)	7485(7)	49(2)
C(10)	2953(10)	860(8)	8148(7)	59(2)
C(11)	4182(9)	398(6)	7666(6)	50(2)
C(12)	4913(8)	948(6)	6535(6)	43(2)
C(13)	6806(6)	1804(5)	4034(5)	36(1)
C(14)	7067(7)	1038(5)	3522(6)	40(1)
C(15)	8314(7)	480(6)	3221(6)	44(2)
C(16)	9290(7)	689(6)	3450(7)	49(2)
C(17)	9026(7)	1450(6)	3968(7)	47(2)
C(18)	7794(6)	1996(5)	4263(6)	38(1)
C(19)	7193(6)	4276(5)	1272(5)	35(1)
C(20)	7936(7)	3266(6)	1288(6)	40(1)
C(21)	8067(8)	2822(7)	493(7)	53(2)
C(22)	7428(9)	3354(8)	-303(7)	58(2)
C(23)	6679(8)	4379(6)	-336(6)	46(2)
C(24)	6559(7)	4815(6)	450(6)	41(1)
C(25)	8458(6)	4645(6)	2553(6)	36(1)
C(26)	9648(6)	4328(6)	1825(6)	45(2)
C(27)	10782(7)	4171(7)	2058(8)	53(2)
C(28)	10770(8)	4378(8)	2967(8)	56(2)
C(29)	9607(8)	4720(7)	3686(8)	56(2)
C(30)	8457(7)	4836(6)	3491(6)	41(1)

C(31)	6816(7)	6346(5)	1450(5)	36(1)
C(32)	7949(7)	6768(6)	610(6)	41(2)
C(33)	7905(9)	7835(7)	-161(7)	52(2)
C(34)	6723(9)	8504(6)	-96(7)	52(2)
C(35)	5603(9)	8100(6)	731(7)	51(2)
C(36)	5643(7)	7019(5)	1519(6)	39(1)
P(1)	5229(2)	2631(1)	4346(1)	30(1)
Cl(1)	3594(2)	5039(1)	3222(1)	38(1)
P(2)	6924(1)	4874(1)	2335(1)	30(1)
Rh(1)	5294(1)	4419(1)	4048(1)	28(1)
O(1)	5223(4)	5949(3)	4106(4)	31(1)
O(2)	6109(4)	3822(4)	5266(4)	35(1)
C(37)	1712(12)	7549(17)	3205(14)	84(5)
Cl(2)	70(6)	7618(4)	4015(5)	86(2)
Cl(3)	1937(8)	8678(6)	1911(7)	121(3)
C(37A)	1640(20)	7495(14)	3550(20)	83(5)
Cl(2A)	317(8)	7602(7)	3159(9)	111(3)
Cl(3A)	2391(5)	8688(5)	2734(5)	82(2)

Table 3. Bond lengths [Å] and angles [°] for 3.5(i).

C(1)-C(2)	1.383(10)	C(17)-C(18)	1.380(10)
C(1)-C(6)	1.386(10)	C(17)-H(17)	0.9300
C(1)-P(1)	1.837(6)	C(18)-H(18)	0.9300
C(2)-C(3)	1.397(10)	C(19)-C(20)	1.393(9)
C(2)-H(2)	0.9300	C(19)-C(24)	1.397(10)
C(3)-C(4)	1.374(11)	C(19)-P(2)	1.830(6)
C(3)-H(3)	0.9300	C(20)-C(21)	1.388(10)
C(4)-C(5)	1.394(11)	C(20)-H(20)	0.9300
C(4)-H(4)	0.9300	C(21)-C(22)	1.375(13)
C(5)-C(6)	1.388(9)	C(21)-H(21)	0.9300
C(5)-H(5)	0.9300	C(22)-C(23)	1.409(12)
C(6)-H(6)	0.9300	C(22)-H(22)	0.9300
C(7)-C(8)	1.386(10)	C(23)-C(24)	1.375(10)
C(7)-C(12)	1.393(10)	C(23)-H(23)	0.9300
C(7)-P(1)	1.823(7)	C(24)-H(24)	0.9300
C(8)-C(9)	1.375(10)	C(25)-C(26)	1.402(9)
C(8)-H(8)	0.9300	C(25)-C(30)	1.404(9)
C(9)-C(10)	1.404(13)	C(25)-P(2)	1.808(7)
C(9)-H(9)	0.9300	C(26)-C(27)	1.389(11)
C(10)-C(11)	1.382(13)	C(26)-H(26)	0.9300
C(10)-H(10)	0.9300	C(27)-C(28)	1.371(13)
C(11)-C(12)	1.396(11)	C(27)-H(27)	0.9300
C(11)-H(11)	0.9300	C(28)-C(29)	1.390(12)
C(12)-H(12)	0.9300	C(28)-H(28)	0.9300
C(13)-C(14)	1.390(9)	C(29)-C(30)	1.391(10)
C(13)-C(18)	1.394(9)	C(29)-H(29)	0.9300
C(13)-P(1)	1.827(7)	C(30)-H(30)	0.9300
C(14)-C(15)	1.400(10)	C(31)-C(36)	1.386(10)
C(14)-H(14)	0.9300	C(31)-C(32)	1.402(9)
C(15)-C(16)	1.391(11)	C(31)-P(2)	1.837(7)
C(15)-H(15)	0.9300	C(32)-C(33)	1.378(11)
C(16)-C(17)	1.390(11)	C(32)-H(32)	0.9300
C(16)-H(16)	0.9300	C(33)-C(34)	1.392(13)

C(33)-H(33)	0.9300	C(5)-C(4)-H(4)	120.1
C(34)-C(35)	1.379(13)	C(6)-C(5)-C(4)	120.1(7)
C(34)-H(34)	0.9300	C(6)-C(5)-H(5)	120.0
C(35)-C(36)	1.399(10)	C(4)-C(5)-H(5)	120.0
C(35)-H(35)	0.9300	C(1)-C(6)-C(5)	120.9(7)
C(36)-H(36)	0.9300	C(1)-C(6)-H(6)	119.6
P(1)-Rh(1)	2.3006(15)	C(5)-C(6)-H(6)	119.6
Cl(1)-Rh(1)	2.3933(15)	C(8)-C(7)-C(12)	118.8(6)
P(2)-Rh(1)	2.2772(15)	C(8)-C(7)-P(1)	118.7(5)
Rh(1)-O(2)	1.980(4)	C(12)-C(7)-P(1)	122.2(5)
Rh(1)-O(1)	2.090(4)	C(9)-C(8)-C(7)	121.4(7)
Rh(1)-O(1)#1	2.188(4)	C(9)-C(8)-H(8)	119.3
O(1)-O(2)#1	1.432(6)	C(7)-C(8)-H(8)	119.3
O(1)-Rh(1)#1	2.188(4)	C(8)-C(9)-C(10)	119.9(8)
O(2)-O(1)#1	1.432(6)	C(8)-C(9)-H(9)	120.0
C(37)-Cl(3)	1.747(10)	C(10)-C(9)-H(9)	120.0
C(37)-Cl(2)	1.748(10)	C(11)-C(10)-C(9)	119.3(7)
C(37)-H(37A)	0.9700	C(11)-C(10)-H(10)	120.4
C(37)-H(37B)	0.9700	C(9)-C(10)-H(10)	120.4
C(37A)-Cl(2A)	1.741(10)	C(10)-C(11)-C(12)	120.3(7)
C(37A)-Cl(3A)	1.748(10)	C(10)-C(11)-H(11)	119.9
C(37A)-H(37C)	0.9700	C(12)-C(11)-H(11)	119.9
C(37A)-H(37D)	0.9700	C(7)-C(12)-C(11)	120.3(7)
		C(7)-C(12)-H(12)	119.8
C(2)-C(1)-C(6)	118.3(6)	C(11)-C(12)-H(12)	119.8
C(2)-C(1)-P(1)	121.8(5)	C(14)-C(13)-C(18)	119.3(6)
C(6)-C(1)-P(1)	119.9(5)	C(14)-C(13)-P(1)	122.3(5)
C(1)-C(2)-C(3)	121.6(7)	C(18)-C(13)-P(1)	118.3(5)
C(1)-C(2)-H(2)	119.2	C(13)-C(14)-C(15)	120.4(7)
C(3)-C(2)-H(2)	119.2	C(13)-C(14)-H(14)	119.8
C(4)-C(3)-C(2)	119.5(7)	C(15)-C(14)-H(14)	119.8
C(4)-C(3)-H(3)	120.3	C(16)-C(15)-C(14)	119.5(7)
C(2)-C(3)-H(3)	120.3	C(16)-C(15)-H(15)	120.3
C(3)-C(4)-C(5)	119.7(6)	C(14)-C(15)-H(15)	120.3
C(3)-C(4)-H(4)	120.1	C(17)-C(16)-C(15)	120.1(6)

C(17)-C(16)-H(16)	119.9	C(27)-C(28)-C(29)	119.9(7)
C(15)-C(16)-H(16)	119.9	C(27)-C(28)-H(28)	120.0
C(18)-C(17)-C(16)	120.1(7)	C(29)-C(28)-H(28)	120.0
C(18)-C(17)-H(17)	119.9	C(28)-C(29)-C(30)	119.9(8)
C(16)-C(17)-H(17)	119.9	C(28)-C(29)-H(29)	120.1
C(17)-C(18)-C(13)	120.6(6)	C(30)-C(29)-H(29)	120.1
C(17)-C(18)-H(18)	119.7	C(29)-C(30)-C(25)	120.7(7)
C(13)-C(18)-H(18)	119.7	C(29)-C(30)-H(30)	119.6
C(20)-C(19)-C(24)	118.0(6)	C(25)-C(30)-H(30)	119.6
C(20)-C(19)-P(2)	123.0(5)	C(36)-C(31)-C(32)	119.4(6)
C(24)-C(19)-P(2)	118.9(5)	C(36)-C(31)-P(2)	122.1(5)
C(21)-C(20)-C(19)	120.9(7)	C(32)-C(31)-P(2)	118.2(5)
C(21)-C(20)-H(20)	119.5	C(33)-C(32)-C(31)	120.7(7)
C(19)-C(20)-H(20)	119.5	C(33)-C(32)-H(32)	119.6
C(22)-C(21)-C(20)	120.6(8)	C(31)-C(32)-H(32)	119.6
C(22)-C(21)-H(21)	119.7	C(32)-C(33)-C(34)	119.6(7)
C(20)-C(21)-H(21)	119.7	C(32)-C(33)-H(33)	120.2
C(21)-C(22)-C(23)	119.2(7)	C(34)-C(33)-H(33)	120.2
C(21)-C(22)-H(22)	120.4	C(35)-C(34)-C(33)	120.2(7)
C(23)-C(22)-H(22)	120.4	C(35)-C(34)-H(34)	119.9
C(24)-C(23)-C(22)	119.8(7)	C(33)-C(34)-H(34)	119.9
C(24)-C(23)-H(23)	120.1	C(34)-C(35)-C(36)	120.5(7)
C(22)-C(23)-H(23)	120.1	C(34)-C(35)-H(35)	119.8
C(23)-C(24)-C(19)	121.4(7)	C(36)-C(35)-H(35)	119.8
C(23)-C(24)-H(24)	119.3	C(31)-C(36)-C(35)	119.6(7)
C(19)-C(24)-H(24)	119.3	C(31)-C(36)-H(36)	120.2
C(26)-C(25)-C(30)	118.2(6)	C(35)-C(36)-H(36)	120.2
C(26)-C(25)-P(2)	124.2(5)	C(7)-P(1)-C(13)	105.4(3)
C(30)-C(25)-P(2)	117.6(5)	C(7)-P(1)-C(1)	101.3(3)
C(27)-C(26)-C(25)	120.4(7)	C(13)-P(1)-C(1)	104.4(3)
C(27)-C(26)-H(26)	119.8	C(7)-P(1)-Rh(1)	107.3(2)
C(25)-C(26)-H(26)	119.8	C(13)-P(1)-Rh(1)	115.1(2)
C(28)-C(27)-C(26)	120.8(7)	C(1)-P(1)-Rh(1)	121.3(2)
C(28)-C(27)-H(27)	119.6	C(25)-P(2)-C(19)	106.6(3)
C(26)-C(27)-H(27)	119.6	C(25)-P(2)-C(31)	101.4(3)

C(19)-P(2)-C(31)	100.6(3)
C(25)-P(2)-Rh(1)	111.0(2)
C(19)-P(2)-Rh(1)	120.8(2)
C(31)-P(2)-Rh(1)	114.3(2)
O(2)-Rh(1)-O(1)	85.20(17)
O(2)-Rh(1)-O(1)	39.80(16)
O(1)-Rh(1)-O(1)	77.47(18)
O(2)-Rh(1)-P(2)	106.47(13)
O(1)-Rh(1)-P(2)	88.93(12)
O(1)-Rh(1)-P(2)	143.77(11)
O(2)-Rh(1)-P(1)	87.46(14)
O(1)-Rh(1)-P(1)	169.49(13)
O(1)-Rh(1)-P(1)	92.08(11)
P(2)-Rh(1)-P(1)	100.37(6)
O(2)-Rh(1)-Cl(1)	157.94(13)
O(1)-Rh(1)-Cl(1)	93.61(12)
O(1)#1-Rh(1)-Cl(1)	118.47(12)
P(2)-Rh(1)-Cl(1)	95.51(6)
P(1)-Rh(1)-Cl(1)	90.38(5)
O(2)#1-O(1)-Rh(1)	102.5(3)
O(2)#1-O(1)-Rh(1)#1	62.2(2)
Rh(1)-O(1)-Rh(1)	102.53(18)
O(1)-O(2)-Rh(1)	78.0(2)
Cl(3)-C(37)-Cl(2)	108.7(7)
Cl(3)-C(37)-H(37A)	110.0
Cl(2)-C(37)-H(37A)	110.0
Cl(3)-C(37)-H(37B)	110.0
Cl(2)-C(37)-H(37B)	110.0
H(37A)-C(37)-H(37B)	108.3
Cl(2A)-C(37A)-Cl(3A)	110.2(7)
Cl(2A)-C(37A)-H(37C)	109.6
Cl(3A)-C(37A)-H(37C)	109.6
Cl(2A)-C(37A)-H(37D)	109.6
Cl(3A)-C(37A)-H(37D)	109.6
H(37C)-C(37A)-H(37D)	108.1

Table 4. Anisotropic displacement parameters ($Å^2 x\ 10^3$)for pge1311b. The anisotropic displacement factor exponent takes the form: $-2\pi^2[h^2 a^{*2} U^{11} + ... + 2 h k a^* b^* U^{12}]$

	U^{11}	U^{22}	U^{33}	U^{23}	U^{13}	U^{12}
C(1)	37(3)	32(3)	44(3)	-20(3)	-16(3)	-3(2)
C(2)	44(3)	42(3)	39(3)	-20(3)	-13(3)	-8(3)
C(3)	45(4)	50(4)	57(4)	-21(3)	-18(3)	-17(3)
C(4)	54(4)	47(4)	42(3)	-16(3)	-24(3)	-10(3)
C(5)	67(5)	40(4)	43(4)	-12(3)	-28(3)	-15(3)
C(6)	46(4)	43(4)	43(3)	-15(3)	-18(3)	-11(3)
C(7)	46(3)	35(3)	33(3)	-16(3)	-12(3)	-12(3)
C(8)	43(4)	42(4)	45(4)	-22(3)	-8(3)	-12(3)
C(9)	49(4)	60(5)	42(4)	-27(3)	-1(3)	-19(3)
C(10)	79(6)	66(5)	41(4)	-20(4)	-9(4)	-39(5)
C(11)	75(5)	40(4)	38(3)	-11(3)	-21(3)	-13(4)
C(12)	54(4)	40(4)	42(3)	-19(3)	-19(3)	-6(3)
C(13)	37(3)	39(3)	35(3)	-15(3)	-12(2)	-5(3)
C(14)	42(3)	33(3)	49(4)	-21(3)	-14(3)	0(3)
C(15)	46(4)	43(4)	45(4)	-23(3)	-15(3)	3(3)
C(16)	41(4)	42(4)	55(4)	-20(3)	-13(3)	7(3)
C(17)	36(3)	49(4)	59(4)	-25(3)	-19(3)	0(3)
C(18)	39(3)	37(3)	46(3)	-20(3)	-22(3)	1(3)
C(19)	38(3)	41(3)	33(3)	-15(3)	-10(2)	-12(3)
C(20)	41(3)	44(4)	39(3)	-24(3)	-10(3)	-3(3)
C(21)	54(4)	62(5)	52(4)	-40(4)	-8(3)	-5(4)
C(22)	65(5)	79(6)	44(4)	-40(4)	-2(3)	-24(4)
C(23)	60(4)	54(4)	35(3)	-22(3)	-15(3)	-15(3)
C(24)	42(3)	48(4)	44(3)	-22(3)	-13(3)	-12(3)
C(25)	36(3)	42(3)	37(3)	-17(3)	-11(2)	-10(3)
C(26)	30(3)	55(4)	48(4)	-25(3)	-2(3)	-8(3)
C(27)	28(3)	60(5)	65(5)	-23(4)	-6(3)	-8(3)
C(28)	38(4)	73(5)	69(5)	-22(4)	-25(3)	-17(4)
C(29)	47(4)	72(6)	65(5)	-30(4)	-21(4)	-18(4)
C(30)	42(3)	44(4)	46(4)	-18(3)	-17(3)	-10(3)
C(31)	43(3)	34(3)	32(3)	-14(2)	-11(2)	-8(3)
C(32)	44(4)	42(4)	34(3)	-13(3)	-6(3)	-12(3)
C(33)	63(5)	57(5)	39(4)	-22(3)	-4(3)	-24(4)

C(34)	82(6)	32(3)	43(4)	-7(3)	-23(4)	-16(4)
C(35)	63(5)	41(4)	57(4)	-21(3)	-29(4)	1(3)
C(36)	49(4)	33(3)	33(3)	-10(3)	-16(3)	-2(3)
P(1)	33(1)	30(1)	35(1)	-16(1)	-12(1)	-5(1)
Cl(1)	39(1)	38(1)	49(1)	-22(1)	-23(1)	-1(1)
P(2)	30(1)	34(1)	31(1)	-16(1)	-9(1)	-5(1)
Rh(1)	28(1)	31(1)	31(1)	-17(1)	-10(1)	-4(1)
O(1)	31(2)	35(2)	37(2)	-21(2)	-12(2)	-6(2)
O(2)	32(2)	40(2)	34(2)	-20(2)	-11(2)	2(2)
C(37)	81(6)	91(7)	80(7)	-31(6)	-39(6)	9(6)
Cl(2)	88(3)	62(3)	81(3)	-17(2)	-18(3)	2(2)
Cl(3)	110(5)	96(4)	126(5)	-48(4)	5(4)	-19(3)
C(37A)	80(7)	85(7)	84(8)	-30(6)	-35(6)	3(6)
Cl(2A)	103(4)	125(5)	137(6)	-52(4)	-67(4)	-9(4)
Cl(3A)	60(3)	78(3)	78(3)	-20(2)	-6(2)	-4(2)

Table 5. Hydrogen coordinates (x 10^4) and isotropic displacement parameters (Å^{2}x 10^3) for 3.5(i).

	x	y	z	U(eq)
H(2)	3128	1366	5151	47
H(3)	2010	942	4311	56
H(4)	2547	1615	2330	53
H(5)	4204	2711	1195	55
H(6)	5253	3181	2048	50
H(8)	2839	3103	5948	50
H(9)	1613	2195	7797	59
H(10)	2468	498	8905	71
H(11)	4523	-282	8096	60
H(12)	5746	639	6221	51
H(14)	6409	895	3379	48
H(15)	8489	-26	2871	52
H(16)	10120	319	3255	58
H(17)	9681	1591	4116	56
H(18)	7622	2498	4618	45
H(20)	8350	2883	1839	47
H(21)	8592	2159	500	63
H(22)	7490	3040	-814	69
H(23)	6267	4760	-888	55
H(24)	6045	5483	436	50
H(26)	9678	4222	1182	54
H(27)	11560	3923	1593	64
H(28)	11539	4289	3102	68
H(29)	9598	4870	4296	67
H(30)	7678	5044	3988	50
H(32)	8740	6323	572	49
H(33)	8660	8107	-720	62
H(34)	6688	9226	-613	62
H(35)	4815	8550	765	61
H(36)	4888	6755	2087	47
H(37A)	2217	7559	3630	100
H(37B)	1997	6872	3049	100
H(37C)	2252	6864	3436	99
H(37D)	1354	7386	4365	99

Time (min)	[Product]/%	[Diethyl diallylmalonate]/%
20	5.8	98.9
40	6.5	97.8
60	7.3	95.1
80	10.2	91.9
100	12.3	89.7
120	14.1	85.5
140	15.4	81.3
160	18.7	77.1
180	21.6	73.2
200	24.8	69.7
220	27.9	65.8
240	31.6	59.6
260	36.6	53.4
280	46.72	49.8
300	56.5	44.5
320	64.2	38.9
340	68.7	35.4
360	72.5	30.1
380	78.7	29.9
400	84.2	28.3
420	84.7	27.7
440	84.8	26.5
460	85.2	25.3
480	85.2	22.3
500	85.2	20.4

Figure 4.7: Data set for the representation plot of Diethyl diallylmalonate and its corresponding cyclopentene diester concentrations vs Time. The representation plot has been graphed in page 128.